Technical Report SL-99-5
August 1999

US Army Corps of Engineers
Waterways Experiment Station

Airblast Effects Research: Small-Scale Experiments and Calculations

by Charles E. Joachim, Gordon W. McMahon, Christo V. Lunderman, Sharon B. Garner

Prepared for Army Materiel Command

The contents of this report are not to be used for advertising, publication, or promotional purposes. Citation of trade names does not constitute an official endorsement or approval of the use of such commercial products.

The findings of this report are not to be construed as an official Department of the Army position, unless so designated by other authorized documents.

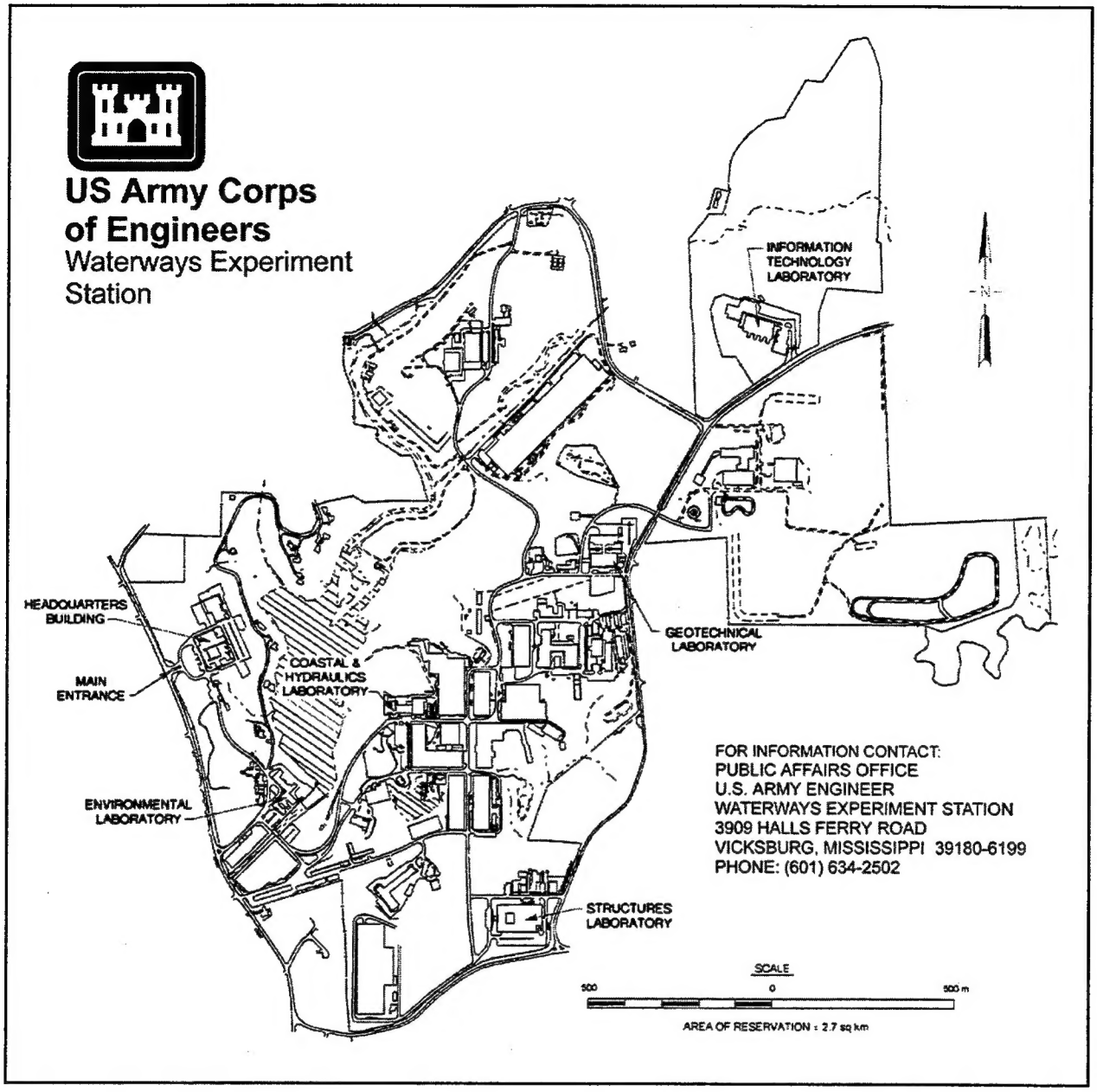

Waterways Experiment Station Cataloging-in-Publication Data

Airblast effects research : small-scale experiments and calculations / by Charles E. Joachim ... [et al.] ;
prepared for Army Materiel Command, Special Projects Support Activity.
99 p. : ill. ; 28 cm. — (Technical report ; SL-99-5)
Includes bibliographic references.

1. Blast effect — Mathematical models. 2. Ammunition — Storage. 3. Explosives — Storage. I. Joachim, Charles E. II. United States. Army. Corps of Engineers. III. U.S. Army Engineer Waterways Experiment Station. IV. Structures Laboratory (U.S. Army Engineer Waterways Experiment Station) V. U.S. Army Materiel Command (1984-). Special Projects Support Activity. VI. Series: Technical report (U.S. Army Engineer Waterways Experiment Station) ; SL-99-5.
TA7 W34 no.SL-99-5

Contents

List of Figures

List of Tables

Preface

The study reported herein was performed by staff members of the Geomechanics and Explosion Effects Division (GEED), Structures Laboratory (SL), U.S. Army Engineer Waterways Experiment Station (WES), Vicksburg, MS, a complex of five laboratories of the Engineer Research and Development Center (ERDC), during September 1997. The investigation was sponsored by Army Materiel Command Special Projects Support Activity, Fort Belvoir, Virginia. Technical monitor for this study was Mr. Jeff Huber.

The Project Manager was Mr. G. W. McMahon. Mr. C. E. Joachim conducted the study and is the primary author of this report, with contributions from Messrs. McMahon, C. V. Lunderman, GEED, and Ms. S. B. Garner, Structural Mechanics Division, SL. Others actively participating in this study were Messrs. Lunderman, T. G. Ray, GEED, and W. D. Townsend, Directorate of Public Works. Instrumentation support was provided by Messrs. H. L. Blake and J. Carter, Instrumentation Systems Development Division, Information Technology Laboratory. The CTH calculations of the experiments were performed by Ms. Garner. Ms. Donna Rowland, GEED, helped in preparation of this report. Mr. A. E. Jackson, Jr., was Acting Chief, GEED. Dr. Bryant Mather was Director, SL.

Commander of ERDC during the conduct of this research was COL Robin R. Cababa, EN. This report was prepared and published at the WES complex of ERDC.

1 Introduction

Background

A considerable amount of research has been performed in the last three decades to develop data and prediction methods for airblast from accidental explosions in underground magazines. The airblast measurements recorded in most experiments related to this work were almost exclusively overpressure (side-on). Few attempts were made to measure dynamic flow properties of the blast wave in the tunnel system. During the recently-completed Joint US/Republic of Korea (ROK) R&D Program for New Ammunition Storage Technologies, an attempt was made to record total pressure waveforms along with the associated overpressure time-histories. The blast waves in these experiments entrained large quantities of fine dust that clogged the small vent ports of the total pressure gage mounts, resulting in total pressure waveforms with an undefined component associated with the entrained dust.

A program of small-scale, high-explosive airblast experiments was conducted in September 1997 at the U.S. Army Waterways Experiment Station (WES) Big Black Test Site near Vicksburg, MS, to evaluate the dynamic flow parameters produced by detonations in underground facilities. The program consisted of six explosive experiments using spherical C-4 explosive charges. Total pressures were measured at two locations within the vent pipe using a WES-designed, miniature total-pressure gage mount. The experimental program was coupled with hydrocode calculations that allowed a comprehensive analysis of the dynamic pressure environment and flow conditions in the model.

Objectives

The overall objectives of this research was to establish quantitatively the dynamic pressure environment and flow parameters from confined detonations in a simple chamber/tunnel system over a range of loading densities from 0.4 to 5.0 kg/m^3 and to establish the ability of the first-principles shock-physics code CTH to model this phenomena. Specific objectives of the research program were to evaluate the effects of explosive loading density (kilograms of explosive per cubic meter of chamber volume), characterize the dynamic flow parameters of the blast wave, and perform validation calculations using CTH.

2 Procedures

Model Layout

The airblast effects research program used the steel detonation chamber constructed for small-scale magazine tests in the US/ROK R&D Program (Joachim, 1994). The model consisted of a detonation chamber connected to a coaxial vent pipe section. The detonation chamber is cylindrical with an inside diameter of 508 mm (20 in.) and a length of 1.8 m (5.9 ft), with 152.4 mm (6 in.) thick walls. The vent pipe consisted of four one-meter long sections of 364-mm (14.3 in.) inside diameter Schedule 80 steel pipe. The chamber was sealed with a 76.2 mm (3 in.) steel backplate. The backplate and all vent pipe sections were secured using 25.4-mm (1 in.) diameter, Grade 8 steel bolts.

The model is shown in elevation cross-section in Figure 1. The model storage chamber has a cross-sectional area of 0.2027 m^2 and a volume of 0.3648 m^3. The vent pipe cross-sectional area was 0.1038 m^2 and the volume was 0.4152 m^3. The total volume of the model storage magazine was 0.7800 m^3.

Instrumentation

Airblast measurements included: (1) chamber pressure, vent pipe pressures (side-on and total), and free-field pressure (side-on and stagnation). The airblast gage locations are shown in Figure 1 and listed in Table 1.

The detonation chamber was instrumented for side-on pressure at three locations; one on the rear wall and two at the side wall. Side-on airblast gages were installed at five locations along the vent pipe wall. In addition, the vent pipe was instrumented at two locations for total pressure/flow velocity measurements. Free-field airblast measurements were made at four ranges along the extended centerline of the tunnel. The internal wall gages were mounted flush with the inside surface of the chamber and vent pipe for side-on pressure measurements. The free-field gages were placed in surface gage mounts

such that the gage sensing surfaces were flush with the ground surface. Gage locations are shown in Figure 1 and tabulated in Table 1. Experiment parameters (charge mass and chamber loading density) are given in Table 2.

Two WES-designed probe mounts were positioned inside the vent pipe. Each probe mount contained two pressure transducers; a total pressure gage at the front of the probe (oriented face-on to the shock wave), and a side-on gage located in a small chamber 70 mm behind the total pressure gage. The probe side-on pressure gage sensor measured the pressure in an arched chamber with a volume of 10,700 mm^3. Pressure entered the chamber through two rows of 1.6-mm-diameter holes drilled at 10° intervals. A schematic showing the position of the probe mount within a section of vent pipe is shown in Figure 2.

The gage signals were amplified, digitized and recorded on computer-controlled transient data recorders. The gage signals were transmitted to the recording trailer on 4-conductor, shielded cable (approximately 300 m long) with a floating ground. Each channel was electronically calibrated at the digitizer by the equivalent voltage method. A zero-time break wire wrapped around the explosive charge triggered the transient data recorders and provided a time reference for each event.

Airblast Predictions

Predicted peak airblast values are plotted versus distance in Figure 3. The predicted peak data were obtained from two sources: BLASTX (Version 3.6) calculations (Britt, et al., 1994), and 1/20-scale US/ROK test data. The data from the US/ROK (Phase 3 Series I) Test 24 are plotted in Figure 3 for comparison. After evaluating the predictions shown in Figure 3, the decision was made to select gages and set ranges to accommodate a peak value twice the BLASTX-calculated value.

Prediction of total pressures were made using Figure 3.8 in the CONWEP software derived from Army TM 5-855. This figure is a plot of overpressure (abscissa) versus dynamic pressure (ordinate axis). Entering the CONWEP Figure 3.8 with the predicted overpressure at the gage station, the corresponding value of dynamic pressure was obtained. The total pressure prediction was simply the sum of the overpressure and dynamic pressure values.

Explosive Charges

Six experiments were conducted in the small-scale model using spherical C-4 charges. The masses of the explosive charges used for these experiments were 0.045, 0.11 (three experiments), 0.28 and 1.36 kg. Charges were formed in a hemispherical mold. The charge diameters were 38, 51, 69, and 118-mm, respectively. A Reynolds Electric Bridge Wire (EBW) detonator was positioned at the center of the diametrical plane of the hemisphere prior to putting the two

hemispherical sections together to form the spherical charge. The charges were suspended at the center of the test chamber using a section of panty-hose and nylon fish line.

Table 1
Airblast Effects Experiments, Gage Location

Gage No.	Distance from Rear Wall of Chamber (m)	Distance from Axis of Chamber/Tunnel (m)	Measurement Location, Type of Measurement
AB-1	0.00	0.107	Back Wall of Chamber, Chamber Pressure
AB-2	0.45	0.254	Side Wall of Chamber, Chamber Pressure
AB-3	1.35	0.254	Side Wall of Vent Pipe, Chamber Pressure
AB-4	1.99	0.182	Side Wall of Vent Pipe, Side-on Pressure
AB-5	2.61	0.182	Side Wall of Vent Pipe, Side-on Pressure
AB-6	3.37	0.019	Probe Mount, Side-on Pressure
AB-7	3.30	0.000	End of Probe Mount, Total Pressure
AB-8	4.37	0.019	Probe Mount, Side-on Pressure
AB-9	4.30	0.000	End of Probe Mount, Total Pressure
AB-10	5.30	0.182	Side Wall of Vent Pipe, Side-on Pressure
AB-11	5.61	0.182	Side Wall of Vent Pipe, Side-on Pressure
AB-12	7.60	0.182	Free-Field, Side-on Pressure
AB-13	8.80	0.182	Free-Field, Side-on Pressure
AB-15	10.60	0.182	Free-Field, Side-on Pressure
AB-17	13.80	0.182	Free-Field, Side-on Pressure

Table 2
Test Parameters for Model Blast Effects Experiments

Test No.	C-4 Explosive Mass (kg)	Chamber Loading Density (kg/m^3)	Total Loading Density (kg/m^3)
1	0.110000	0.404	0.184
2	0.110000	0.404	0.184
3	0.110000	0.404	0.184
4	0.280000	1.028	0.468
5	1.360000	4.995	2.273
6	0.045000	0.165	0.075
7[1]	1049.000000	1.028	0.468

[1] CTH computational model for prototype underground magazine.

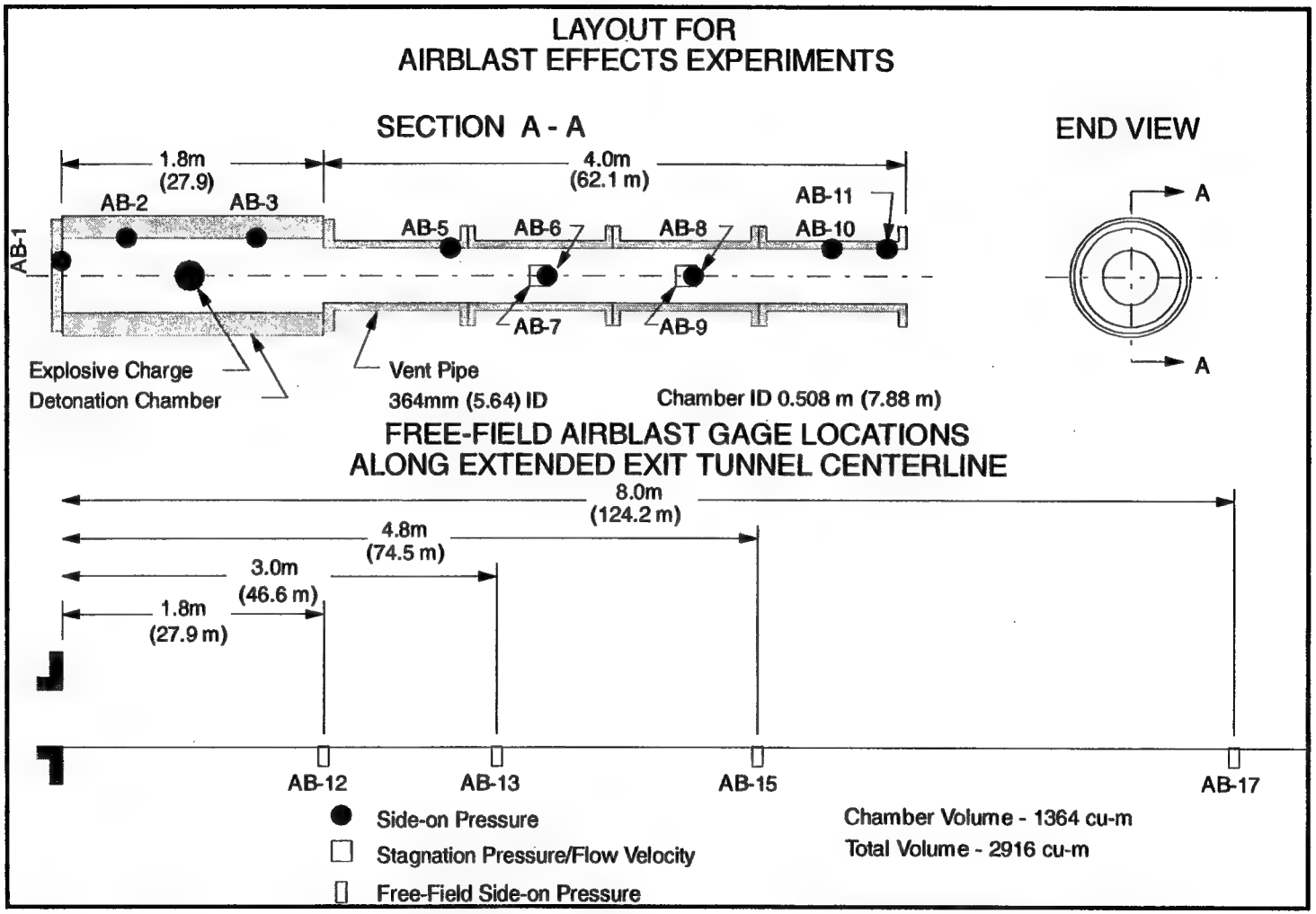

Figure 1. Layout for small-scale blast effects experiments. Full-scale distances are given in parenthesis

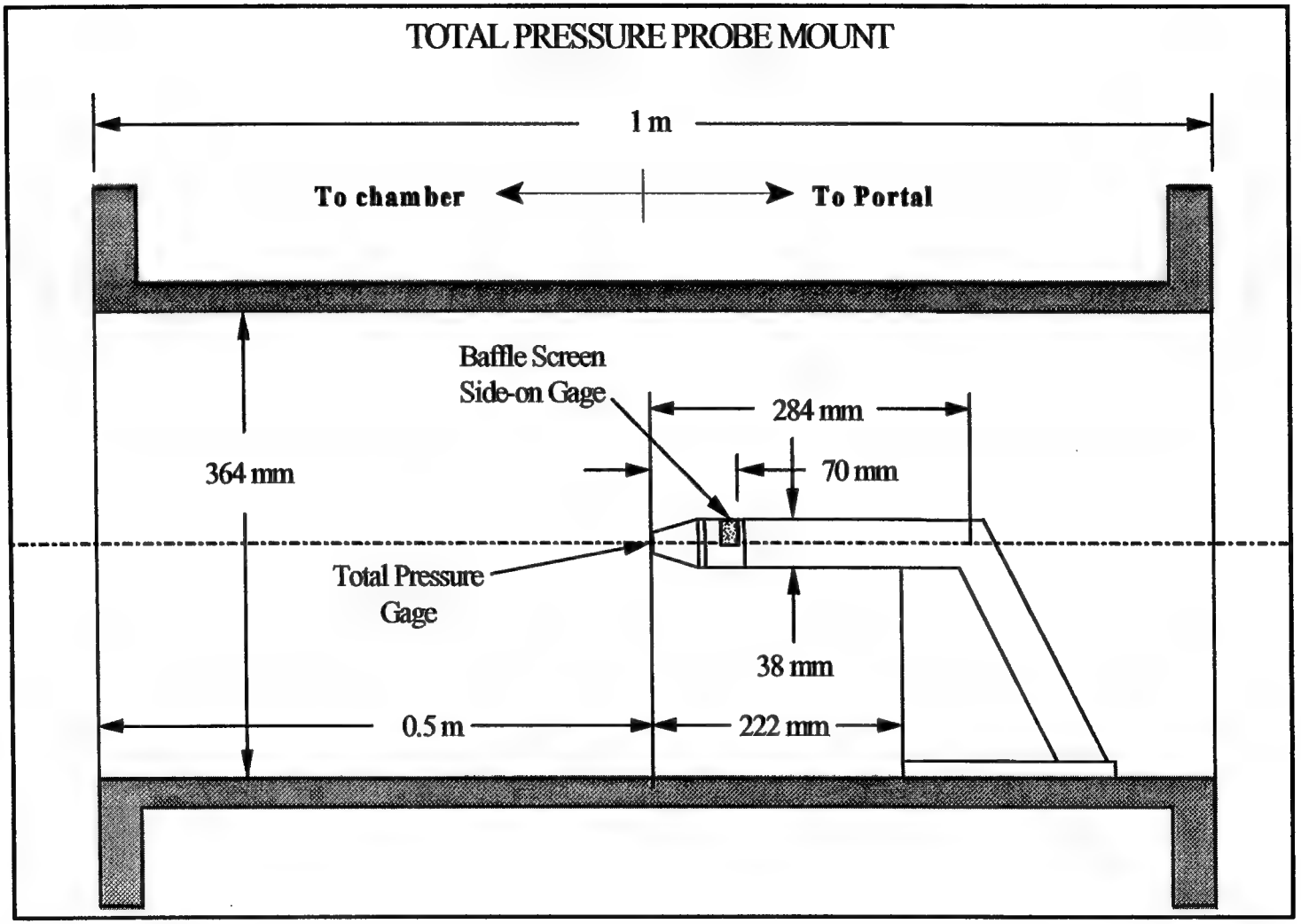

Figure 2. Schematic showing position of total pressure probe mount within vent pipe and the relative position of side-on pressure blast screen with respect to the total pressure gage

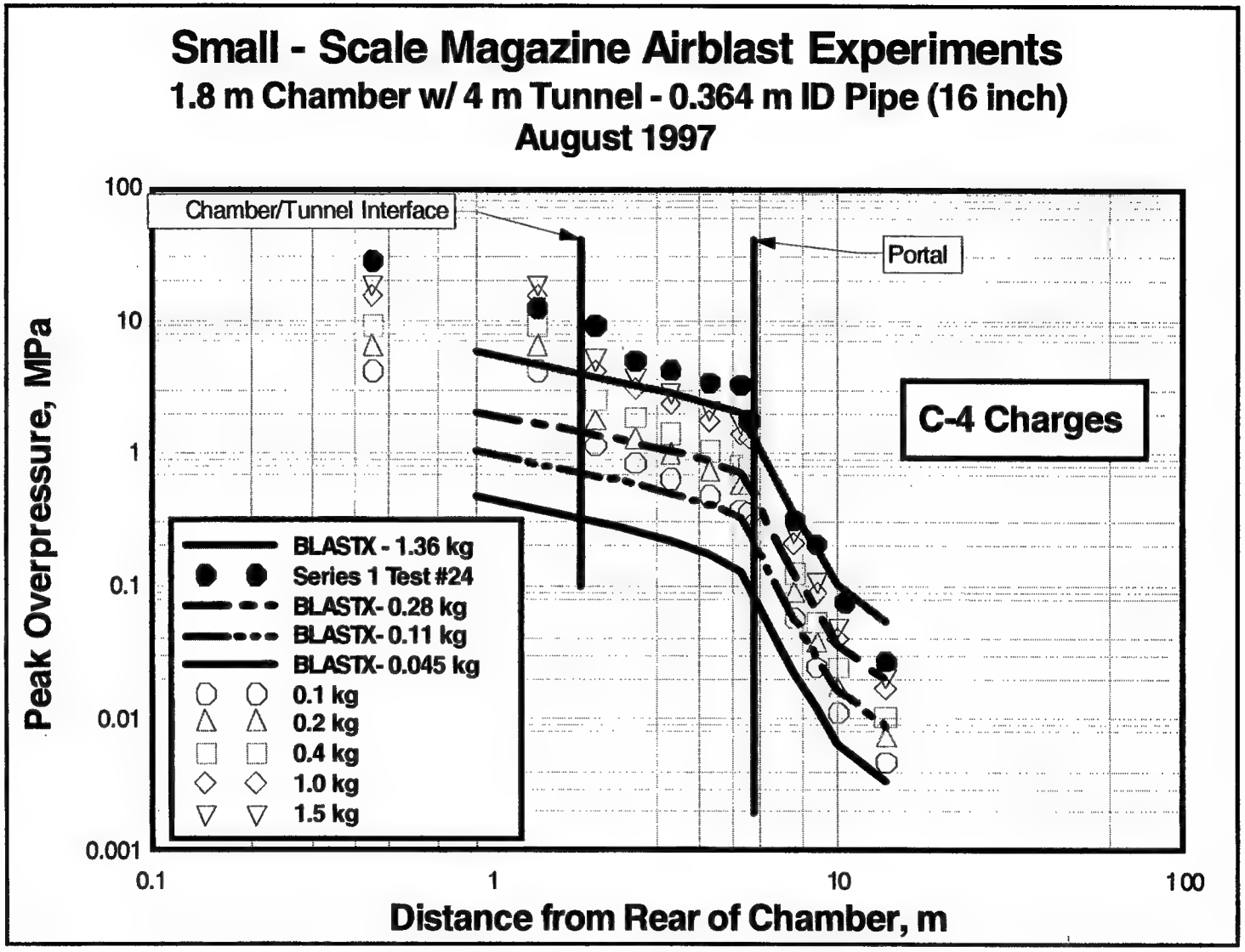

Figure 3. Predicted peak overpressure versus distance from rear wall of the chamber, Small-Scale Magazine airblast experiments

3 Computer Model

Computer Code

The computer model was developed using CTH, a family of codes developed at Sandia National Laboratories for modeling problems characterized by large deformations or strong shocks (see McGaun, et al., 1990, and Hertel, et al, 1993). CTH uses an Eulerian mesh to solve the mass, momentum and energy conservation equations. The mesh is fixed in space, and the material flows through the mesh in response to boundary and initial conditions. The mesh is made up of computational cells, each of which can contain multiple materials and voids.

The solution of the conservation equations (in the CTH codes) is performed in two steps: a Lagrangian step and a remap step. In the Lagrangian step, the Lagrangian forms of the governing equations are integrated across a time step, resulting in a distorted mesh with no mass flux across cell boundaries. In the remap step, the distorted cells are remapped back into the original mesh. As a result of this solution scheme, mass is conserved. The remaining conservation equations are replaced with explicit finite volume approximations.

CTH contains models for material strength, fracture, porous materials, and high explosive initiation and detonation. These models are applied during the Lagrangian step, and the resulting velocities, energies, stress deviators and internal state variables are mapped back into the initial mesh. Thermodynamic material behavior is incorporated through two equation-of-state packages, the Analytic Equation-Of State (ANEOS) package and the tabular SNL-SESAME package. Tabular equation-of-state data for explosive materials are provided in the JWL data package. Tables in this package are derived from the Jones-Wilkinson-Lee formula.

Computer Model Development

The scaling relation between model and prototype was developed as follows. The access tunnel in the prototype was assumed to have a rectangular

cross-section, 5 m wide by 5 m high. Assuming a circular cross-section of the same area, the equivalent diameter was computed to be 5.64 m. The diameter of the access tunnel in the small-scale model was 0.364 m. Therefore, the geometric scale factor relating model and prototype is the ratio of the access tunnel diameters (5.64/0.364 = 15.52). Assuming that the chamber loading density was 1.028 kg/m^3 and the charge mass in the model was 0.28 kg C-4, the equivalent charge mass of C-4 in the prototype computes to be 1,049 kg. The dimensions of the model were scaled to prototype size by multiplying by the scale factor of 15.52 (note: for convenience, this is referred to as the 1/15-scale model). A grid was superimposed on the prototype magazine (2.5 cm square cells) and the dimensions of the prototype were adjusted to make grid boundaries coincide with cell boundaries. After gridding the prototype for the CTH calculation, the actual prototype charge mass used in the calculation was 1,049 kg C-4.

The prototype underground magazine was numerically modeled as axisymmetric. The computational model included three materials: C-4 explosive, steel, and air. The SNL-SESAME tabular equations-of-state were used to define the properties of the air and steel materials throughout the CTH computations. The C-4 equation-of-state properties were obtained from interpolation of the JWL tables in CTH. A uniform cell spacing of 2.5 cm was applied to the x and y coordinate directions in the prototype underground magazine problem. A graph of the initial state (before charge detonation) of the axisymmetric computational model is shown in Figure 4. The x coordinate axis is the axis of symmetry for the calculation. The prototype calculation contained a total of 1,131,900 cells.

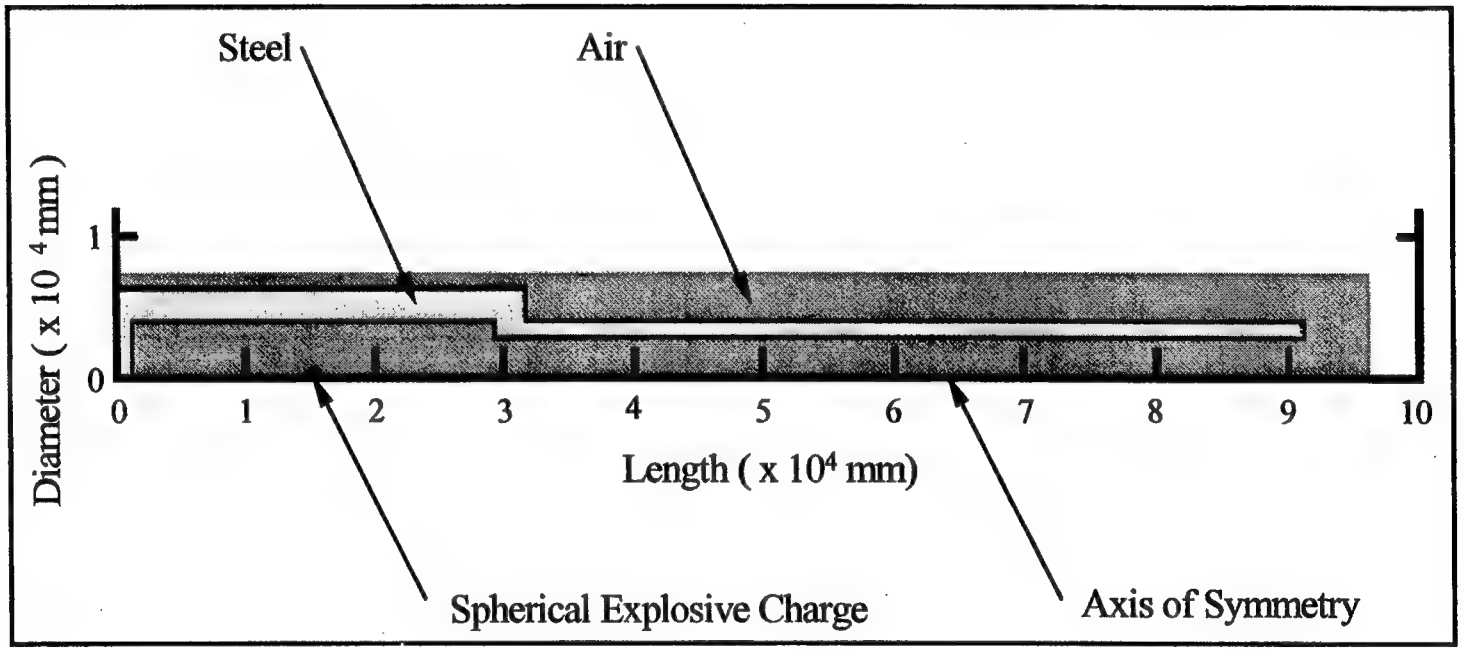

Figure 4. Visual display of prototype magazine computational model for airblast effects study. Note: dark shaded area depicts a diameter of 7.35 m (294 cells) and a length of 96.25 m (3850 cells)

4 Results and Discussions

Airblast Data

Fourteen pressure channels were recorded on each of the six experiments. One channel was lost during Experiment 5 (1.36 kg C-4) due to gage failure at the airblast shock front arrival. Five gages on this experiment were overdriven when the airblast pressure exceeded the maximum range of the recording system. The remaining gages yielded excellent data. The airblast arrival times, peak pressures, peak impulse values (from integration of the time histories) and gage location data from the airblast effects experiments are presented in Tables 3 through 8. Plots of the recorded waveforms are given in Appendix A through F at the end of this report.

Arrival Time

The arrival time data recorded from the pressure gages are plotted versus distance from the center of the explosive charge in Figure 5. Lines derived from least-square fits to the data are shown for each charge weight. The arrival time data exhibits a consistency, the shock wave arrival times from decrease as the charge weight is increased. Figure 5 also shows that the shock velocity approaches the sonic velocity in air (358 m/s) at greater distances from the source.

Measured Peak Pressure

Peak measured pressure data are plotted versus distance from the center of the explosive charge in Figures 6 through 9, respectively. The peak pressure data from a 0.045 kg spherical C-4 detonation are plotted in Figure 6. Separate least-square lines have been fit to the internal and free-field data. As shown in Figure 6, the side-on peak pressure data from the probe gages (square symbol) plots below the trend for the wall-mounted gages (least-squares line). It is apparent that the baffle on the probe gages reduced the measured peak value. Peak total pressure (diamond symbol) measured at the front end of the probe

mount is also presented in Figure 6. The peak total pressure is approximately 1.6 times greater than the side-on pressure curve (least-squares data fit).

Peak pressure data from three 0.11-kg C-4 experiments are presented in Figure 7. Although the internal gages show some peak data scatter, the trend is similar to that shown for the 0.045 kg experiment (Figure 6). The free-field peak pressure data exhibit good repeatability with a low degree of scatter. The peak total pressure values are approximately 2.5 time greater than the side-on pressure curve (least-squares data fit).

Figure 8 presents peak pressure data from a 0.28-kg spherical C-4 detonation in the small-scale vented "shot-gun" magazine. Here again, the probe-mounted side-on pressure gages record slightly lower vales of peak pressure than at the vent tube side-on pressure gages. The peak total pressure values are approximately three times greater than the side-on pressure curve (least-squares data fit). The increase in total pressure is due to the factor of two increase in the explosive charge mass, from 0.11 kg to 0.28 kg.

A comparison of pressures produced by spherical and rectangular parallel piped charge geometries is presented in Figure 9. A 1.36-kg experiment was conducted in the US/ROK R&D Program using a rectangular charge that measured 51 by 76 by 220 mm which gives an L/Ds ratio = 3.1. As shown in Figure 9, data from the two charge geometries plot within normal measurement scatter and are essentially equal. The side-on pressures recorded by the gages inside the probe mount cannot be differentiated from the vent tube side-on peak data.

The stagnation pressure values recorded from the US/ROK experiment are less than the total (stagnation) pressure data measured with the probe mounts. The stagnation gages were placed 12.7 mm in front of a 25.4-mm steel cube welded to the inside wall of the vent tube. The measured stagnation pressures are influenced by wall turbulence and drag, which reduces the peak values. The peak total (stagnation) pressure values at the center of the tube are approximately five times greater than the side-on pressure curve (least-squares data fit). The increase in total pressure compared to side-on pressure for this experiment is due to the factor of 10 increase in the explosive charge mass, from 0.28 kg to 1.36 kg.

Total or stagnation pressure is the pressure exerted on a stationary object in a flow field. The pressure recorded on this stationary object is greater than the overpressure (side-on) within the flow. Total pressure is equal to the sum of the overpressure and dynamic pressure at a point within an incompressible flow where dynamic pressure is the impact component of the flow (King, 1985).

Peak Impulse

The pressure waveforms were integrated to obtain impulse time histories. The peak impulse data from the 0.045-kg experiment is plotted in Figure 10. As shown in Figure 10, the impulse data from the probe-mounted gages behind the baffle are indistinguishable from the impulse, values measured at the vent tube side-on pressure gages. The value of the impulse lost through the baffle reduction of the peak pressure is very small compared to the total impulse, and does not significantly affect the peak impulse values. The total pressure impulse values are approximately 1.7 times greater than the side-on impulse curve (least-squares data fit).

Peak impulse data from the three 0.11-kg spherical C-4 detonations are plotted in Figure 11. Although there the data exhibits some scatter it falls within normal bounds for typical experimental data. The total pressure impulse is approximately 1.7 times greater than the side-on impulse curve (least-squares data fit).

Figure 12 shows the peak impulse data from the 0.28-kg spherical C-4 charge detonation. The total pressure impulse is approximately 1.7 time greater than the side-on impulse curve (least-squares data fit).

A comparison of measured impulse data produced by spherical and rectangular parallelepiped charge geometries is presented in Figure 13. The 1.36-kg experiment using the rectangular charge was conducted in the US/ROK R&D Program. As shown in Figure 9, internal data from the two charge geometries plot within normal measurement scatter and are essentially equal. The side-on pressure recorded by the gages inside the probe mount cannot be differentiated from the vent tube side-on peak data. The external impulse data from the US/ROK experiment decrease much faster than the spherical charge data. This is attributed to a difference in the experimental setup. The portal of the US/ROK experiment vented onto a horizontal platform (0.61 m long by 0.91 m wide) that was connected to a sloped section to the ground. The spherical charge experiments of this program were conducted with the portal venting at ground level. Therefore, the decreased free-field impulse values are attributed to the presence of the sloped section. The total pressure impulse is approximately 1.7 time greater than the side-on impulse curve (least-squares data fit).

Loading Density

Peak pressure data are plotted versus loading density in Figure 14. Total loading density is the explosive weight divided by the total volume of the chamber/tunnel system that is pressurized by the detonation at the time the pressure wave reaches the gage. A least-squares curve has been fit to all the side-on pressure data (spherical and rectangular charges) for all shots in this

series. The slope of the total pressure least-squares data fit is a factor of four times the slope of the side-on pressure curve.

Peak airblast impulse is plotted versus loading density in Figure 15. A least-squares curve has been fit to all the side-on impulse data (spherical and rectangular charges). The slope of the total impulse curve (least-squares data fit) is a factor of two times the slope of the side-on impulse curve. Thus, the impluse loading on targets along the flow path is a factor of two greater than that on targets subjected to side-on loading.

Calculated Data

The CTH code was used to calculate pressure profiles for a detonation of 1049 kg in a full-scale version of the model magazine. Six contour plots are plotted in Figure 16, giving a sequence of pressure contours for the shock front and detonation products. The shock front is shown impinging on the storage chamber walls at 1 ms after detonation. The pressure contour plot at 2 ms shows the shock front reflecting from the chamber wall. At 4 ms the reflected waves meet at the chamber centerline, amplifying the pressure on that axis of symmetry. The contour plot at 4 ms also shows the shock wave traveling at a higher velocity through the steel of the chamber wall. The remaining pressure contour plots, at 26, 47 and 69 ms after detonation, show the progress of the shock front along the access tunnel toward the portal.

Figure 17 compares the measured side-on pressure waveform for Gage AB-5 in the model, scaled up by the 1:15-scale factor, to the CTH calculation for the same location in the full-scale tunnel. As shown here, there is a very good comparison in arrival times of the various portions of the waveform. The major difference is for the second peak of the calculation, which is the reflection of the incident wave off the rear wall of the detonation chamber. This calculated peak is approximately twice the measured value. It is postulated that the reflecting surface is much stiffer in the calculational model than it was in the small-scale physical model.

A comparison of three calculated waveforms -- for side-on, dynamic, and total pressure -- is shown in Figure 18. The CTH computer code calculated the side-on pressure waveform directly, but not the dynamic pressure. The calculated air density and particle velocity waveforms for each gage location were used to calculate the dynamic pressure waveform using the following equation:

$$P_{dyn} = \rho u^2 \qquad (1)$$

where

P_{dyn} = the dynamic pressure component at each time increment,

ρ = the air density component at each time increment, and

u = the particle velocity component.

The total pressure waveform was computed using the following relation,

$$P_t = P_{dyn} + P_{so} \quad (2)$$

where

P_t = the total pressure component at each time increment, and

P_{so} = the side-on pressure component.

The calculated waveform comparison shown in Figure 18 is for the gage location in the full-scale computational model corresponding to Gage AB-7 in the small-scale physical model.

A comparison of the calculated full-scale total pressure waveform and the scaled up waveform from the physical model is presented in Figure 19. The small-scale data is converted to full-scale by multiplying the time scale by the scale factor (15.52). As shown in Figure 19, the waveforms are in good agreement except for the reflected peak value (second pressure peak at approximately 46 msec), where the calculated peak is more than twice the measured value.

An overpressure waveform comparison at a full-scale distance of 38.3 m from the center of the explosive charge is shown in Figure 20. This location corresponds to Gage AB-6 in the physical model. The measured and calculated waveforms are in relatively good agreement. The measured waveform does not have the rapid rise time response seen in the calculation because this gage is located behind a baffle on the side of the total pressure probe. A CONWEP (Hyde 1988) calculated full-scale free-field overpressure waveform at the same distance from the same charge is included in Figure 20 for an additional comparison. This comparison emphasizes how the confinement of the detonation chamber and tunnel increases the pressure at a given location, compared to an open air detonation.

Figure 21 compares the total pressure and side-on overpressure impulse waveforms in the confined space of the underground facility to calculated (CONWEP, Hyde 1988) free-field waveforms produced by an unconfined explosive source of the same yield at the same distance. Note the dramatic increase in impulse resulting from confinement. As shown in Figure 21, the calculated total impulse is a factor of 1.5 greater than the measured side-on impulse at this location.

Calculated waveforms on the centerline of the access tunnel at 52.8 m (full-scale) from the center of the explosive charge (Gage AB-9 in the physical model)

are shown in Figure 22. CTH calculated the side-on pressure, air density and particle velocity waveforms at this position in the tunnel. The dynamic pressure waveform was computed using Equation 1. The sum of the side-on and dynamic pressure waveforms yields the total pressure waveform (Equation 2).

A comparison of the calculated full-scale total pressure waveform (from Figure 22) and the scaled up measured waveform from the physical model (full-scale distance of 52.8 m) is presented in Figure 23. The small-scale data is converted to full-scale by multiplying the time scale by the scale factor (15.52). As shown in Figure 23, the waveforms are in good agreement. The calculated waveform does not exhibit the large peak reflection seen in previous waveform comparisons.

An overpressure waveform comparison at a full-scale distance of 53.9 m from the center of the explosive charge is shown in Figure 24. This location corresponds to Gage AB-8 in the physical model. The measured and calculated waveforms are in relatively good agreement. The measured waveform does not have the rapid rise time response seen in the calculation because this gage is located behind a baffle on the side of the total pressure probe. A CONWEP (Hyde 1988) calculated full-scale free-field overpressure waveform is included in Figure 24 for an additional comparison. This comparison emphasizes how the confinement of the chamber and tunnel increases the pressure.

Figure 25 compares the total airblast impulse, and overpressure impulse waveforms in the confined space of the underground facility, to the free-field calculated (CONWEP, Hyde 1988) impulse waveform produced by an explosive source of the same explosive yield at the same distance from the source. Note the dramatic increase in impulse resulting from confinement. As shown in Figure 25, the peak total calculated impulse is a factor of 1.7 greater than the peak side-on (measured overpressure) impulse at this location.

A plot of peak overpressure versus distance from the rear wall of the detonation chamber is shown in Figure 26. Overpressures were calculated on the centerline and side wall throughout the chamber/tunnel facility. The measured peak overpressure data are plotted in Figure 26 for comparison. The calculated (wall) curve is a factor of two or more greater than the measured data. As was shown in Figures 17, 18, 19, 20, 22, and 24, the greater calculated overpressure values are due to the reflected (second) peak found in these waveforms.

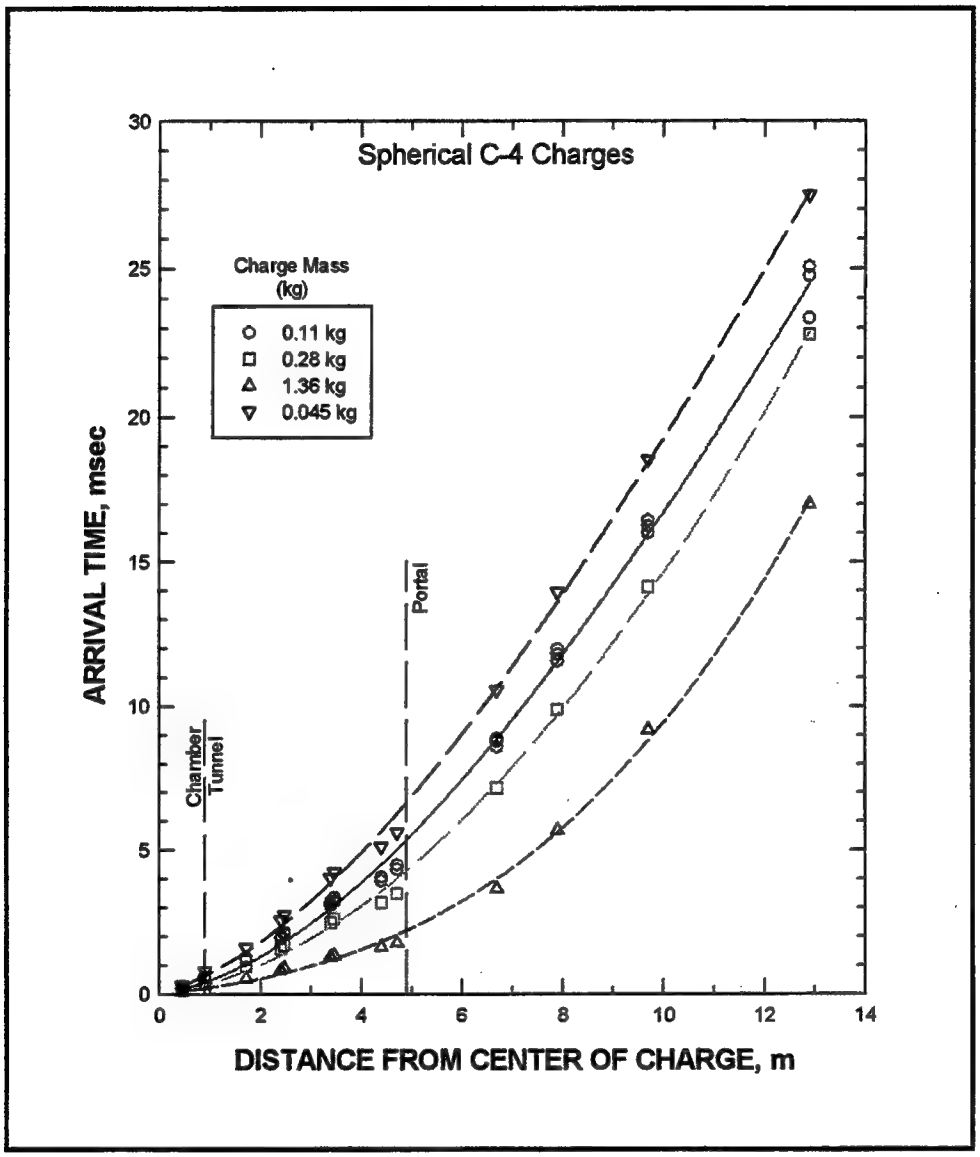

Figure 5. Airblast shock front arrival time versus distance from the center of the explosive charge, from airblast effects experiments with spherical C-4 charges in small-scale vented "shot-gun" magazines

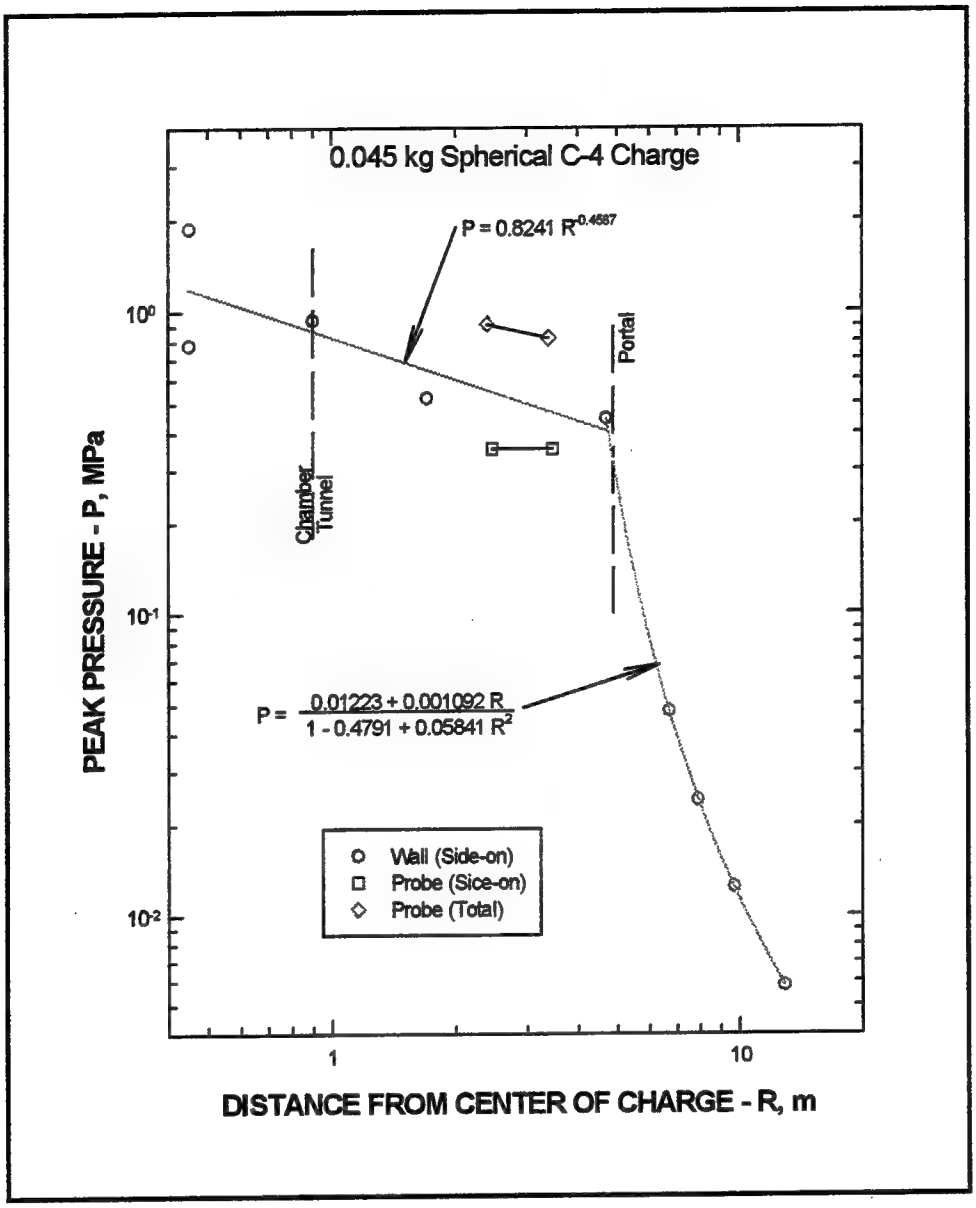

Figure 6. Peak airblast pressure versus distance from the center of the explosive charge for a 0.045 kg spherical C-4 charge detonation, from airblast effects experiments in small-scale vented "shot-gun" magazines

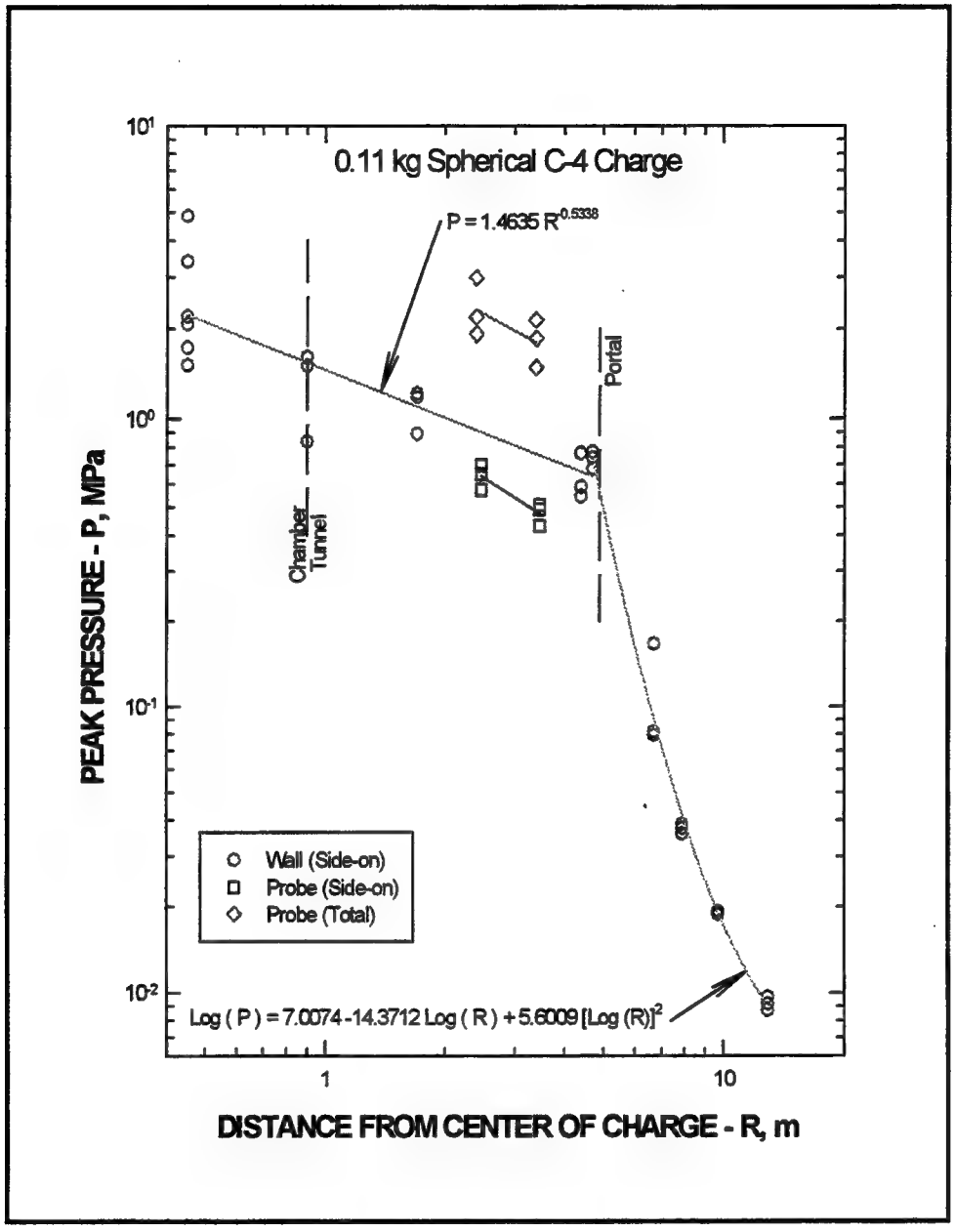

Figure 7. Peak airblast pressure versus distance from center of the explosive charge for a 0.11 kg spherical C-4 charge detonation (three experiments), from airblast effects experiments in small-scale vented "shot-gun" magazines

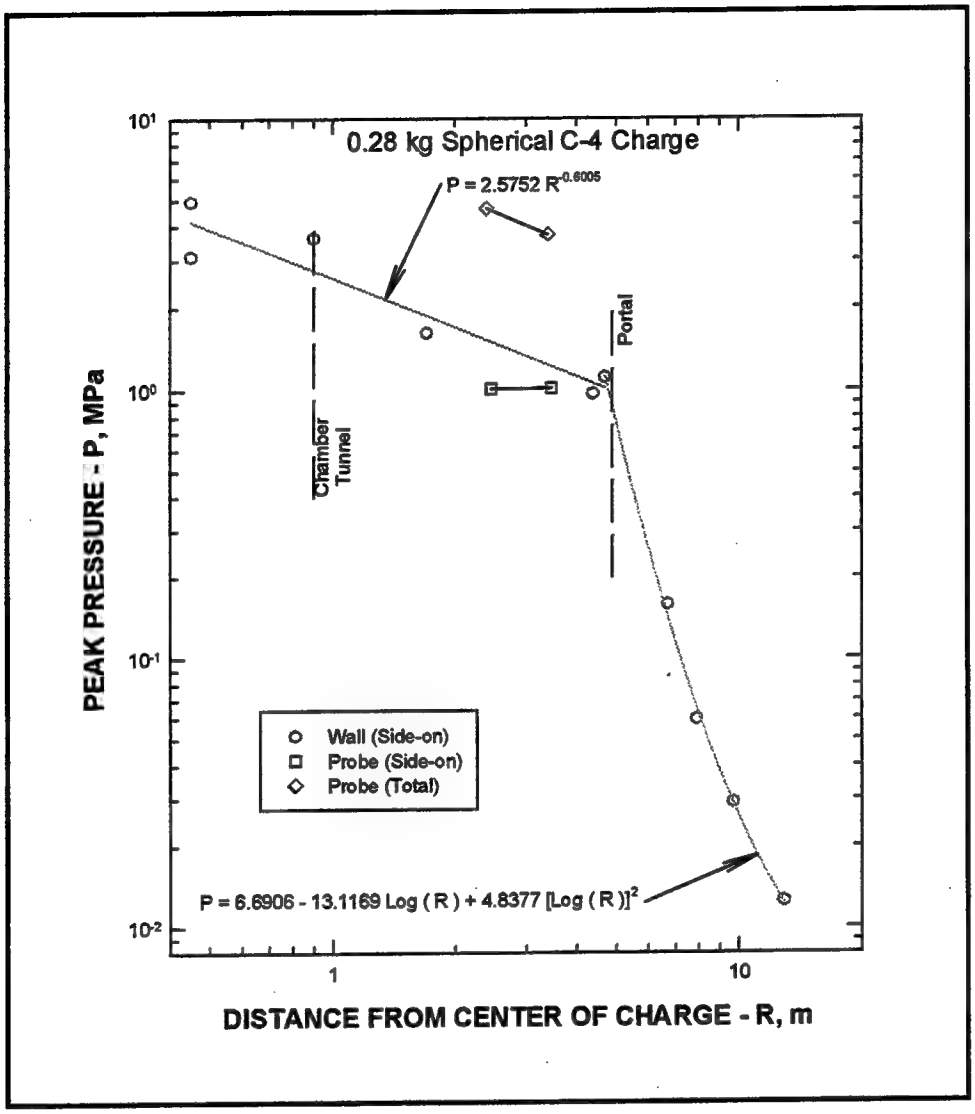

Figure 8. Peak airblast pressure versus distance from the center of the explosive charge for 0.28 kg spherical C-4 charge detonation, from airblast effects experiments in small-scale vented "shot-gun" magazines

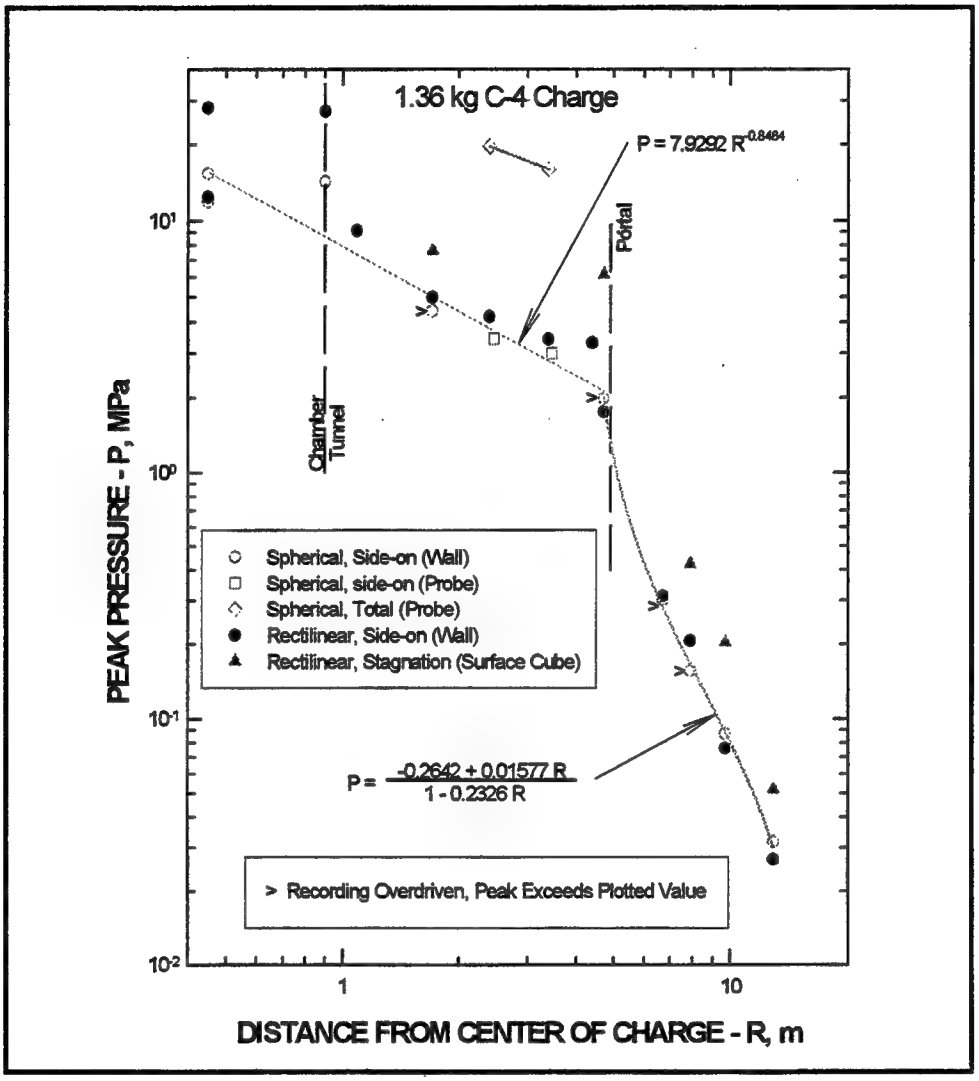

Figure 9. Peak airblast pressure versus distance from the center of the explosive charge for a 1.36 kg C-4 charge detonation, from airblast effects experiments in small-scale vented "shot-gun" magazines. Comparison is shown between peak pressure data from spherical and parallelepiped (rectilinear) charge geometries

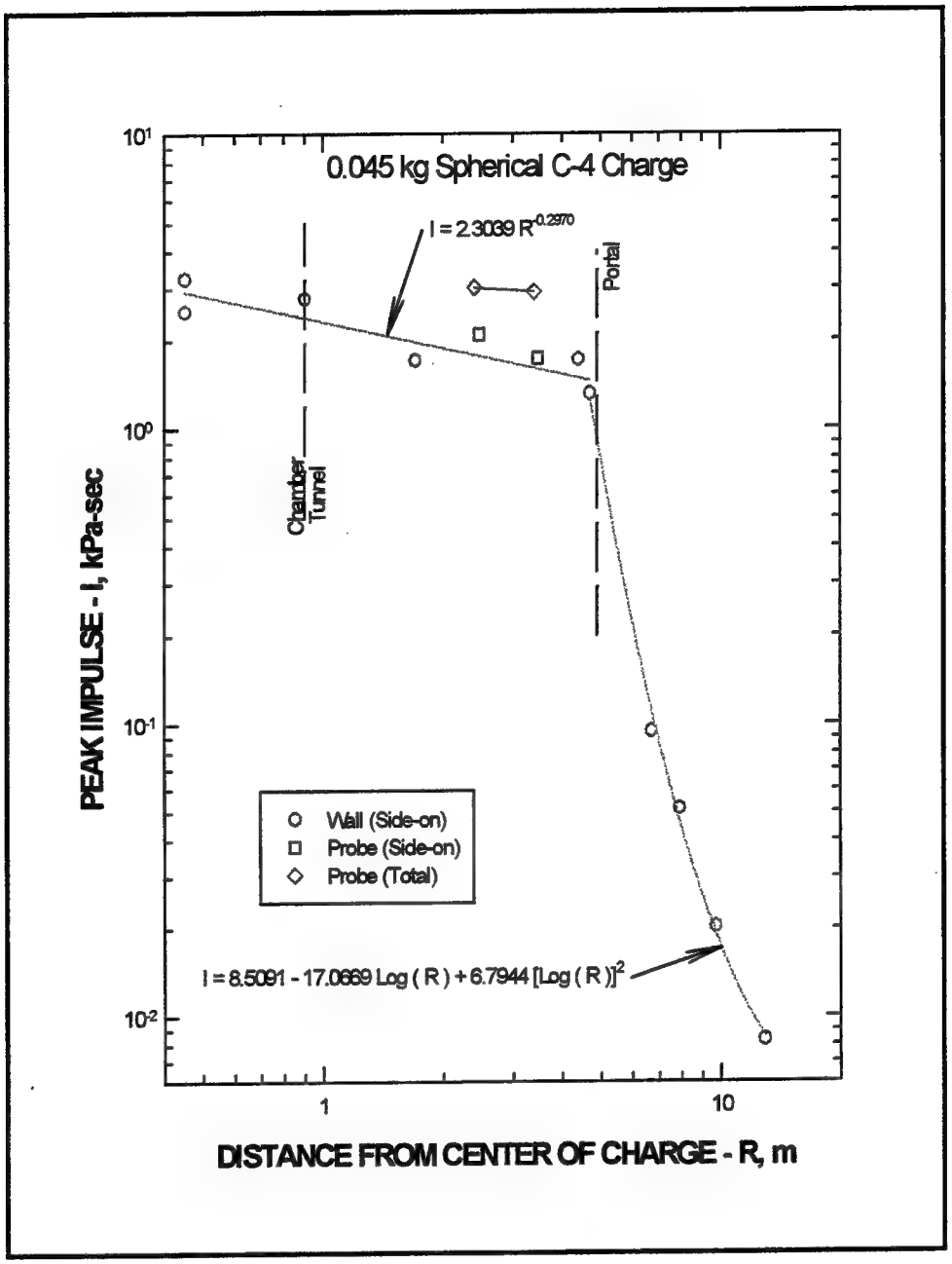

Figure 10. Peak airblast impulse versus distance from the center of the explosive charge for a 0.045 kg spherical C-4 charge detonation, from airblast effects experiments in small-scale vented "shot-gun" magazines

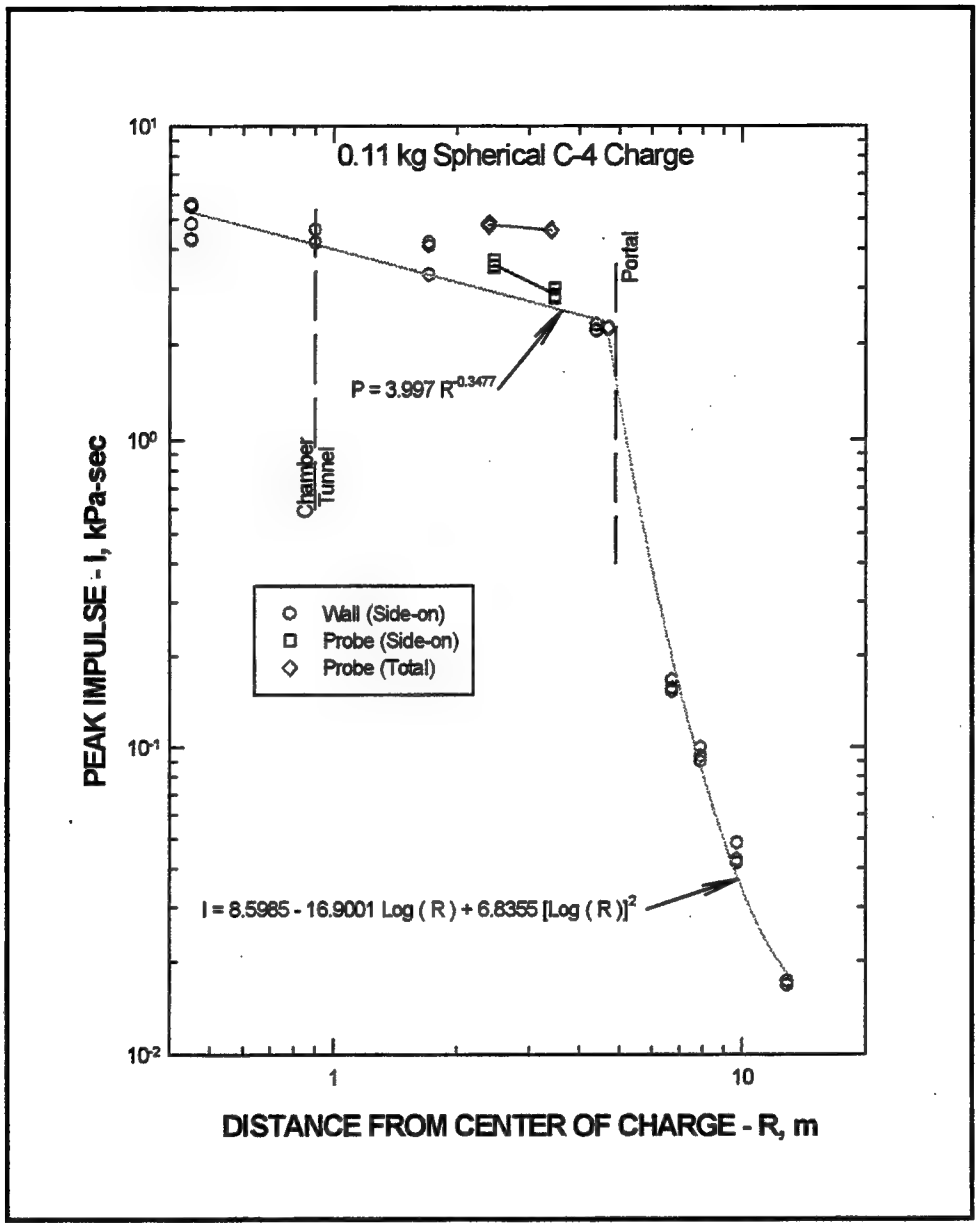

Figure 11. Peak airblast impulse versus distance from the center of the explosive charge for a 0.11 kg spherical C-4 charge detonation, from airblast effects experiments in small-scale vented "shot-gun" magazines

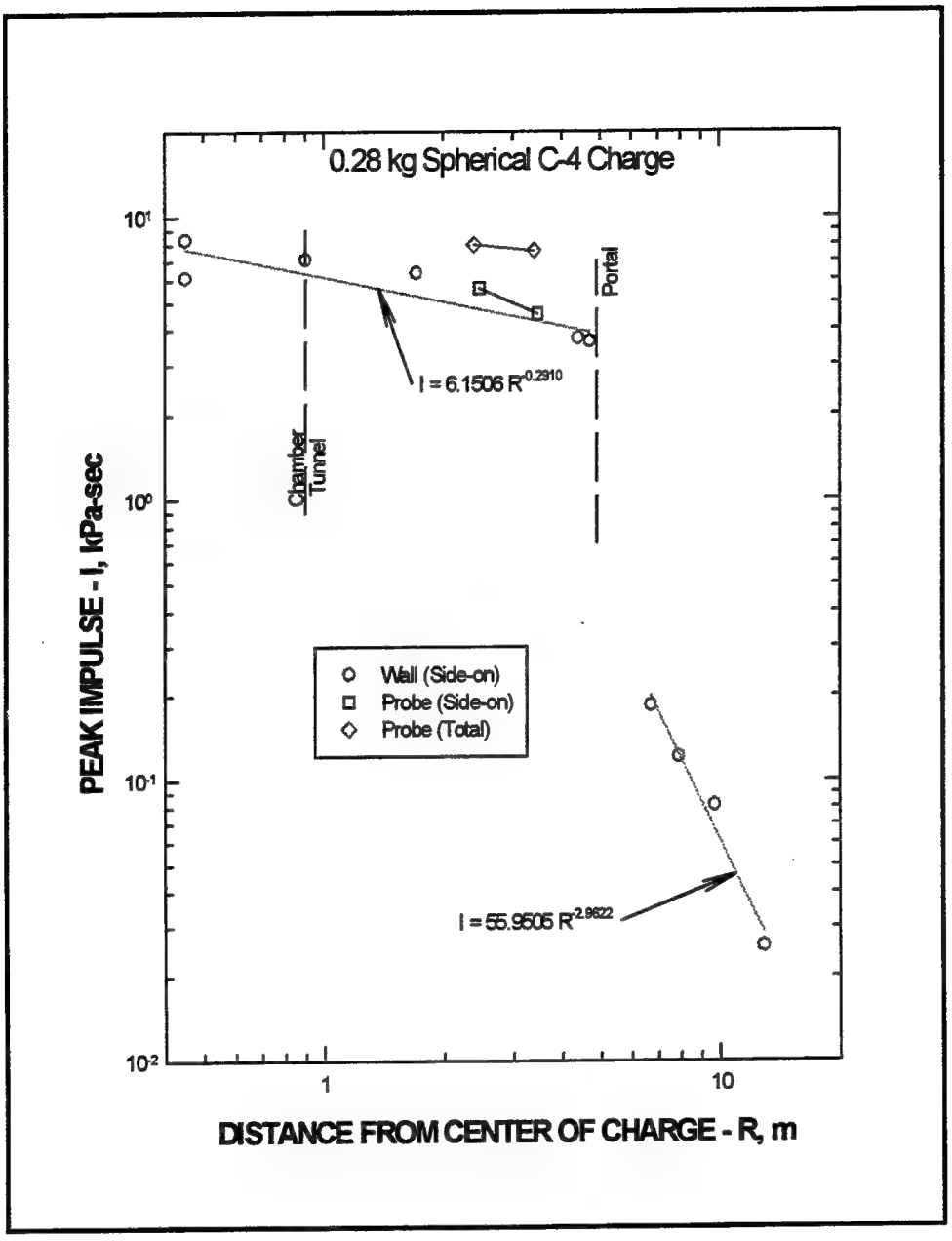

Figure 12. Peak airblast impulse versus distance from the center of the explosive charge for a 0.28 kg spherical C-4 charge detonation, from airblast effects experiments in small-scale vented "shot-gun" magazines

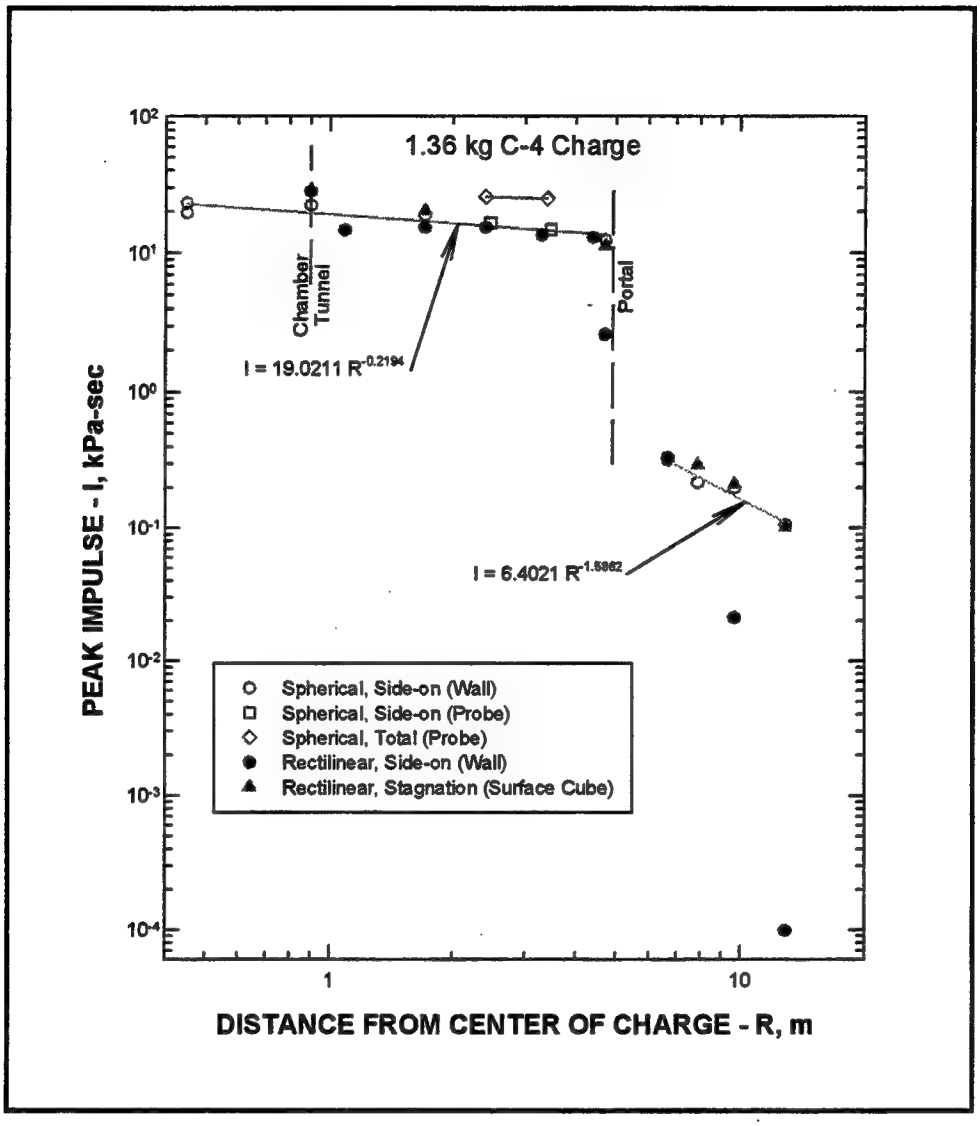

Figure 13. Peak airblast impulse versus distance from the center of the explosive charge for a 1.36 kg C-4 charge detonation, from airblast effects experiments in small-scale vented "shot-gun" magazines. Comparison is shown between peak impulse data from spherical and rectangular parallel piped (rectilinear) charge geometries

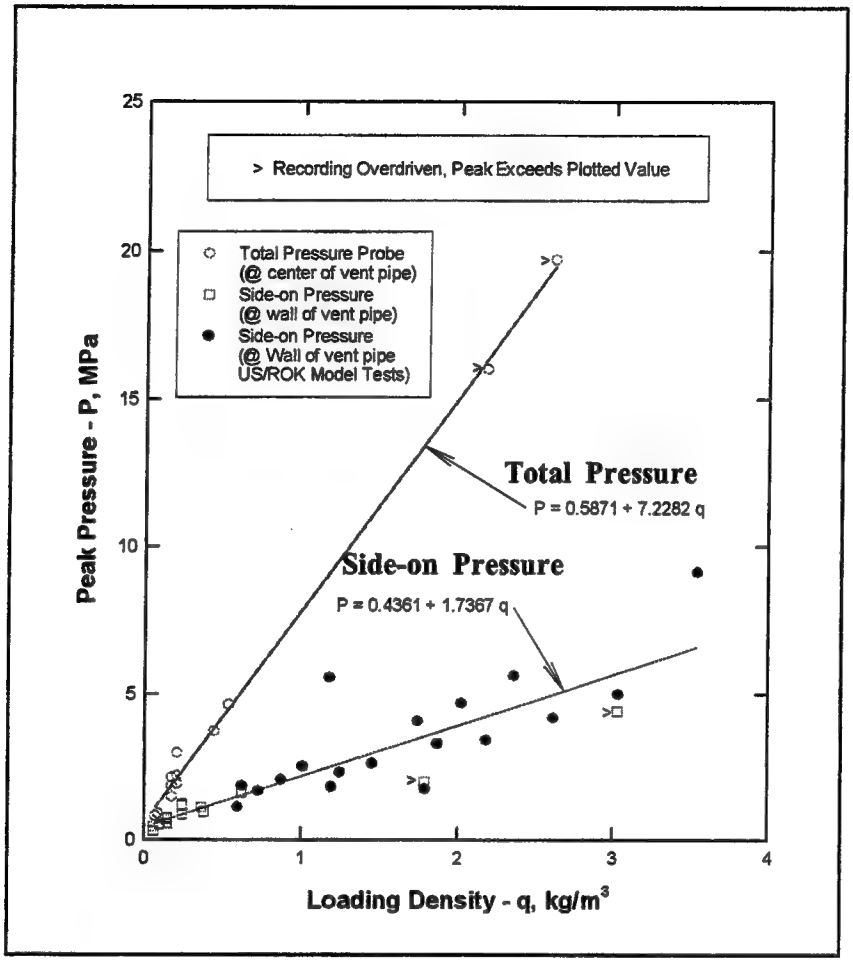

Figure 14. Peak airblast pressure in vent pipe versus explosive loading density, from airblast effects experiments in small-scale vented "shot-gun" magazines (loading density is the explosive mass divided by the total encompassed volume to the measurement point). Open symbols are for tests in this program using spherical charges; solid symbols are for rectangular charges used in the US/ROK program

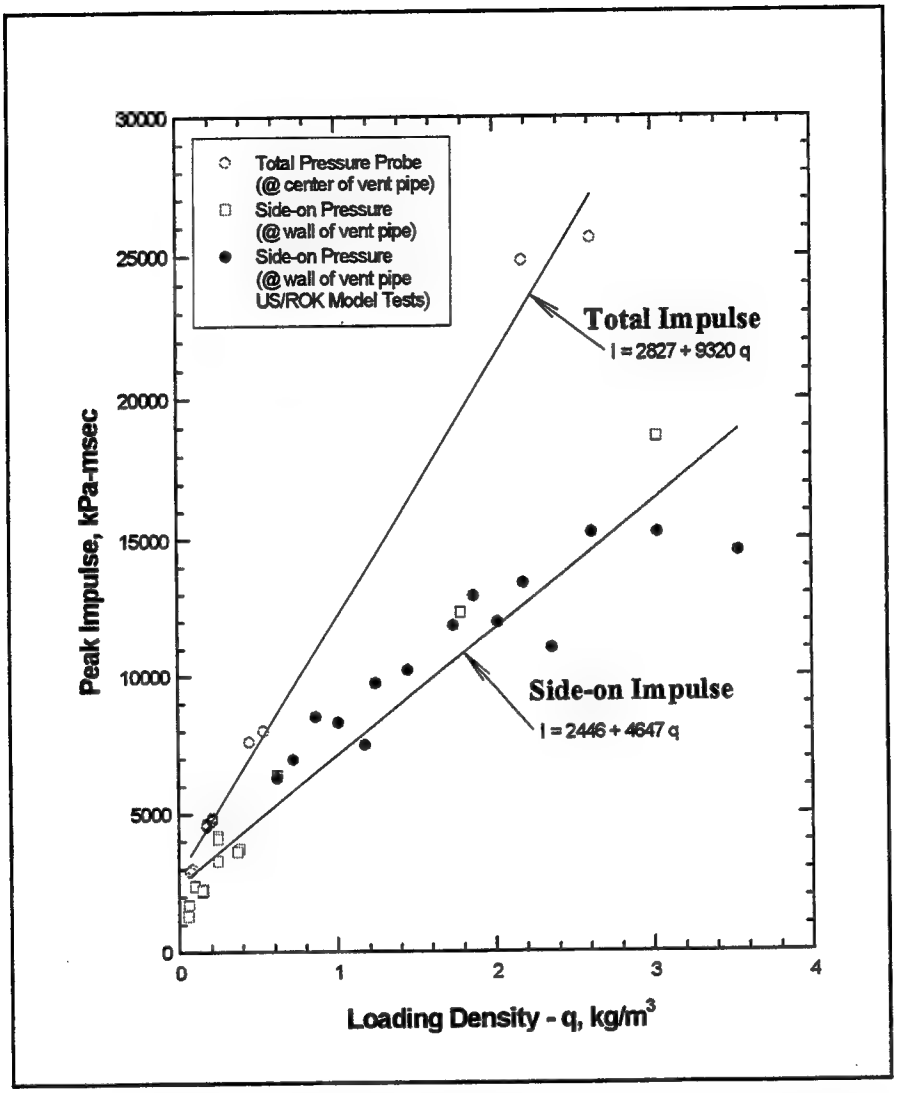

Figure 15. Peak airblast impulse in vent pipe versus explosive loading density for small-scale "shot-gun" magazines. Open symbols are for tests in this program using spherical charges; solid symbols are for rectangular charges used in the US/ROK program

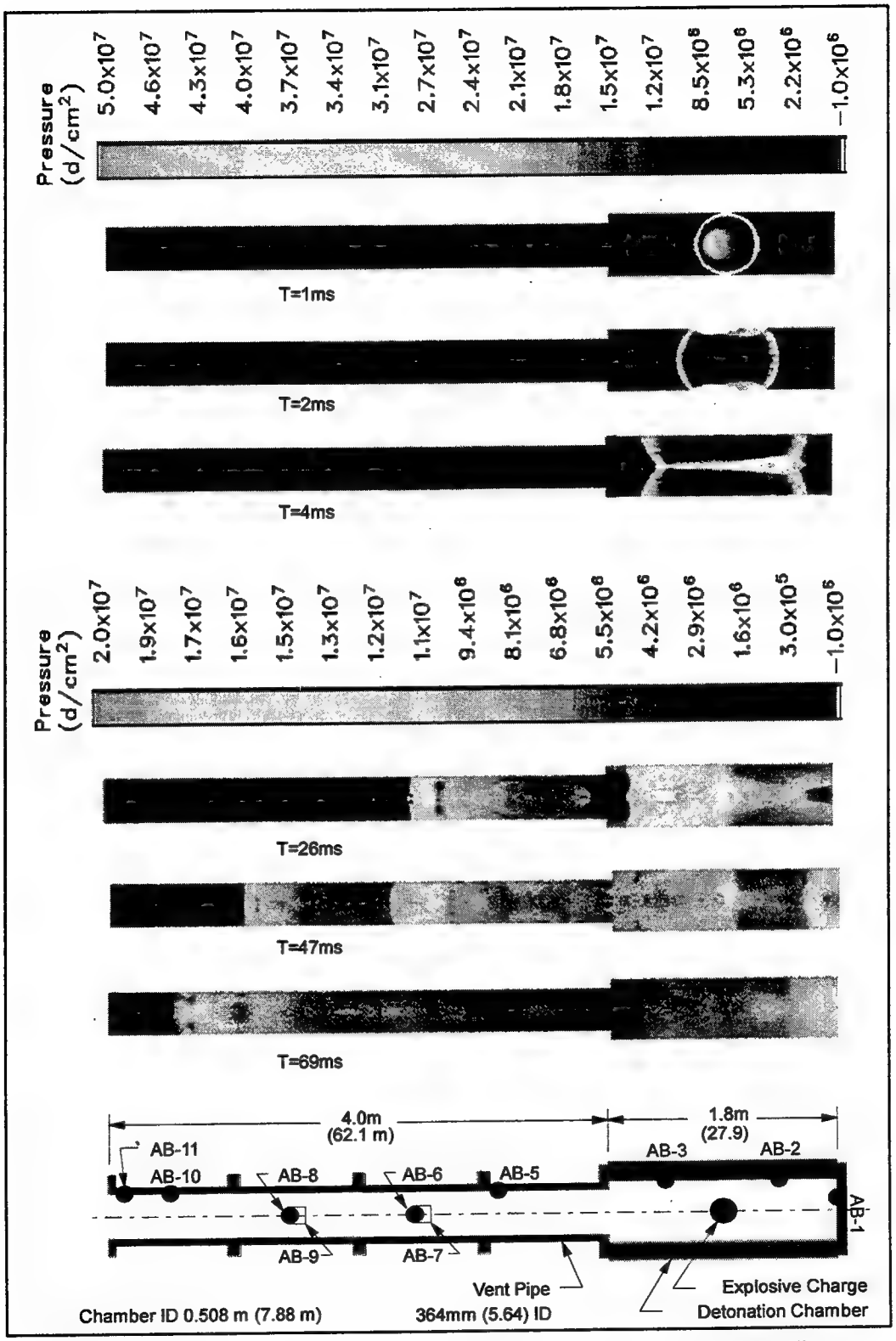

Figure 16. Pressure contour plots at 1, 2, 4, 26, 47 and 69 ms after detonation from CTH calculation of a detonation in a full-scale magazine

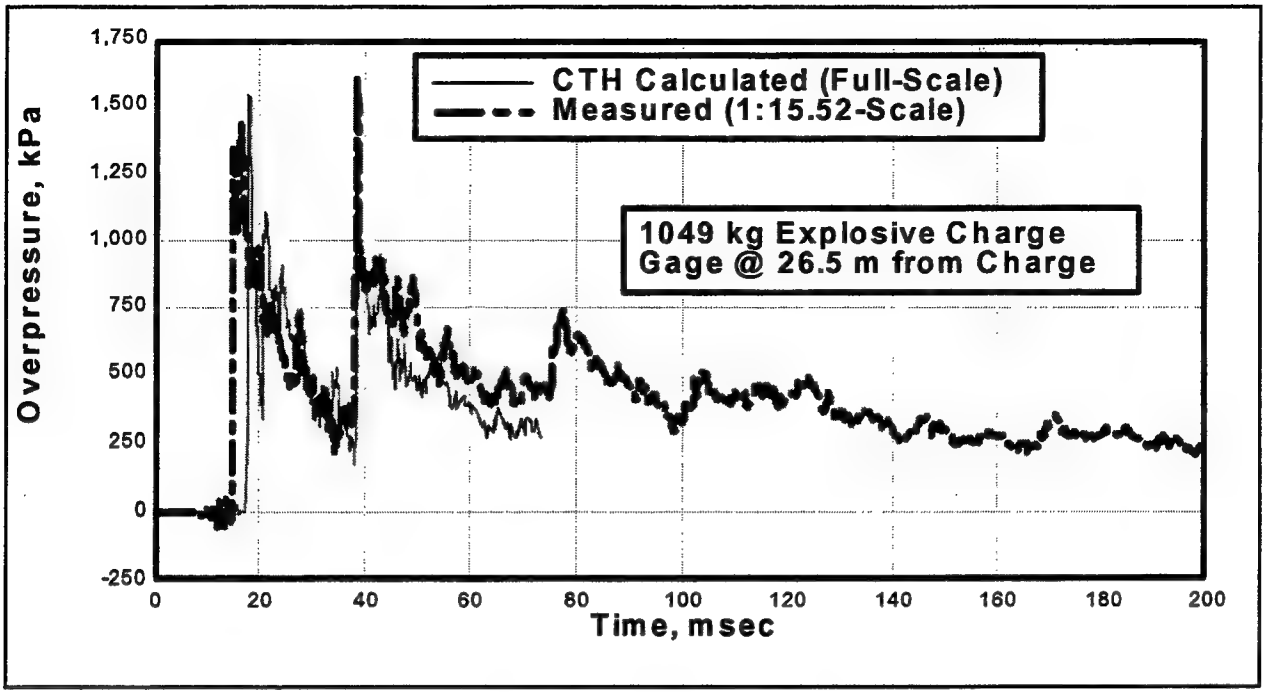

Figure 17. Comparison of measured (1:15-scale) and calculated (CTH full-scale) overpressure waveforms on the side wall of the exit tunnel at 26.5 m (full-scale distance) from the center of the explosive charge. The explosive charge was 0.28 kg for the model experiment that scaled to 1049 kg in the full-scale calculation

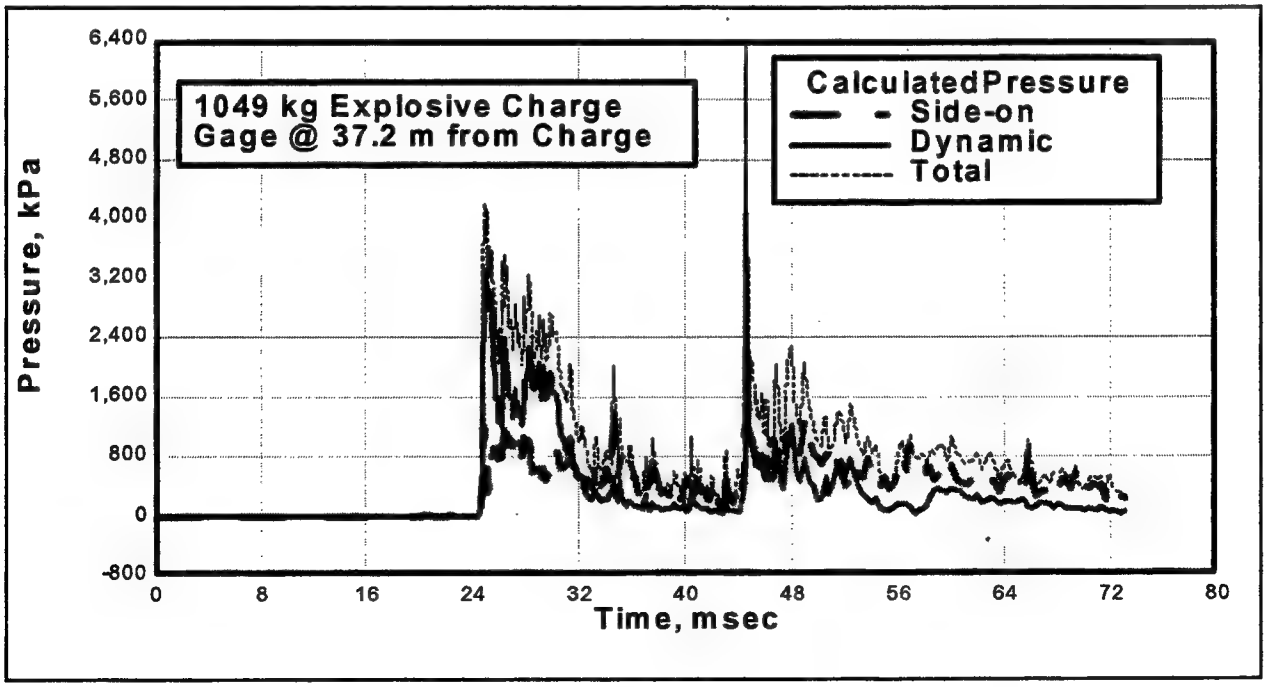

Figure 18. Calculated (CTH) pressure waveforms on the center line of the exit tunnel at 37.2 m from the center of the explosive charge. The calculated overpressure waveform (CTH) is compared with dynamic pressure (from CTH-calculated air density and shock velocity) and total pressure (sum of side-on and dynamic pressure waveforms)

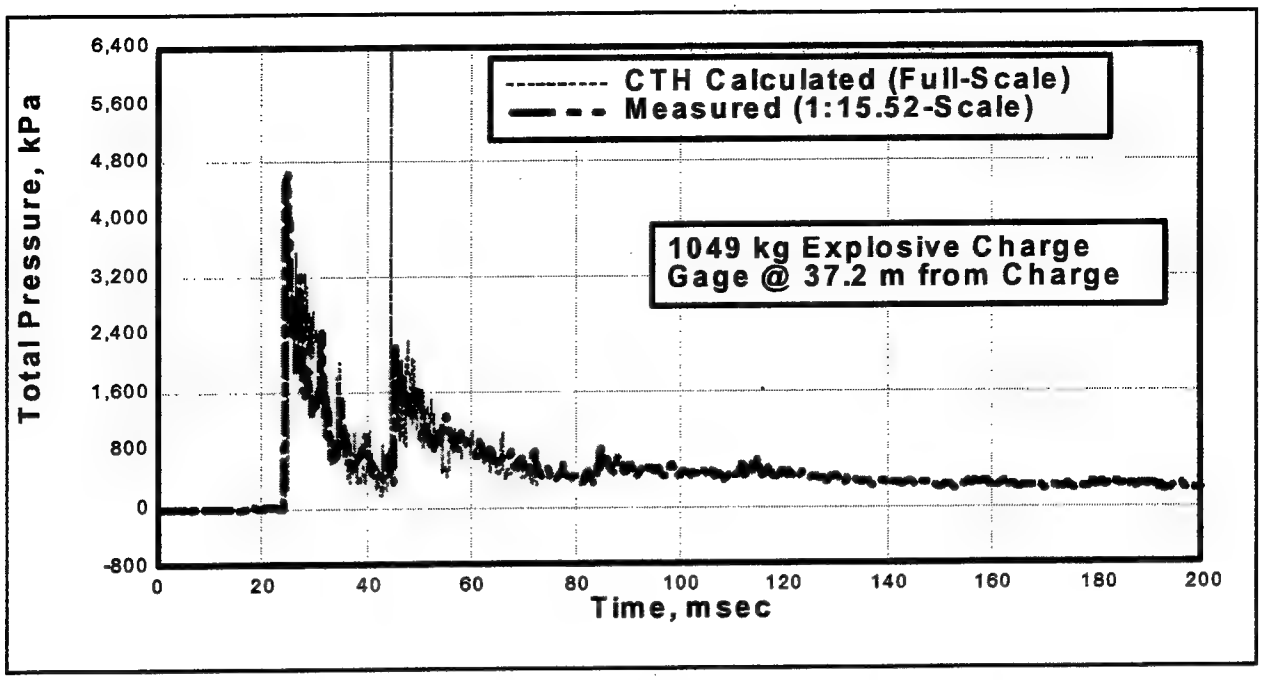

Figure 19. Comparison of measured (1:15-scale) and calculated (CTH derived full-scale) total pressure waveforms on the center line of the exit tunnel at 37.2 m from the center of the explosive charge. The explosive charge was 0.28 kg for the model experiment that scaled to 1049 kg in the full-scale calculation

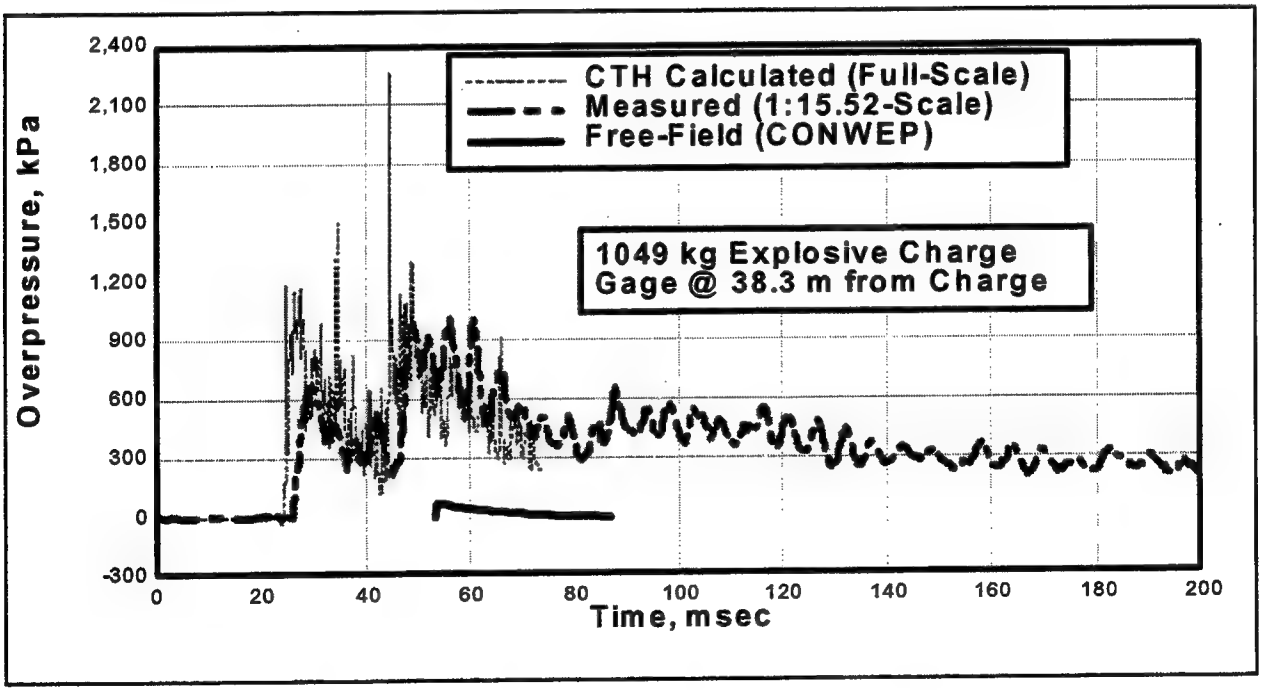

Figure 20. Comparison of measured (1:15-scale) and calculated (CTH and CONWEP) full-scale overpressure waveforms on the center line of the exit tunnel at 38.3 m from the center of the explosive charge. The measured waveform was recorded from a gage located behind a baffle on the side of the total pressure probe

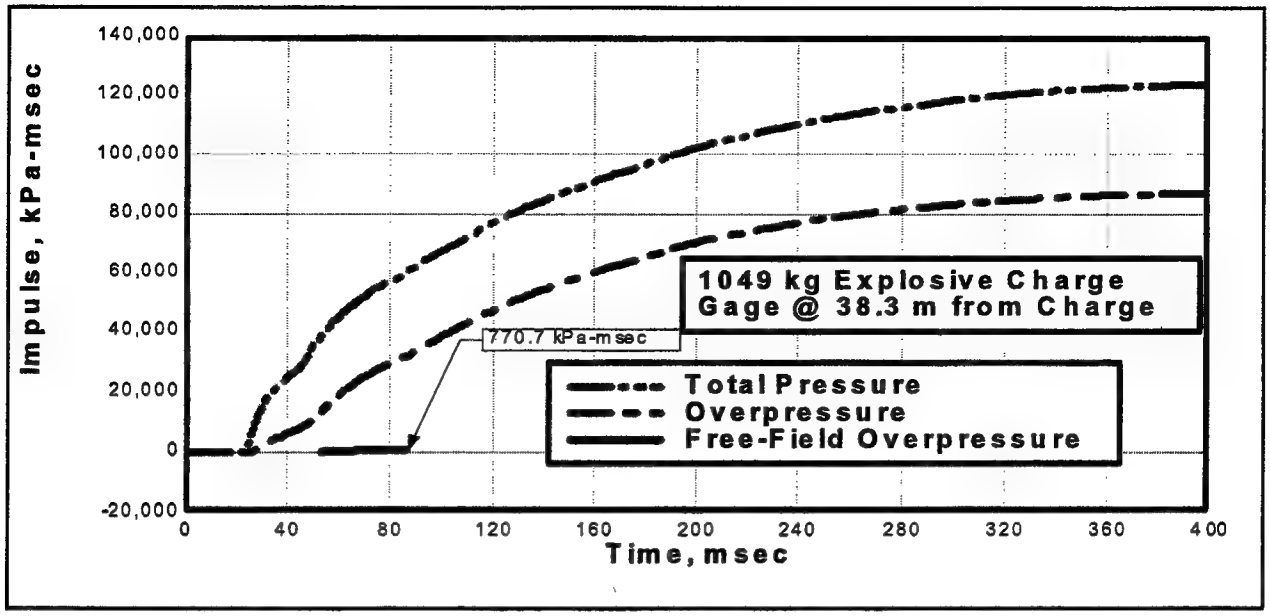

Figure 21. Airblast impulse waveforms obtained by integrating the total and side-on pressure waveforms presented in Figure 16

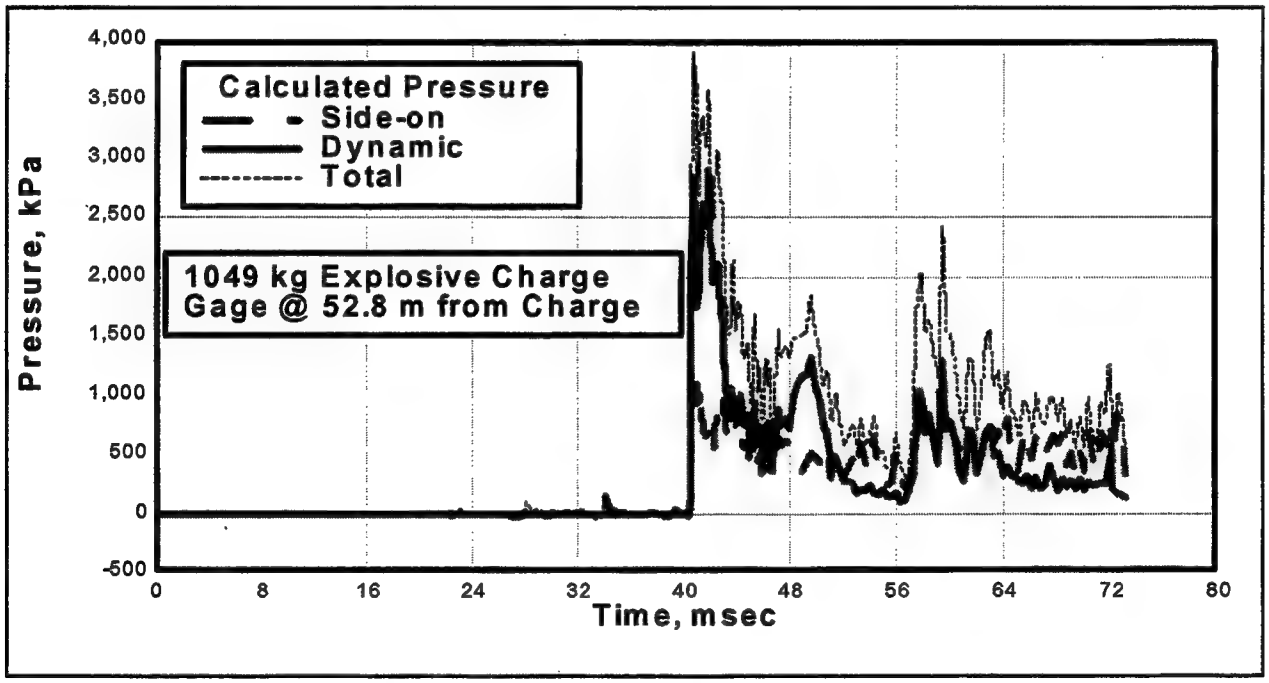

Figure 22. Calculated (CTH) pressure waveforms on the center line of the exit tunnel at 52.8 m from the center of the explosive charge. The calculated overpressure waveform (CTH) is compared with dynamic pressure (from CTH-calculated air density and shock velocity) and total pressure (sum of side-on and dynamic pressure waveforms)

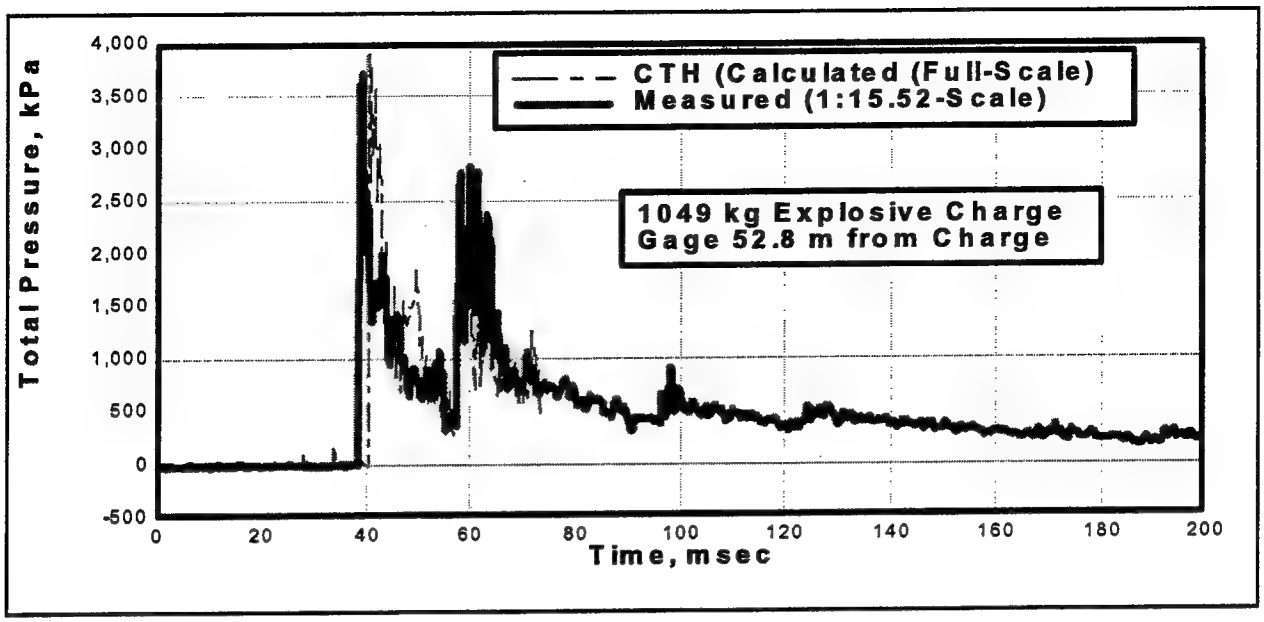

Figure 23. Comparison of measured (1:15-scale) and calculated (CTH derived full-scale) total pressure waveforms on the center line of the exit tunnel at 52.8 m from the center of the explosive charge. The explosive charge was 0.28 kg for the model experiment that scaled to 1049 kg in the full-scale calculation

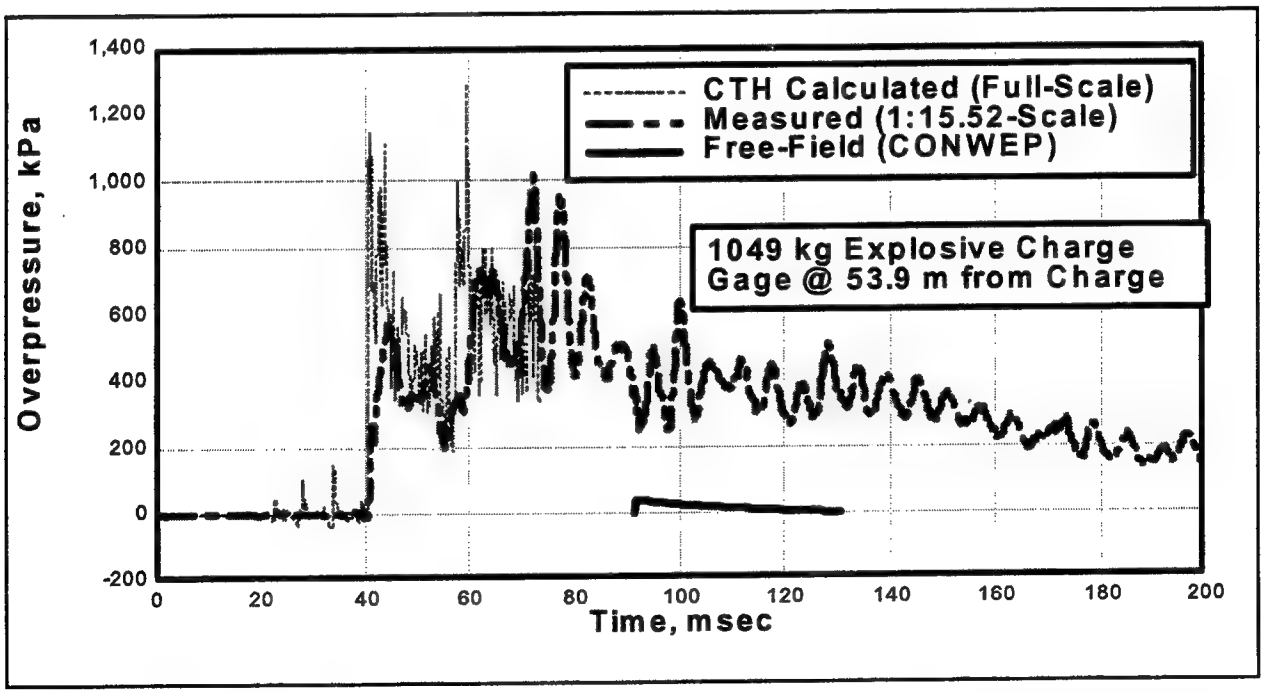

Figure 24. Comparison of measured (1:15-scale) and calculated (CTH and CONWEP) full-scale overpressure waveforms on the center line of the exit tunnel at 53.9 m from the center of the explosive charge. The measured waveform was recorded from a gage located behind a baffle on the side of the total pressure probe

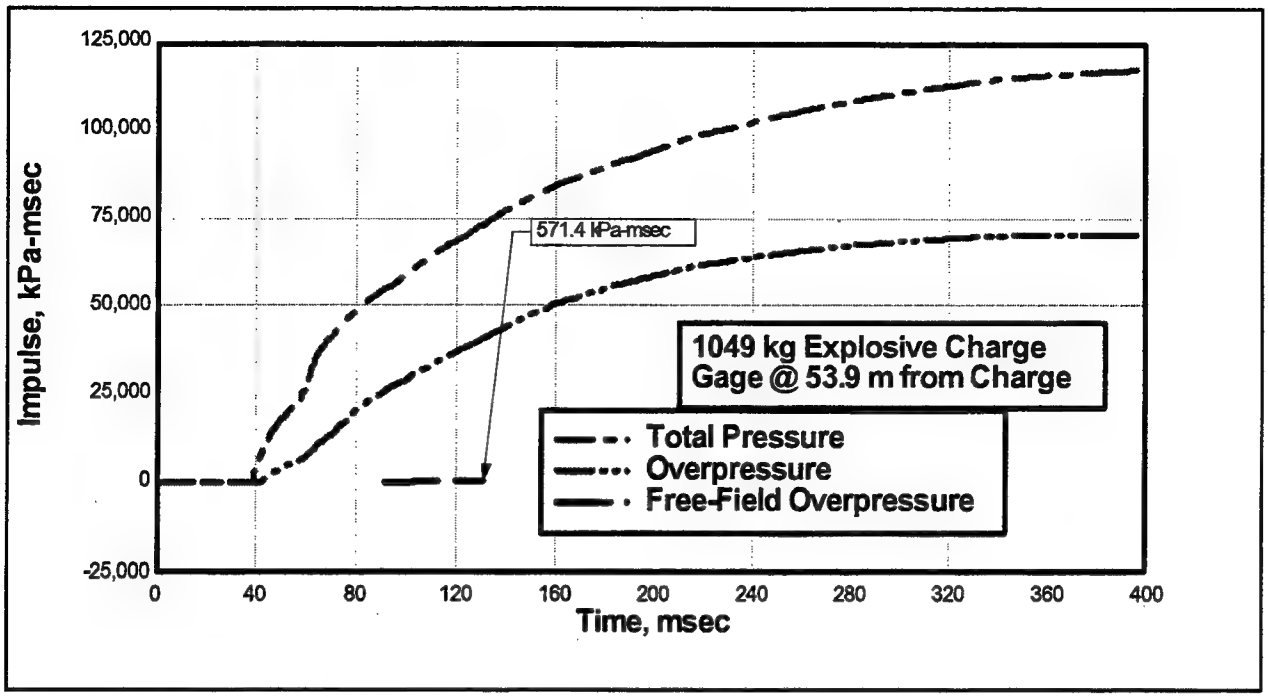

Figure 25. Airblast impulse waveforms obtained by integrating the total and side-on pressure waveforms presented in Figure 21

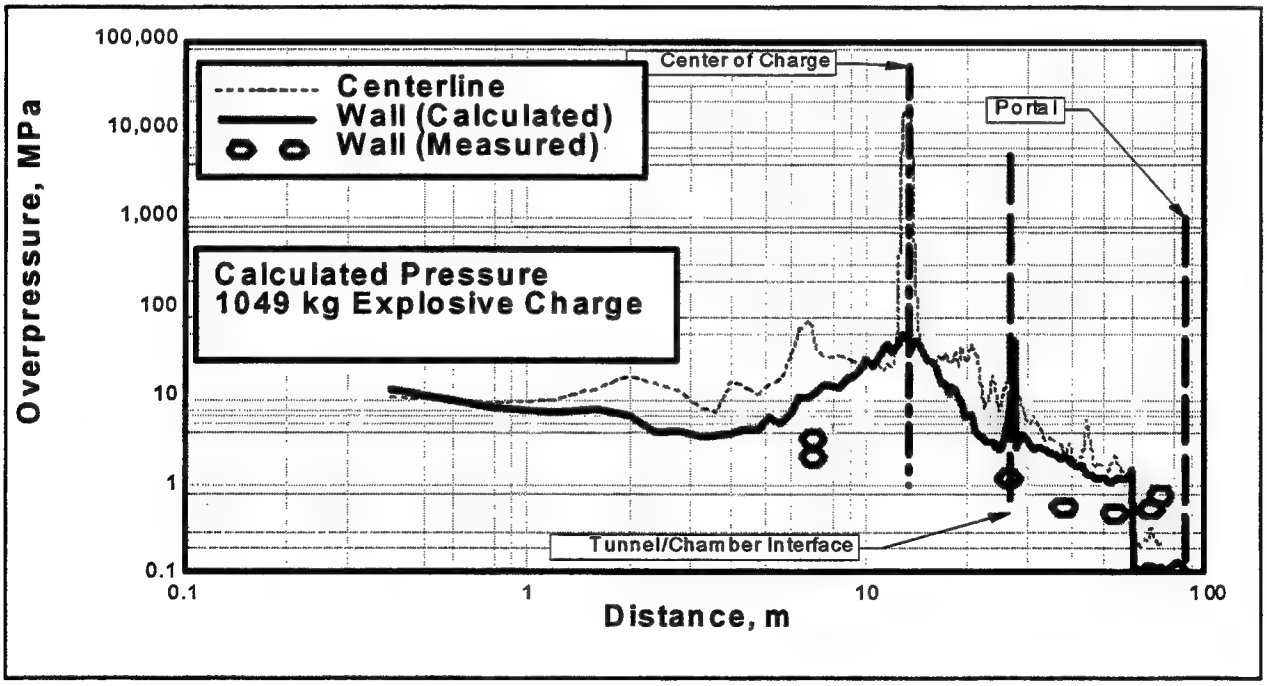

Figure 26. Comparison of peak overpressures along the surface of the wall(1:15- and full-scale) and center line (full-scale) of the chamber/tunnel, from airblast effects experiments in small-scale vented "shot-gun" magazines

Table 3
Small-Scale Chamber/Tunnel Airblast Experiments: Experiment 1, 0.11-kg Spherical C-4 Charge

Gage No.	Measurement Type	Gage Location		Measured Values			Remarks
		Distance From Rear Wall of Chamber (m)	Distance from Tunnel/Chamber Axis (m)	Arrival Time (msec)	Peak Pressure (MPa)	Impulse (kPa-msec)	
AB-1	Chamber	0.00	0.107	0.61	0.838	4191	Back Wall of Chamber
AB-2	Chamber	0.45	0.254	0.23	1.512	5585	Side Wall of Chamber
AB-3	Chamber	1.35	0.254	0.19	2.210	4829	Side Wall of Chamber
AB-5	Side-on	2.61	0.182	1.18	0.887	3318	Side Wall of Vent Pipe
AB-6	Side-on	3.37	0.019	2.11	0.697	3670	Side Wall of Probe
AB-7	Total	3.30	0.000	1.97	2.981	4837	Front End of Probe
AB-8	Side-on	4.37	0.019	3.24	0.510	2988	Side Wall of Probe
AB-9	Total	4.30	0.000	3.09	2.139	4632	Front End of Probe
AB-10	Side-on	5.30	0.182	4.06	0.761	2293	Side Wall of Vent Pipe
AB-11	Side-on	5.61	0.182	4.47	0.675	2248	Side Wall of Vent Pipe
AB-12	Side-on	7.60	0.182	8.87	0.0794	153.0	Ground Surface, Free-Field
AB-13	Side-on	8.80	0.182	11.44	0.0359	99.70	Ground Surface, Free-Field
AB-15	Side-on	10.60	0.182	16.44	0.0190	42.70	Ground Surface, Free-Field
AB-17	Side-on	13.80	0.182	25.13	0.00869	17.15	Ground Surface, Free-Field

Table 4
Small-Scale Chamber/Tunnel Airblast Experiments: Experiment 2, 0.11-kg Spherical C-4 Charge

Gage No.	Measurement Type	Gage Location		Measured Values			Remarks
		Distance From Rear Wall of Chamber (m)	Distance from Tunnel/Chamber Axis (m)	Arrival Time (msec)	Peak Pressure (MPa)	Impulse (kPa-msec)	
AB-1	Chamber	0.00	0.107	0.58	1.51	4617	Back Wall of Chamber
AB-2	Chamber	0.45	0.254	0.22	2.08	5572	Side Wall of Chamber
AB-3	Chamber	1.35	0.254	0.17	3.38	4316	Side Wall of Chamber
AB-5	Side-on	2.61	0.182	1.25	1.21	4186	Side Wall of Vent Pipe
AB-6	Side-on	3.37	0.019	2.15	0.575	3533	Side Wall of Probe
AB-7	Total	3.30	0.000	2.01	1.92	4778	Front End of Probe
AB-8	Side-on	4.37	0.019	3.33	0.492	2840	Side Wall of Probe
AB-9	Total	4.30	0.000	3.18	1.48	4580	Front End of Probe
AB-10	Side-on	5.30	0.182	4.06	0.544	2210	Side Wall of Vent Pipe
AB-11	Side-on	5.61	0.182	4.47	0.772	2225	Side Wall of Vent Pipe
AB-12	Side-on	7.60	0.182	8.77	0.0814	156.4	Ground Surface, Free-Field
AB-13	Side-on	8.80	0.182	11.78	0.0375	89.91	Ground Surface, Free-Field
AB-15	Side-on	10.60	0.182	16.24	0.0188	41.73	Ground Surface, Free-Field
AB-17	Side-on	13.80	0.182	25.05	0.00913	17.17	Ground Surface, Free-Field

Table 5
Small-Scale Chamber/Tunnel Airblast Experiments: Experiment 3, 0.11-kg Spherical C-4 Charge

Gage No.	Measurement Type	Gage Location		Measured Values			Remarks
		Distance From Rear Wall of Chamber (m)	Distance from Tunnel/Chamber Axis (m)	Arrival Time (msec)	Peak Pressure (MPa)	Impulse (kPa-msec)	
AB-1	Chamber	0.00	0.107	0.6	1.61	4628	Back Wall of Chamber
AB-2	Chamber	0.45	0.254	0.22	1.74	5482	Side Wall of Chamber
AB-3	Chamber	1.35	0.254	0.18	4.86	4280	Side Wall of Chamber
AB-5	Side-on	2.61	0.182	1.21	1.18	4095	Side Wall of Vent Pipe
AB-6	Side-on	3.37	0.019	2.08	0.647	3511	Side Wall of Probe
AB-7	Total	3.30	0.000	1.94	2.20	4732	Front End of Probe
AB-8	Side-on	4.37	0.019	3.22	0.432	2790	Side Wall of Probe
AB-9	Total	4.30	0.000	3.08	1.85	4547	Front End of Probe
AB-10	Side-on	5.30	0.182	3.93	0.588	2204	Side Wall of Vent Pipe
AB-11	Side-on	5.61	0.182	4.33	0.736	2233	Side Wall of Vent Pipe
AB-12	Side-on	7.60	0.182	8.58	0.167	166.6	Ground Surface, Free-Field
AB-13	Side-on	8.80	0.182	11.56	0.0386	93.29	Ground Surface, Free-Field
AB-15	Side-on	10.60	0.182	15.98	0.0193	48.46	Ground Surface, Free-Field
AB-17	Side-on	13.80	0.182	24.75	0.00965	16.68	Ground Surface, Free-Field

Table 6
Small-Scale Chamber/Tunnel Airblast Experiments: Experiment 4, 0.28-kg Spherical C-4 Charge

Gage No.	Measurement Type	Gage Location		Measured Values			Remarks
		Distance From Rear Wall of Chamber (m)	Distance from Tunnel/Chamber Axis (m)	Arrival Time (msec)	Peak Pressure (MPa)	Impulse (kPa-msec)	
AB-1	Chamber	0.00	0.107	0.48	3.60	7124	Back Wall of Chamber
AB-2	Chamber	0.45	0.254	0.16	3.09	8328	Side Wall of Chamber
AB-3	Chamber	1.35	0.254	0.14	4.94	6149	Side Wall of Chamber
AB-5	Side-on	2.61	0.182	0.95	1.62	6361	Side Wall of Vent Pipe
AB-6	Side-on	3.37	0.019	1.68	1.01	5601	Side Wall of Probe
AB-7	Total	3.30	0.000	1.56	4.64	7999	Front End of Probe
AB-8	Side-on	4.37	0.019	2.61	1.02	4542	Side Wall of Probe
AB-9	Total	4.30	0.000	2.48	3.72	7593	Front End of Probe
AB-10	Side-on	5.30	0.182	3.17	0.966	3737	Side Wall of Vent Pipe
AB-11	Side-on	5.61	0.182	3.49	1.11	3628	Side Wall of Vent Pipe
AB-12	Side-on	7.60	0.182	7.15	0.158	184.8	Ground Surface, Free-Field
AB-13	Side-on	8.80	0.182	9.88	0.0593	121.3	Ground Surface, Free-Field
AB-15	Side-on	10.60	0.182	14.13	0.0290	81.56	Ground Surface, Free-Field
AB-17	Side-on	13.80	0.182	22.77	0.0124	25.72	Ground Surface, Free-Field

Table 7
Small-Scale Chamber/Tunnel Airblast Experiments: Experiment 5, 1.36-kg Spherical C-4 Charge

Gage No.	Measurement Type	Gage Location		Measured Values			Remarks
		Distance From Rear Wall of Chamber (m)	Distance from Tunnel/Chamber Axis (m)	Arrival Time (msec)	Peak Pressure (MPa)	Impulse (kPa-msec)	
AB-1	Chamber	0.00	0.107	0.31	14.2	22207	Back Wall of Chamber
AB-2	Chamber	0.45	0.254	0.13	11.9	22986	Side Wall of Chamber
AB-3	Chamber	1.35	0.254	0.096	15.3	19518	Side Wall of Chamber
AB-5	Side-on	2.61	0.182	0.54	>4.41	18652	Side Wall of Vent Pipe
AB-6	Side-on	3.37	0.019	0.90	3.43	16451	Side Wall of Probe
AB-7	Total	3.30	0.000	0.83	>19.7	25635	Front End of Probe
AB-8	Side-on	4.37	0.019	1.35	3.01	14747	Side Wall of Probe
AB-9	Total	4.30	0.000	1.29	>16.0	24842	Front End of Probe
AB-10	Side-on	5.30	0.182	1.63	-----	-----	Side Wall of Vent Pipe
AB-11	Side-on	5.61	0.182	1.78	>1.98	12317	Side Wall of Vent Pipe
AB-12	Side-on	7.60	0.182	3.66	>0.301	320.5	Ground Surface, Free-Field
AB-13	Side-on	8.80	0.182	5.69	0.156	217.3	Ground Surface, Free-Field
AB-15	Side-on	10.60	0.182	9.18	0.0869	198.1	Ground Surface, Free-Field
AB-17	Side-on	13.80	0.182	17.00	0.0317	105.8	Ground Surface, Free-Field

Table 8
Small-Scale Chamber/Tunnel Airblast Experiments: Experiment 6, 0.045-kg Spherical C-4 Charge

Gage No.	Measurement Type	Gage Location		Measured Values			Remarks
		Distance From Rear Wall of Chamber (m)	Distance from Tunnel/Chamber Axis (m)	Arrival Time (msec)	Peak Pressure (MPa)	Impulse (kPa-msec)	
AB-1	Chamber	0.00	0.107	0.81	0.938	2762	Back Wall of Chamber
AB-2	Chamber	0.45	0.254	0.31	0.780	3241	Side Wall of Chamber
AB-3	Chamber	1.35	0.254	0.24	1.86	2506	Side Wall of Chamber
AB-5	Side-on	2.61	0.182	1.60	0.521	2396	Side Wall of Vent Pipe
AB-6	Side-on	3.37	0.019	2.74	0.354	2084	Side Wall of Probe
AB-7	Total	3.30	0.000	2.57	0.908	3003	Front End of Probe
AB-8	Side-on	4.37	0.019	4.22	0.353	1730	Side Wall of Probe
AB-9	Total	4.30	0.000	4.05	0.818	2910	Front End of Probe
AB-10	Side-on	5.30	0.182	5.12	0.286	1712	Side Wall of Vent Pipe
AB-11	Side-on	5.61	0.182	5.62	0.446	1311	Side Wall of Vent Pipe
AB-12	Side-on	7.60	0.182	10.56	0.0476	94.46	Ground Surface, Free-Field
AB-13	Side-on	8.80	0.182	13.94	0.0241	51.30	Ground Surface, Free-Field
AB-15	Side-on	10.60	0.182	18.54	0.0124	20.28	Ground Surface, Free-Field
AB-17	Side-on	13.80	0.182	27.48	0.00579	8.308	Ground Surface, Free-Field

5 Conclusions and Recommendations

Conclusions

Tunnel airblast effects from an explosion in a full-scale underground storage chamber were calculated with the CTH hydrocode, and the results were compared to measurements obtained from experiments in a 1:15-scale model of the same geometry. A total pressure waveform was computed using the CTH- calculated side-on pressure, air density, and particle velocity waveforms. Excellent agreements were shown when the calculated results were compared to full-scale conversions of the model tests data.

Confinement in an underground facility dramatically increases the amplitudes of pressure and impulse waveforms compared to those generated by detonations in the free-field. Comparisons show that the internal pressure and impulse waveforms are orders of magnitude greater than the free-field pressures for equal yield and distance.

Analysis of the data indicates that a 1 kg/m^3 increase in loading density produces a corresponding 1.7 MPa (approximately) increase in overpressure and 7.2 MPa increase in total pressure. Similarly, a 1 kg/m^3 increase in loading density produces a corresponding 4.7 MPa-msec increase in side-on impulse and 9.3 MPa-msec increase in total impulse. Total impulse is on the order of 1.5 to 2.0 times the side-on impulse. These observations are site specific and limited to the magazine design used in these experiments and to the range of explosive mass and loading density of the experiments.

Recommendations

These experiments and corresponding calculations demonstrate that CTH is capable of calculating the internal airblast environment from an explosion in a simple tunnel/chamber system. The CTH analysis can provide insight and understanding of the airblast environment beyond that allowed by the limited data

from the small-scale testing. It is recommended that the CTH code be used to study increasingly more complex tunnel/chamber systems that are more representative of actual underground ammunition storage facilities. This code can also be utilized to investigate multiple detonations within the tunnel chamber systems. Additional small-scale experiments should be conducted to ensure that CTH is providing accurate results for these more complex tunnel/chamber arrangements.

References

Britt, J. R. and Lumsden, M. G. (1994). "Internal Blast and Thermal Environment from Internal and External Explosions: A User's guide for the BLASTX Code, Version 3.0." SAIC 405-94-2, Science Applications International Corporation, St. Joseph, LA.

Hertel, G. I., McGaun, J. M., Petney, S. V., Silling, S. A., Tayor, P. A., and Yarrington, L. (1993). "CTH: A Software Family for Multi-Dimensional Shock Physics Analysis," Proceedings of the 19th International Symposium on Shock Waves, Vol. 1.

Hyde, David W. (1988). "User's Guide for Microcomputer Programs CONWEP and FUNPRO, Applications of TM5-855-1, Fundamentals of Protective Design for Conventional Weapons," Instruction Report SL-88-1, U.S. Army Engineer Waterways Experiment Station, Vicksburg, MS.

Joachim, C. E.. (1994). "Parameter Study for Underground Ammunition Storage Magazines: Results of Explosion Tests in Small-Scale Models," Twenty-Sixth Explosives Safety Seminar, Miami, FL.

Kinney, Gilbert F., and Graham, Kenneth J. (1985). "Explosive Shocks in Air," Springer-Verlag, New York, NY.

McGaun, J. M., Thompson, S. L., and Elrick, M. G. (1990). "CTH: A Three Dimensional Shock Wave Physics Code," International Journal of Impact Engineering, Vol. 10, 351-360.

Appendix A
Airblast Effects Research Small-Scale Magazine Experiment 1

Pressure-Time Histories from the Detonation of 0.11 kg Spherical C-4 Charge

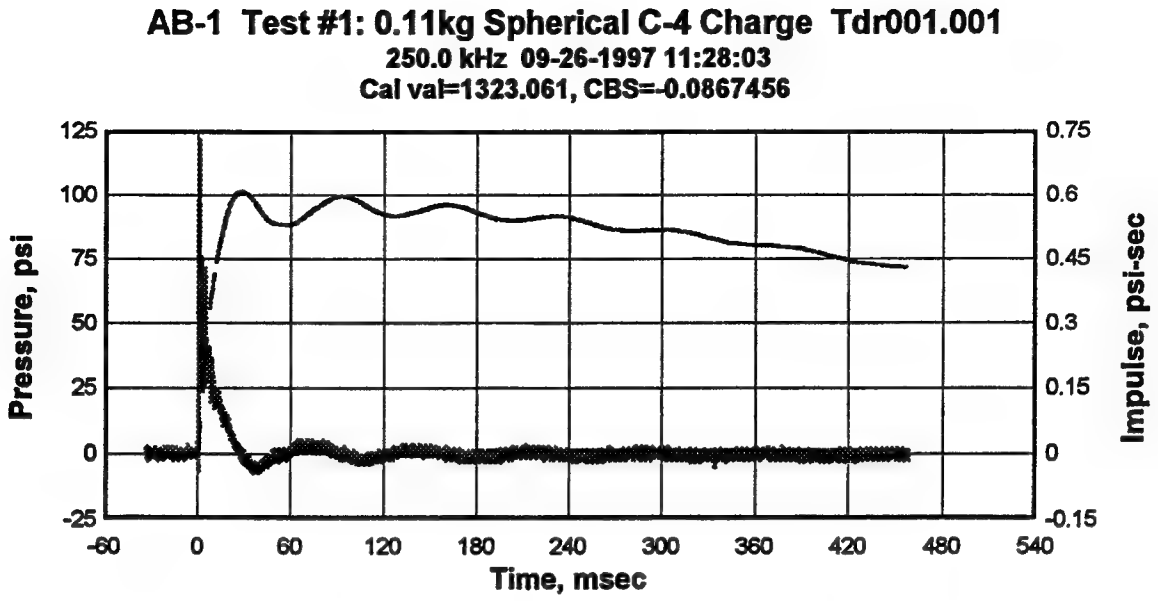

Figure A1. Pressure and impulse-time histories, Gage AB-1 on rear wall of the detonation chamber at a horizontal distance of 0.90 m from the center of the explosive charge, Experiment 1.

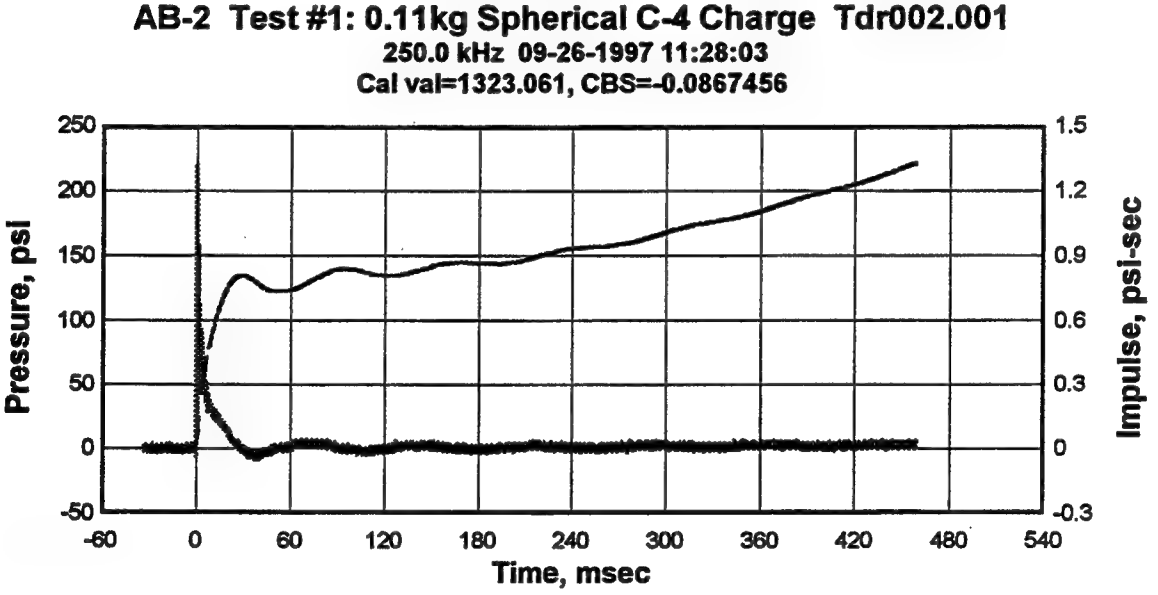

Figure A2. Pressure and impulse-time histories, Gage AB-2 on side wall of the detonation chamber at a horizontal distance of 0.45 m from the rear wall of the detonation chamber, Experiment 1.

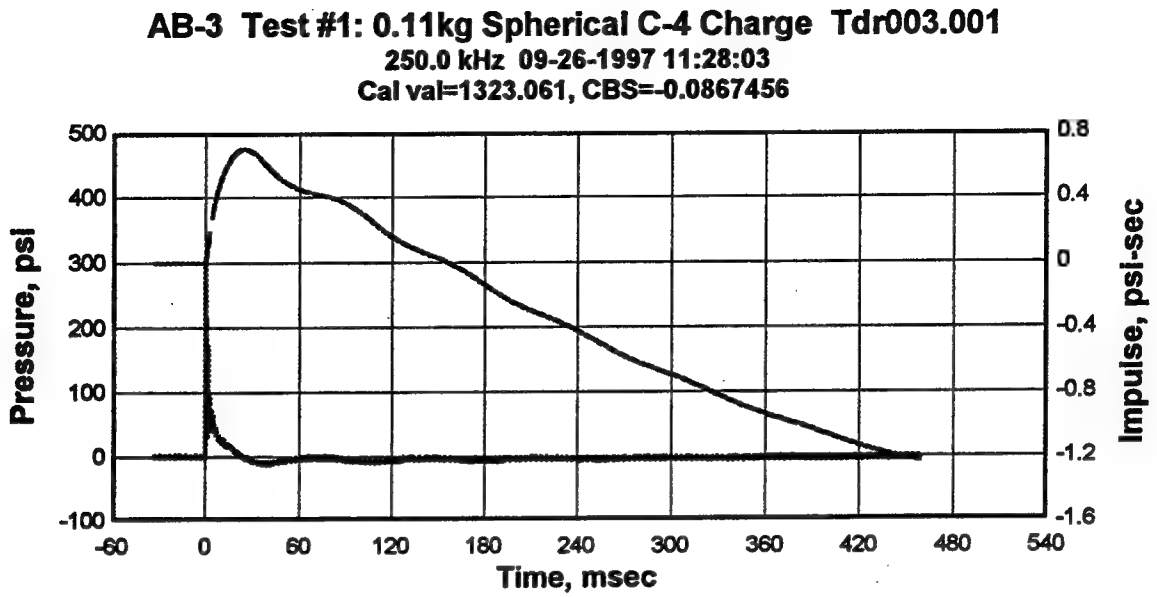

Figure A3. Pressure and impulse-time histories, Gage AB-3 on side wall of the detonation chamber at a horizontal distance of 1.35 m from the rear wall of the detonation chamber, Experiment 1.

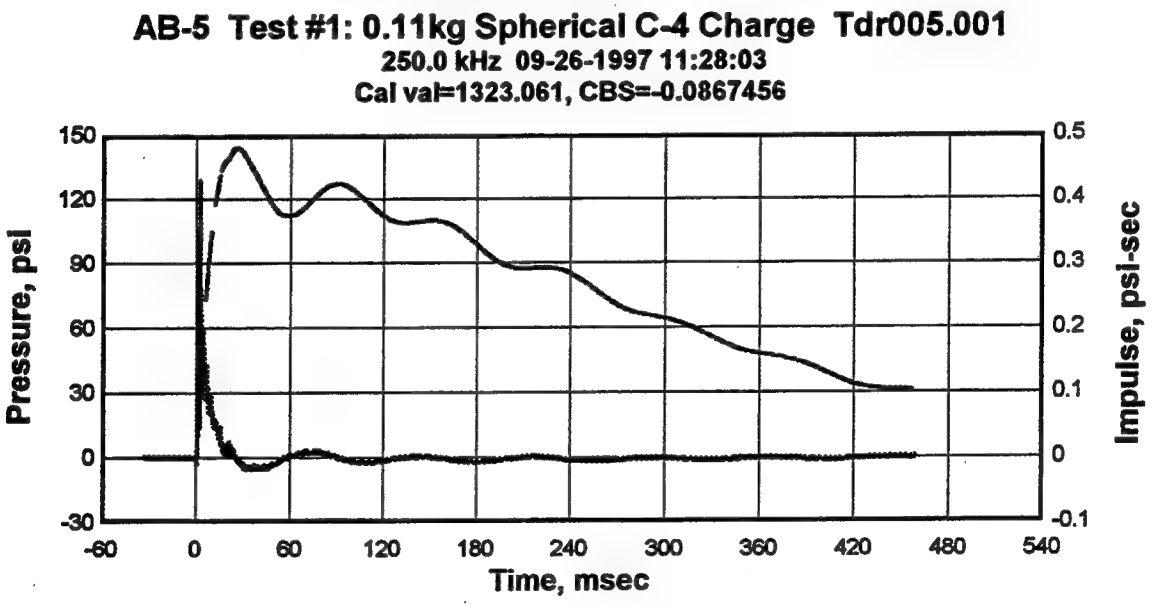

Figure A4. Pressure and impulse-time histories, Gage AB-5, on wall of the access tunnel at a horizontal distance of 2.61 m from rear wall of detonation chamber, Experiment 1.

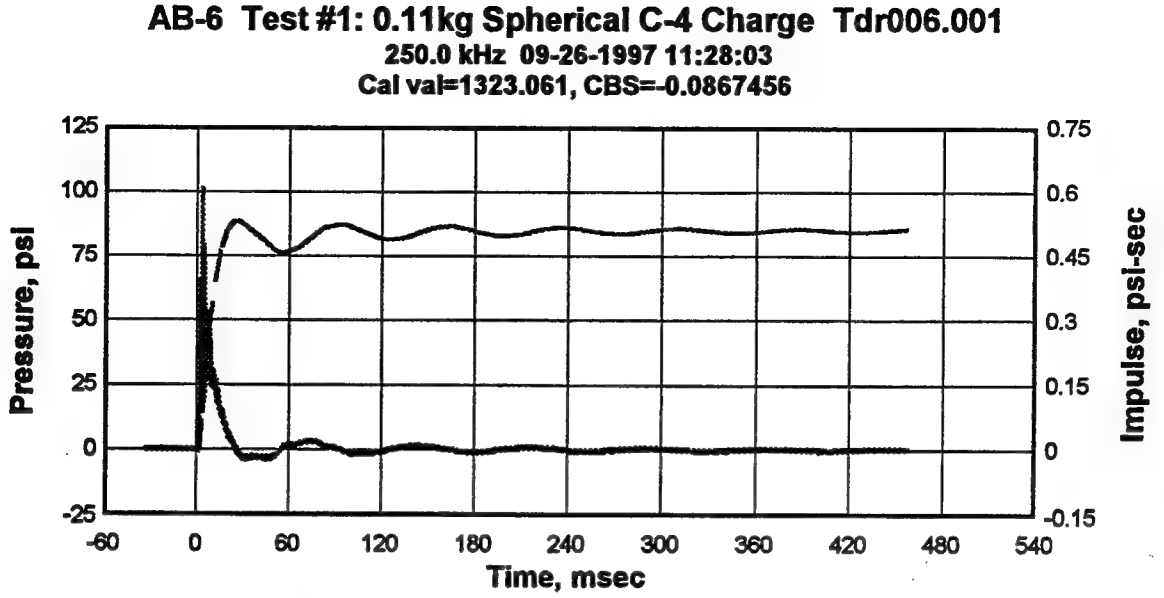

Figure A5. Pressure and impulse-time histories, Gage A-6 in baffled chamber on side of probe mount at a horizontal distance of 3.37 m from the rear wall of the detonation chamber, Experiment 1.

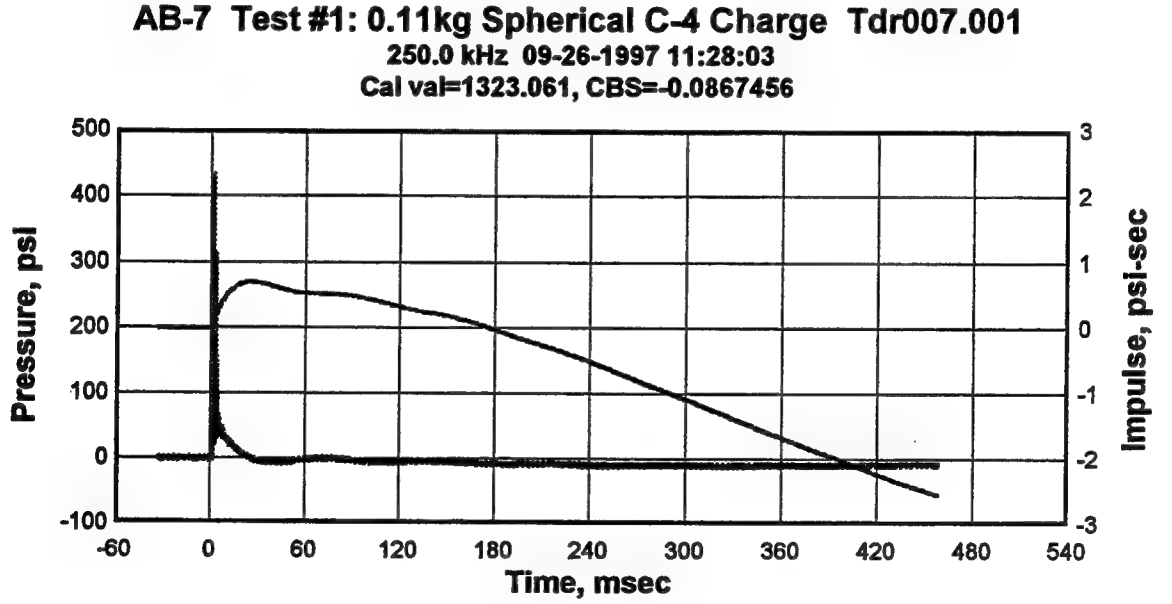

Figure A6. Total pressure and impulse-time histories, Gage AB-7 on probe mount at a horizontal distance of 3.30m from the rear wall of the detonation chamber, Experiment 1.

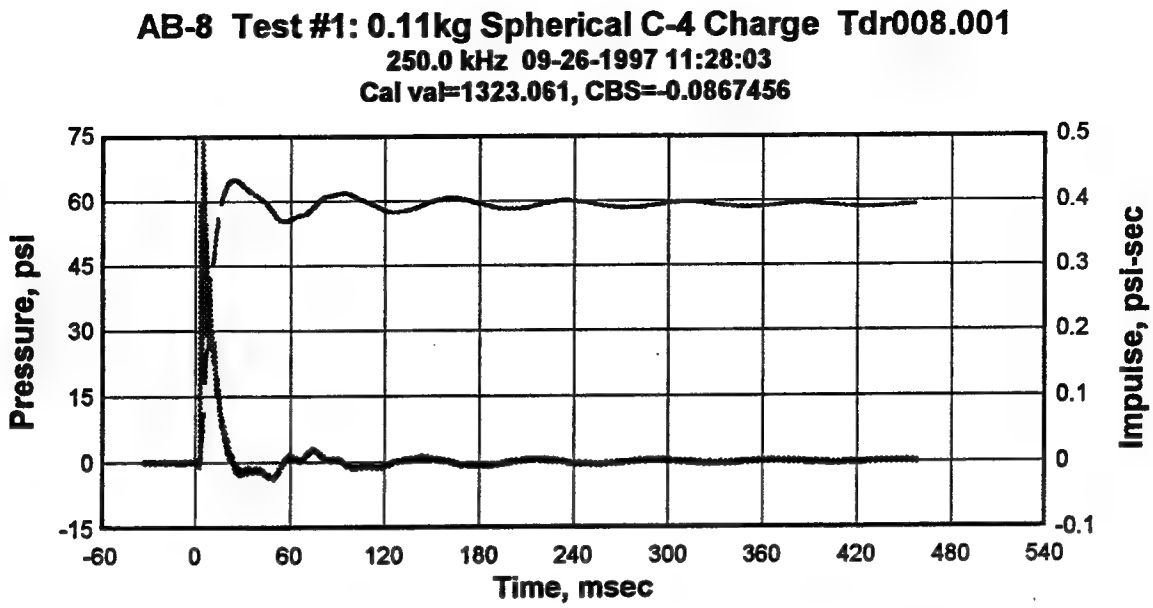

Figure A7. Pressure and impulse-time histories, Gage AB-8 in baffled chamber on the side of probe mount at a horizontal distance of 4.37 m from the rear wall of the detonation chamber,

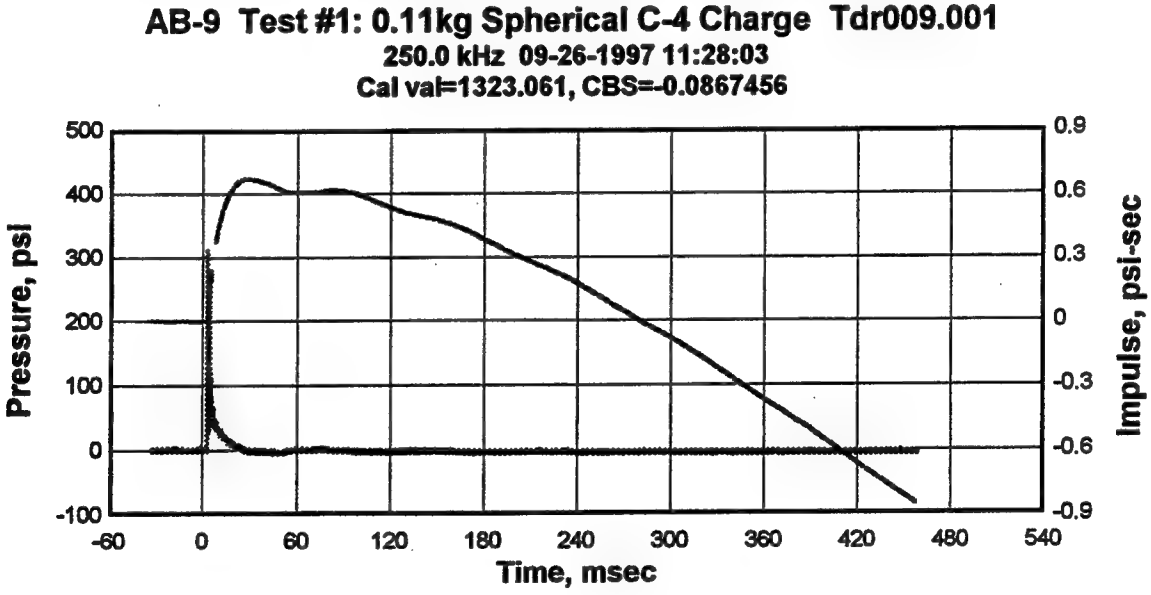

Figure A8. Total pressure and impulse-time histories, Gage AB-9 on probe mount at a horizontal distance of 4.30 m from the rear wall of the detonation chamber, Experiment 1.

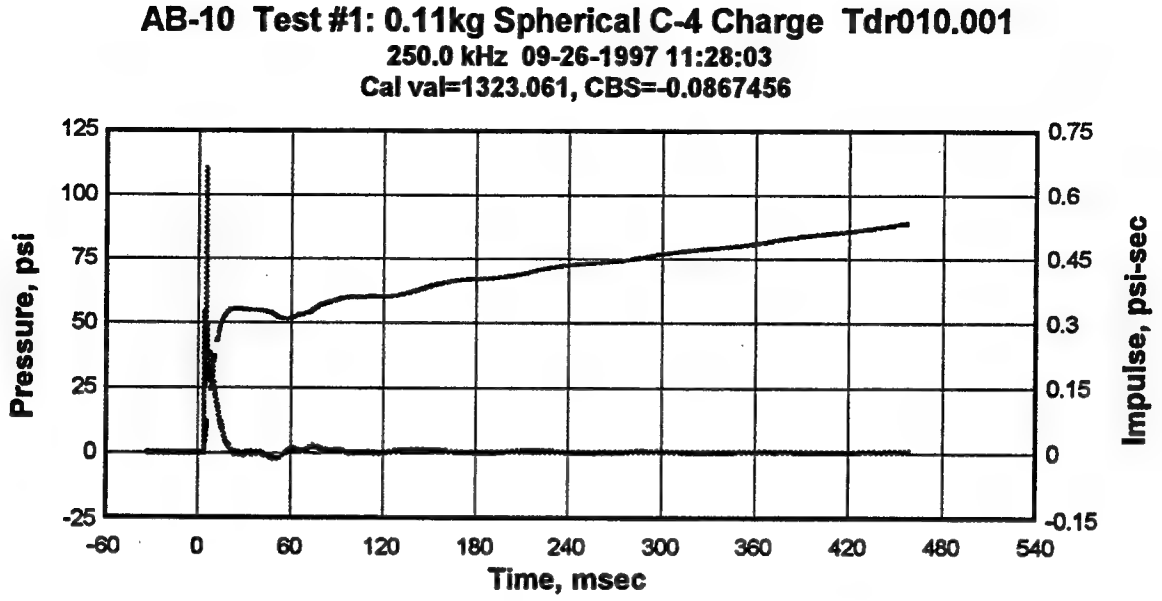

Figure A9. Pressure and impulse-time histories, Gage AB-10 on wall of access tunnel at a horizontal distance of 5.30 m from the rear wall of the detonation chamber, Experiment 1.

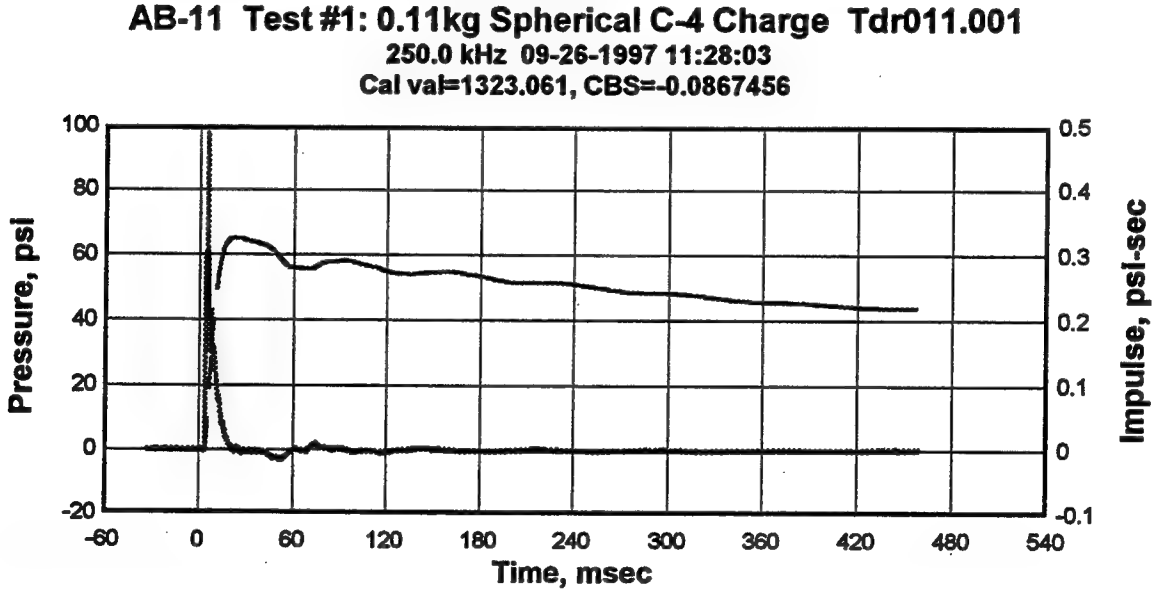

Figure A10. Pressure and impulse-time histories, Gage AB-11 on wall of the access tunnel at a horizontal distance of 5.61 m from the rear wall of the detonation chamber, Experiment 1.

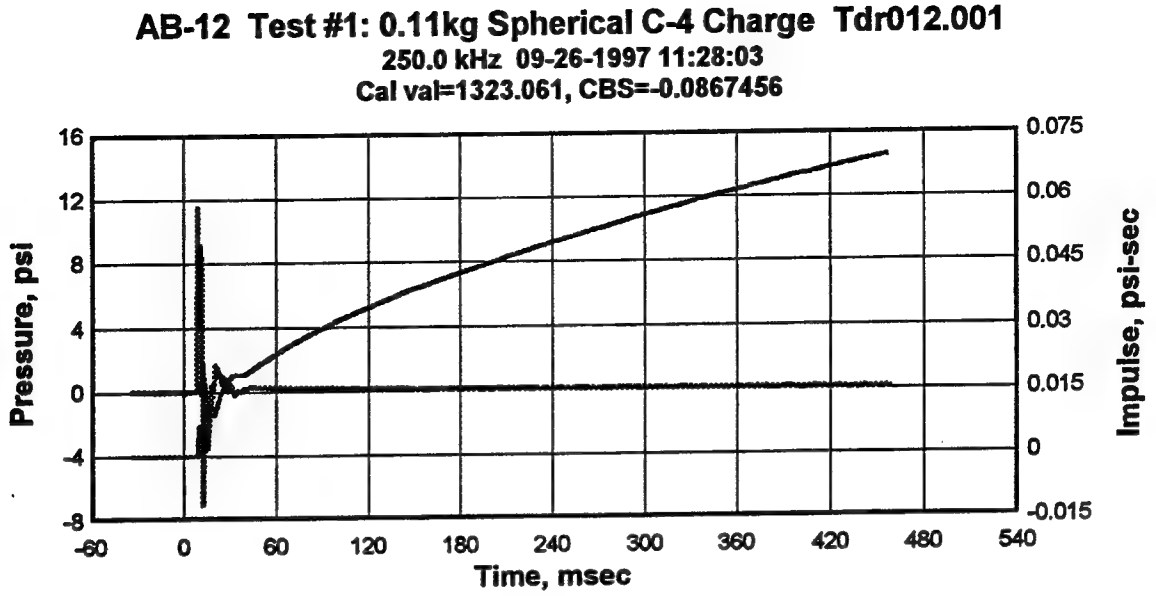

Figure A11. Pressure and impulse-time histories, free-field Gage AB-12 at the surface of the ground at a horizontal distance of 1.80 m from the portal, Experiment 1.

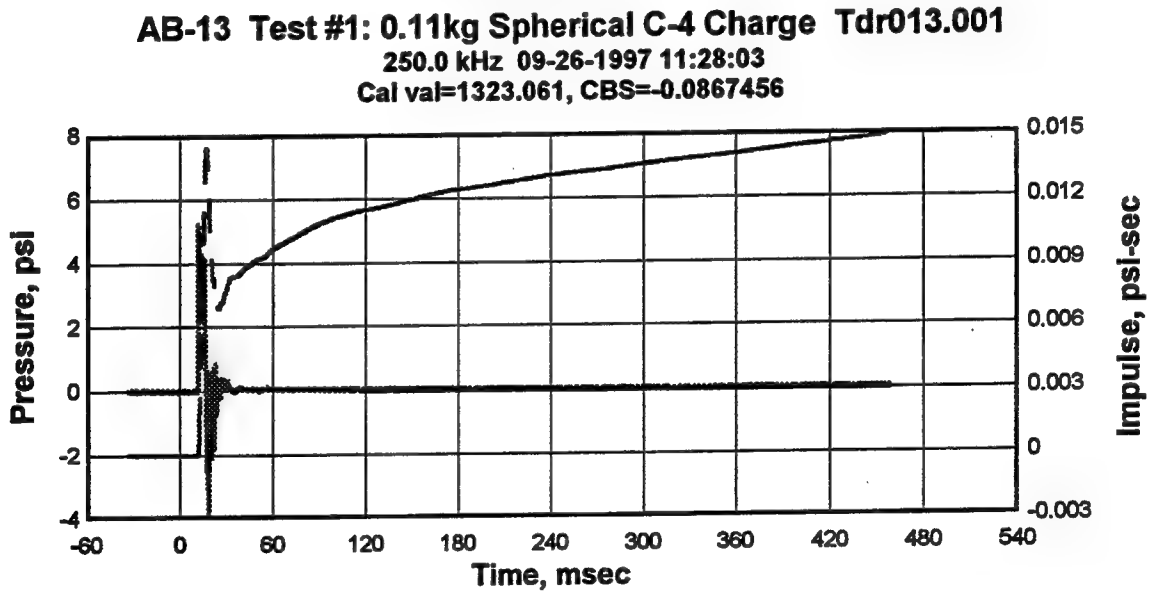

Figure A12. Pressure and impulse-time histories, free-field Gage AB-13 on the surface of the ground at a horizontal distance of 3.00 m from the portal, Experiment 1.

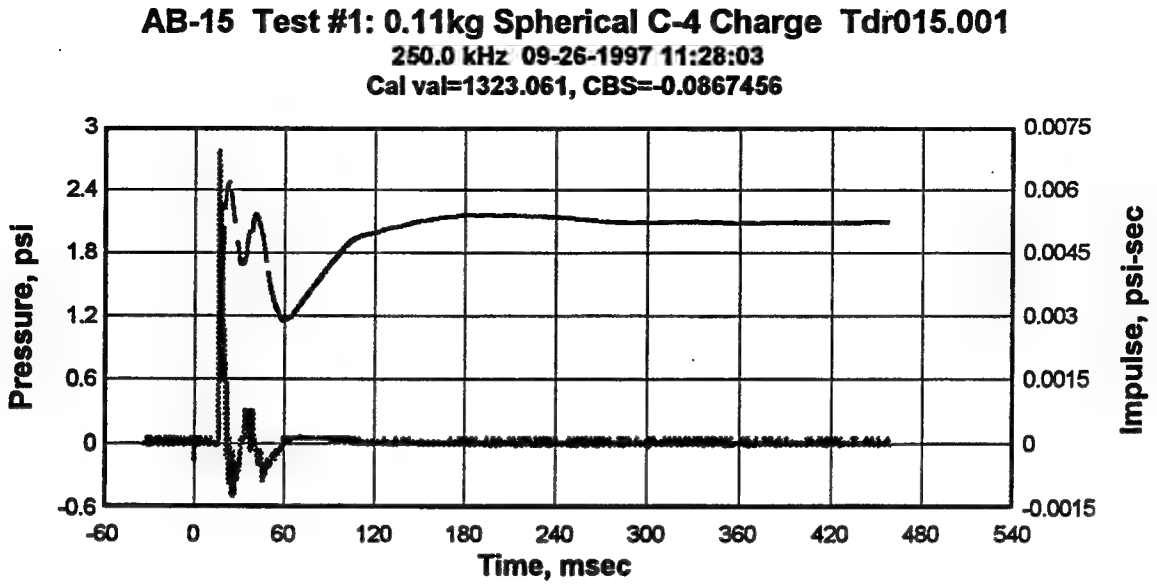

Figure A13. Pressure and impulse-time histories, free-field Gage AB-15 on the surface of the ground at a horizontal distance of 4.80 m from the portal, Experiment 1.

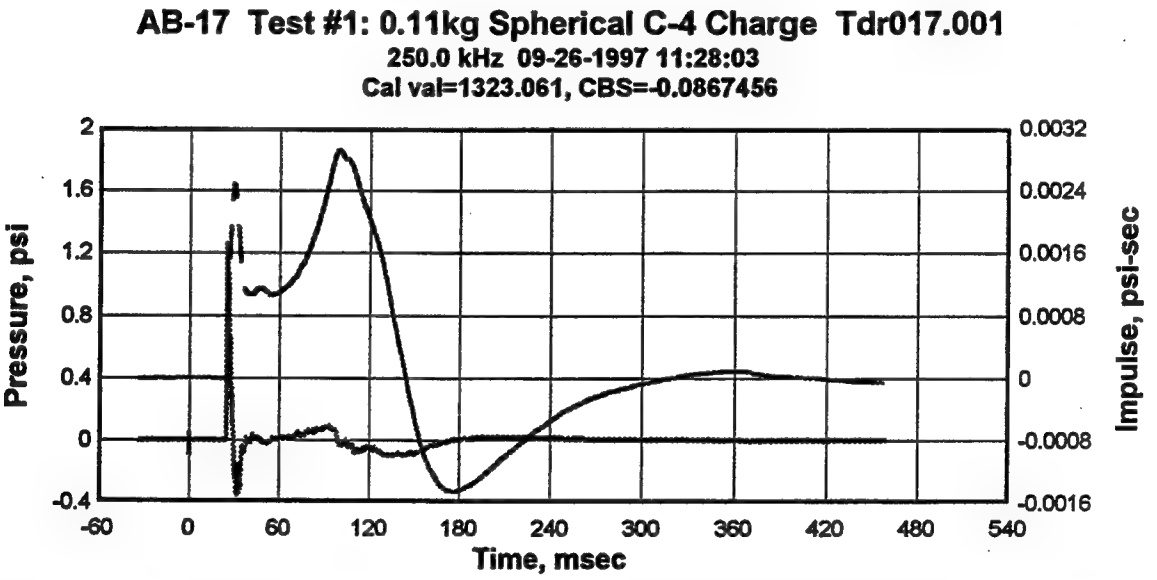

Figure A14. Pressure and impulse-time histories, field-field Gage AB-17 on the surface of the ground at a horizontal distance of 8.00 m from the portal, Experiment 1.

Appendix B
Airblast Effects Research Small-Scale Magazine Experiment 2

Pressure-Time Histories from the Detonation of 0.11 kg Spherical C-4 Charge

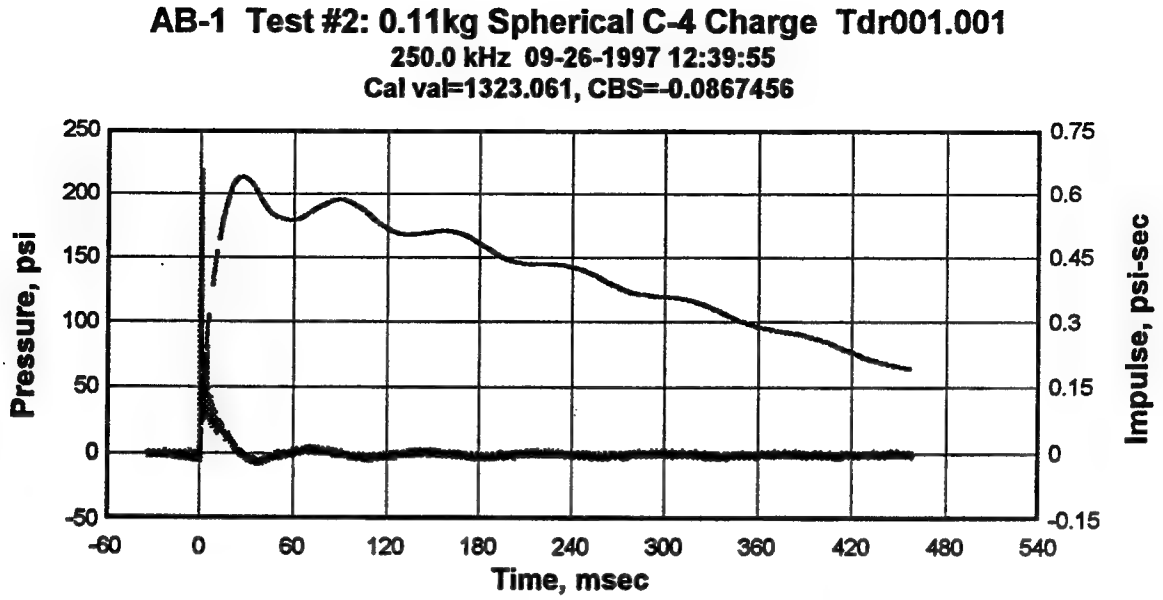

Figure B1. Pressure and impulse-time histories, Gage AB-1 on rear wall of the detonation chamber at a horizontal distance of 0.90 m from the center of the explosive charge, Experiment 2.

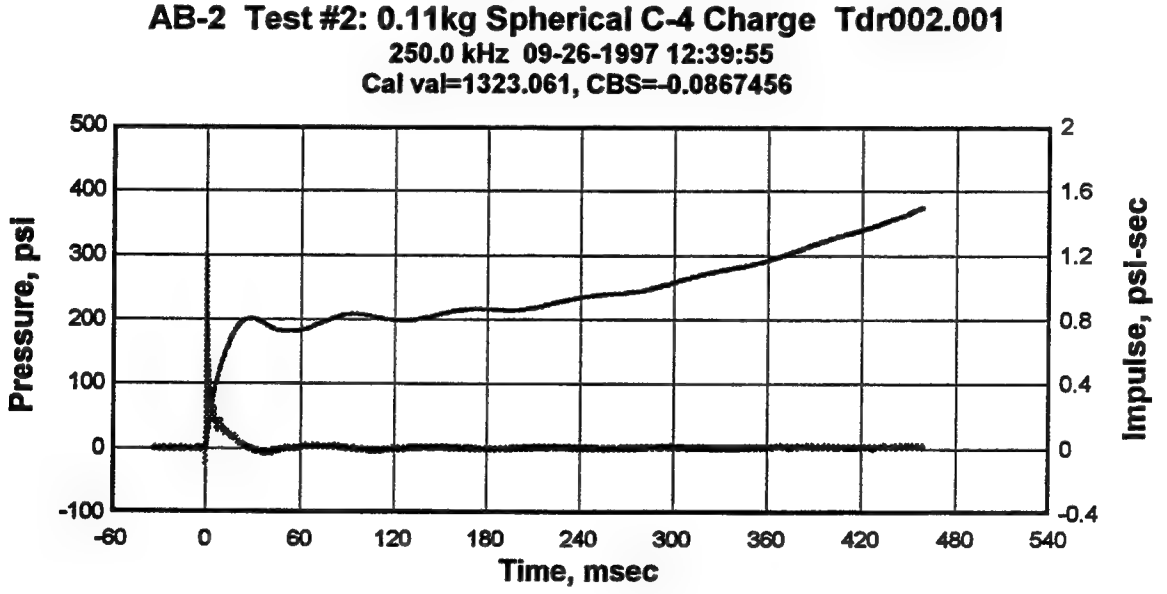

Figure B2. Pressure and impulse-time histories, Gage AB-2 on side wall of the detonation chamber at a horizontal distance of 0.45 m from the rear wall of the detonation chamber, Experiment 2.

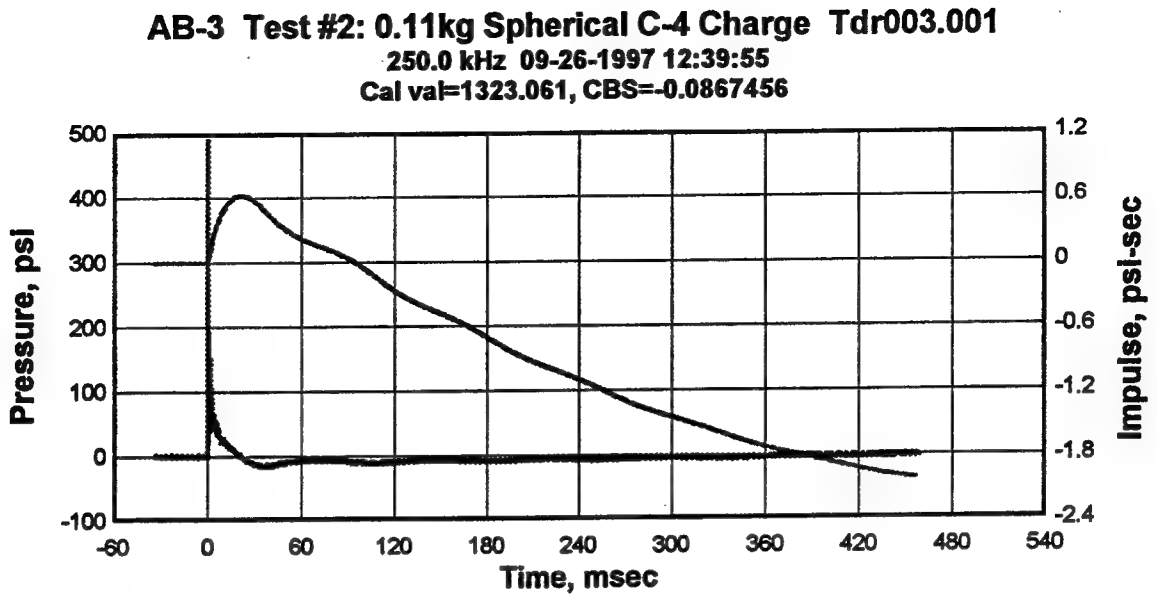

Figure B3. Pressure and impulse-time histories, Gage AB-3 on the side wall of the detonation chamber at a horizontal distance of 1.35 m from the rear wall of the detonation chamber, Experiment 2.

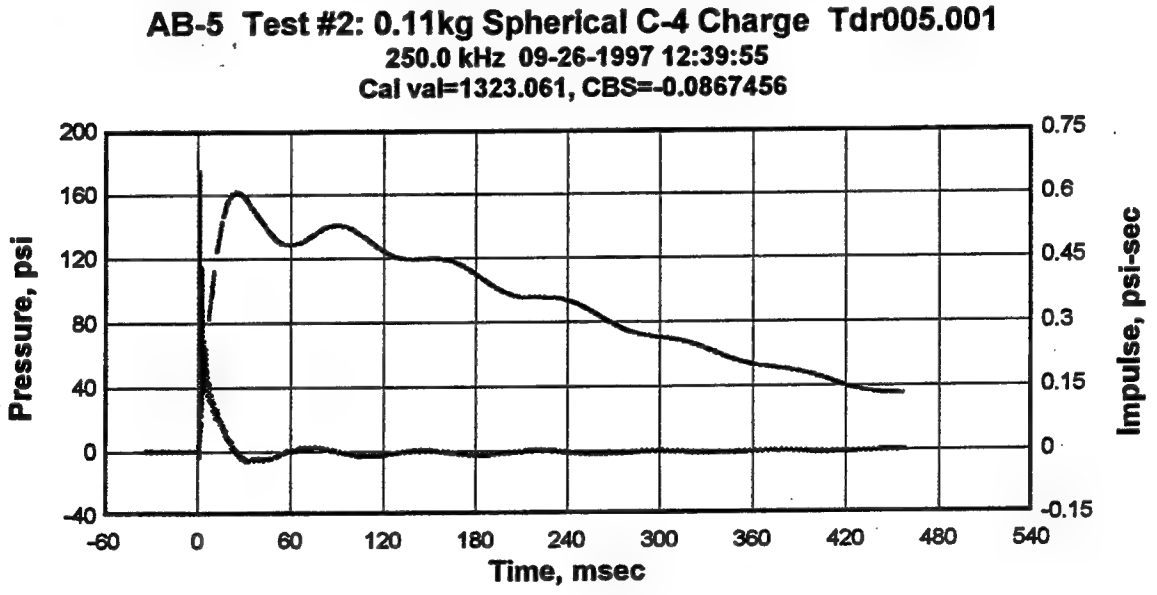

Figure B4. Pressure and Impulse-time histories, Gage AB-5 on wall of the access tunnel at a horizontal distance of 2.61 m from the rear wall of the detonation chamber, Experiment 2.

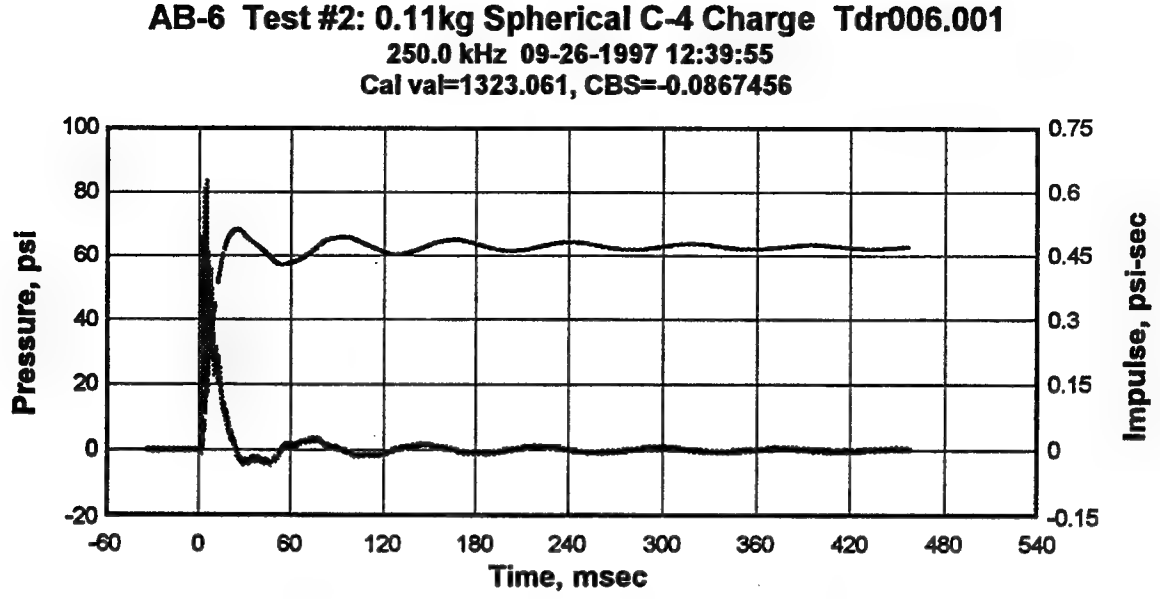

Figure B5. Pressure and impulse-time histories, Gage AB-6 in baffled chamber on the side of probe mount at horizontal distance of 3.37 m from the rear wall of the detonation chamber, Experiment 2.

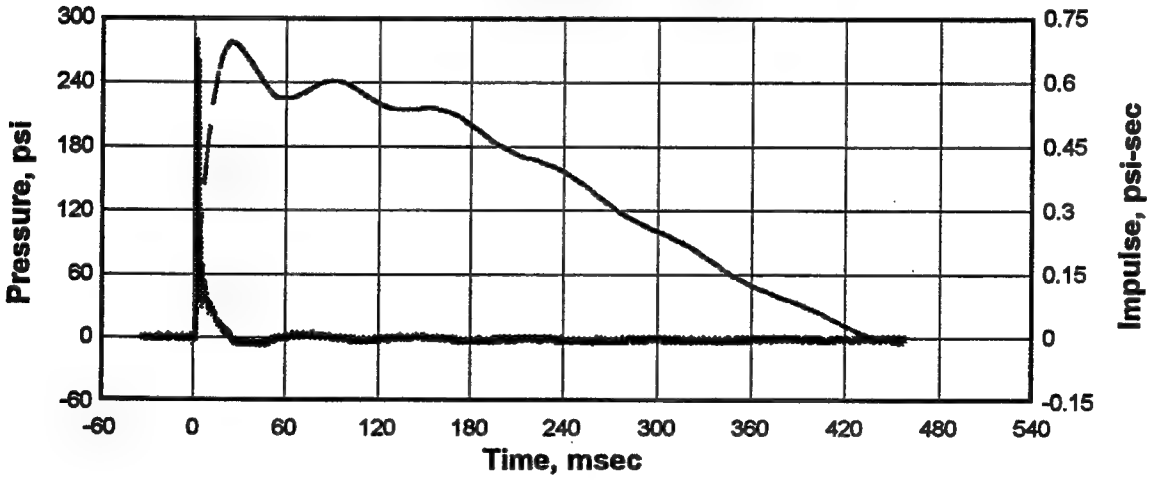

Figure B6. Total pressure and impulse-time histories, Gage AB-7 on probe mount at horizontal distance of 3.30 m from the rear wall of the detonation chamber, Experiment 2.

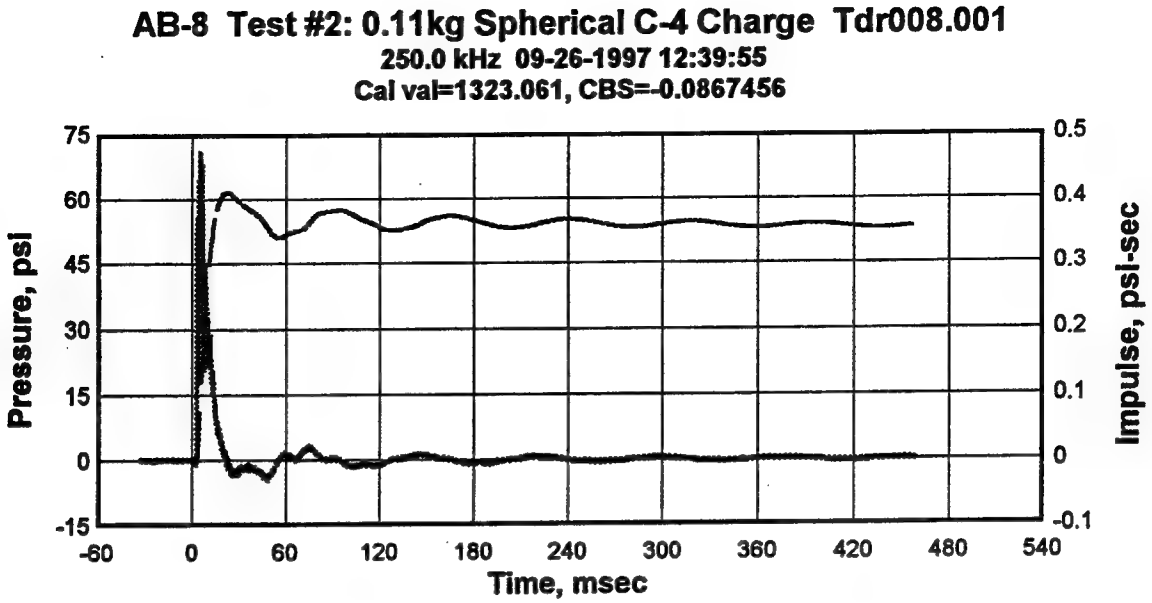

Figure B7. Pressure and impulse-time histories, Gage AB-8 in baffled chamber on the side of probe mount at a horizontal distance of 4.37 m from the rear wall of the detonation chamber, Experiment 2.

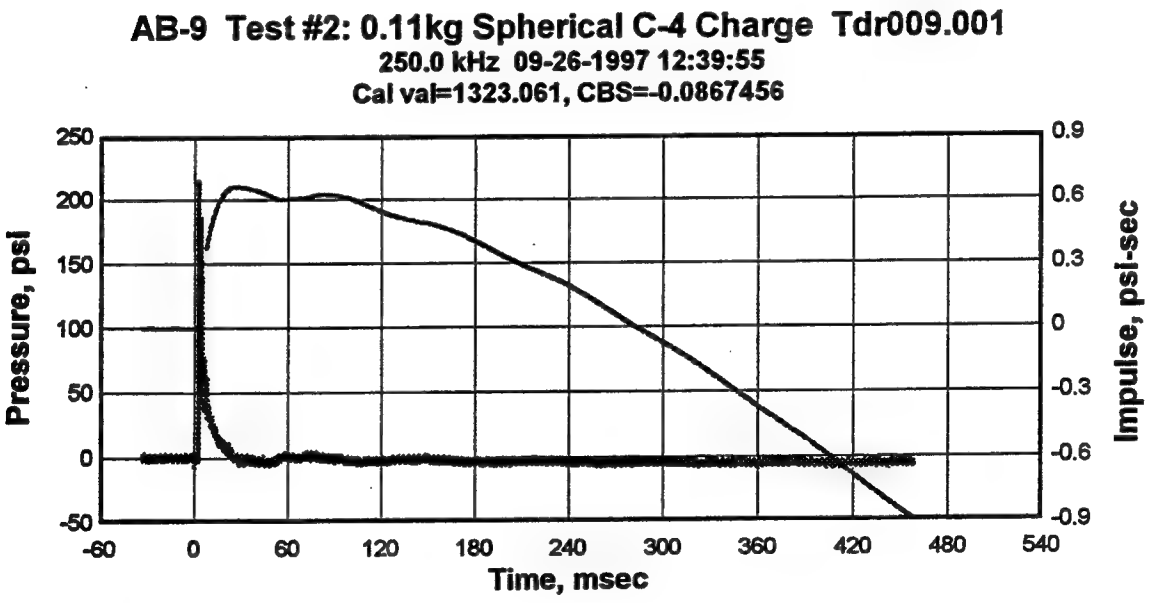

Figure B8. Total pressure and impulse-time histories, Gage AB-9 on probe mount at a horizontal distance of 4.30 m from the rear wall of the detonation chamber, Experiment 2.

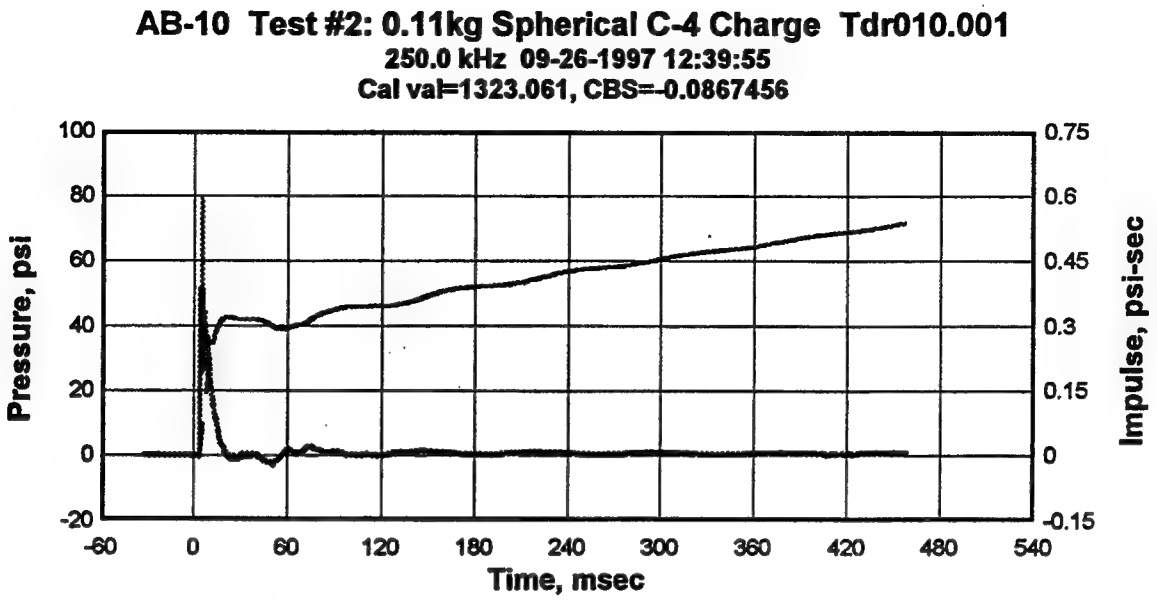

Figure B9. Pressure and impulse-time histories, Gage AB-10 on wall of the access tunnel at a horizontal distance of 5.30 m from the rear wall of the detonation chamber, Experiment 2.

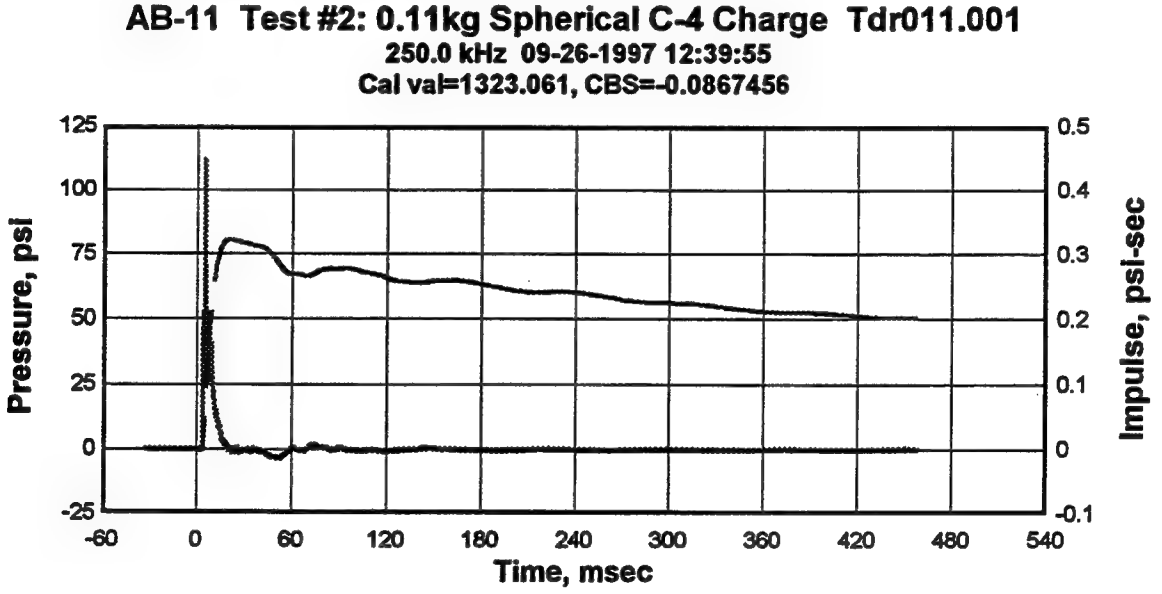

Figure B10. Pressure and impulse-time histories, Gage AB-11 on the wall of the access tunnel at a horizontal distance of 5.61 m from the rear wall of the detonation chamber, Experiment 2.

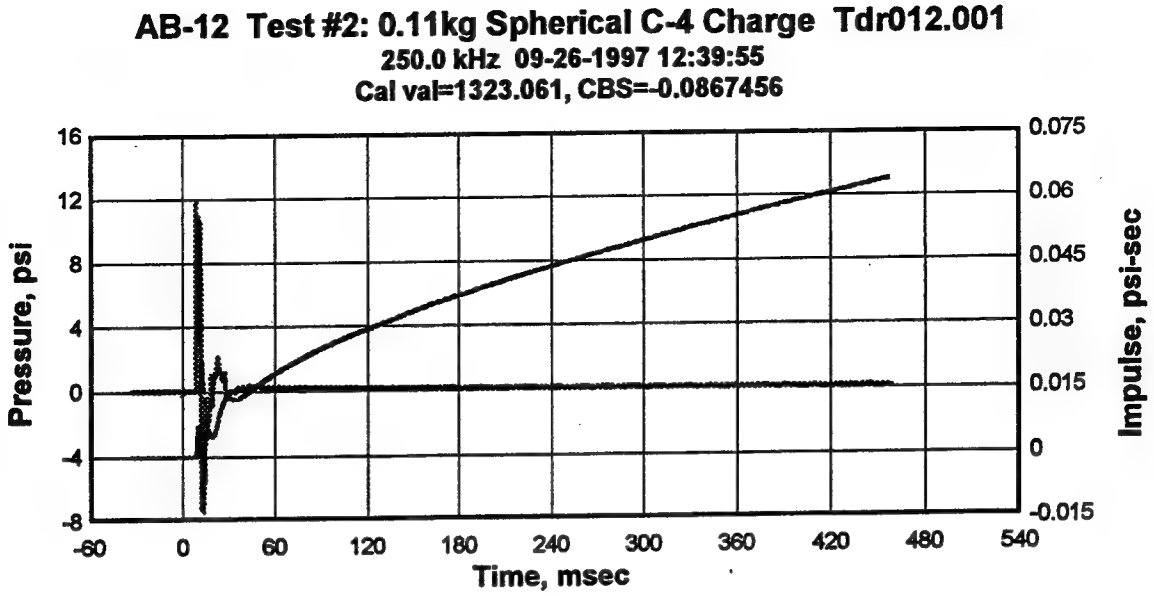

Figure B11. Pressure and impulse-time histories, free-field Gage AB-12 on the surface of the ground at a horizontal distance of 1.80 m from the portal, Experiment 2.

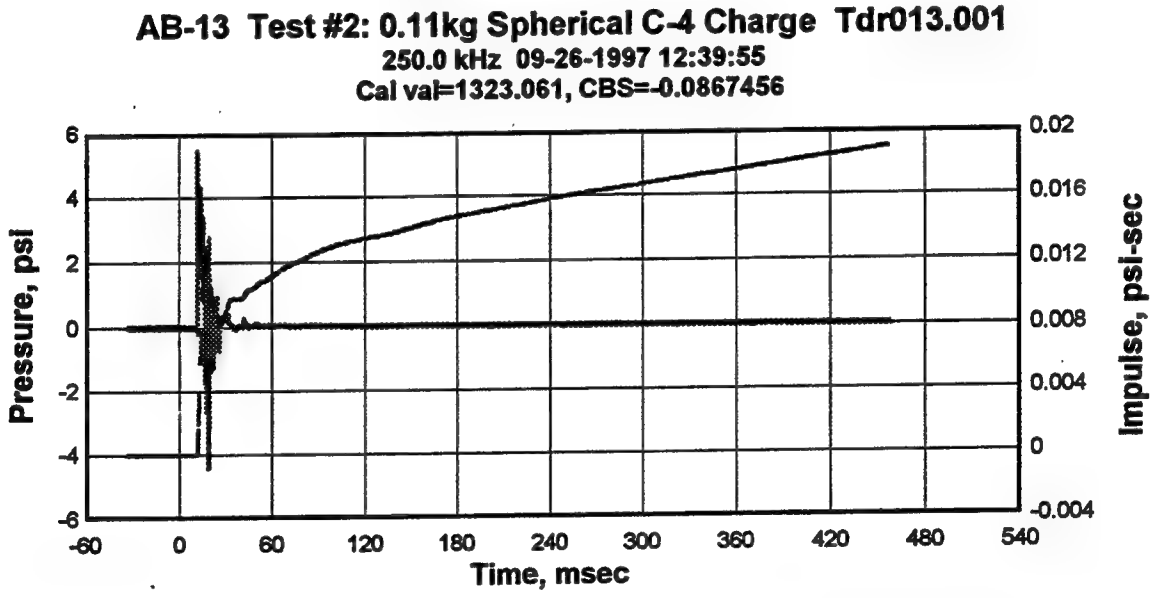

Figure B12. Pressure and impulse-time histories, free-field Gage AB-13 on the surface of the ground at a horizontal distance of 3.00 m from the portal, Experiment 2.

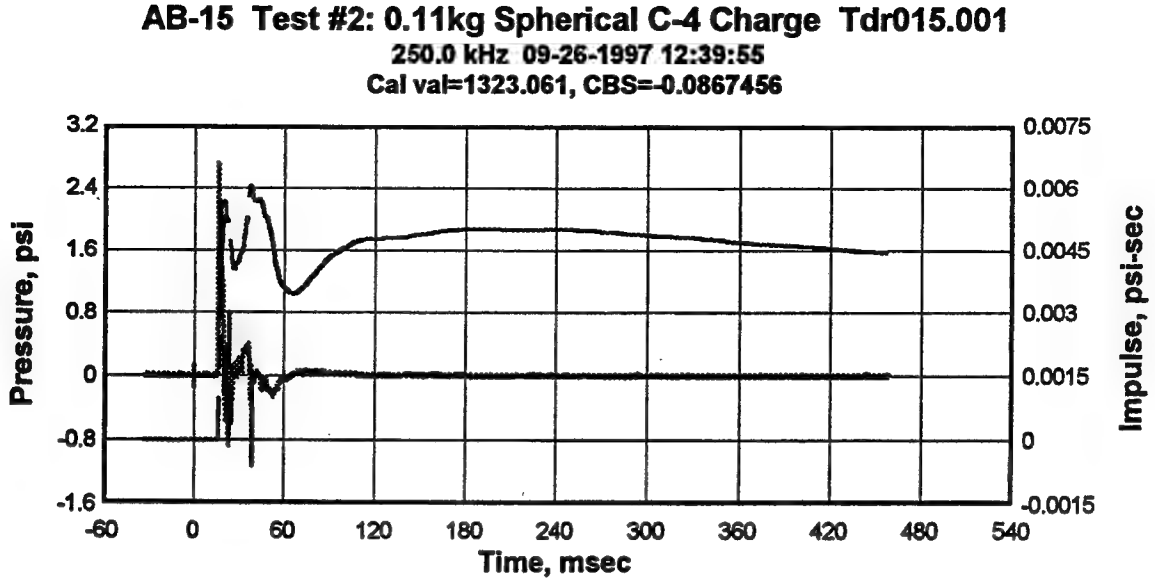

Figure B13. Pressure and impulse-time histories, free-field Gage AB-15 on the surface of the ground at a horizontal distance of 4.80 m from the portal, Experiment 2.

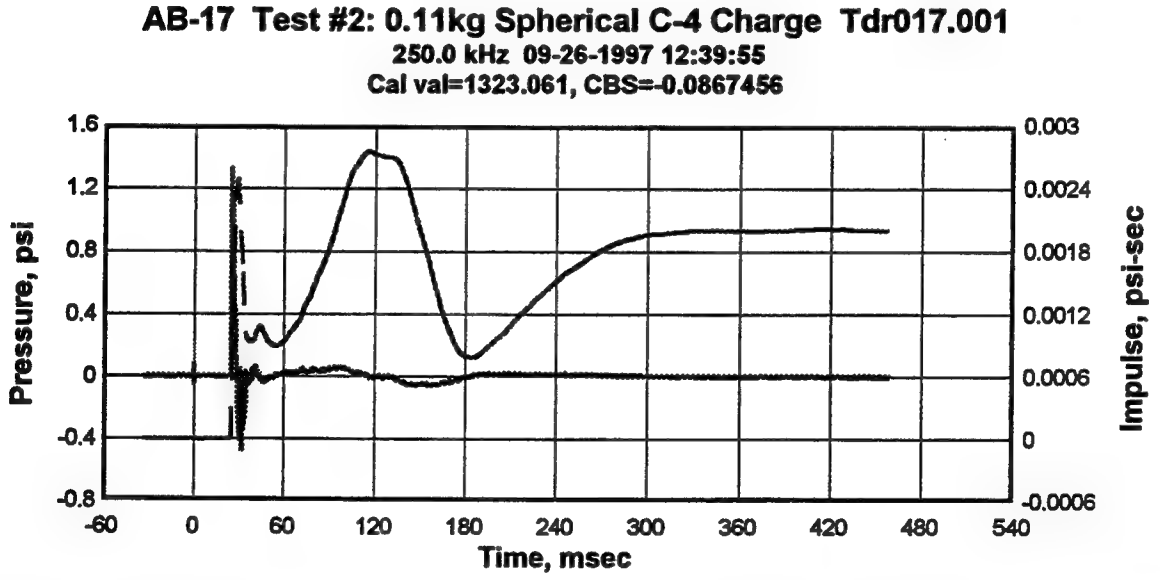

Figure B14. Pressure and impulse-time histories, free-field Gage AB-17 on the surface of the ground at a horizontal distance of 8.00 m from the portal, Experiment 2.

Appendix C
Airblast Effects Research Small-Scale Magazine Experiment 3

Pressure-Time Histories from the Detonation of 0.11 kg Spherical C-4 Charge

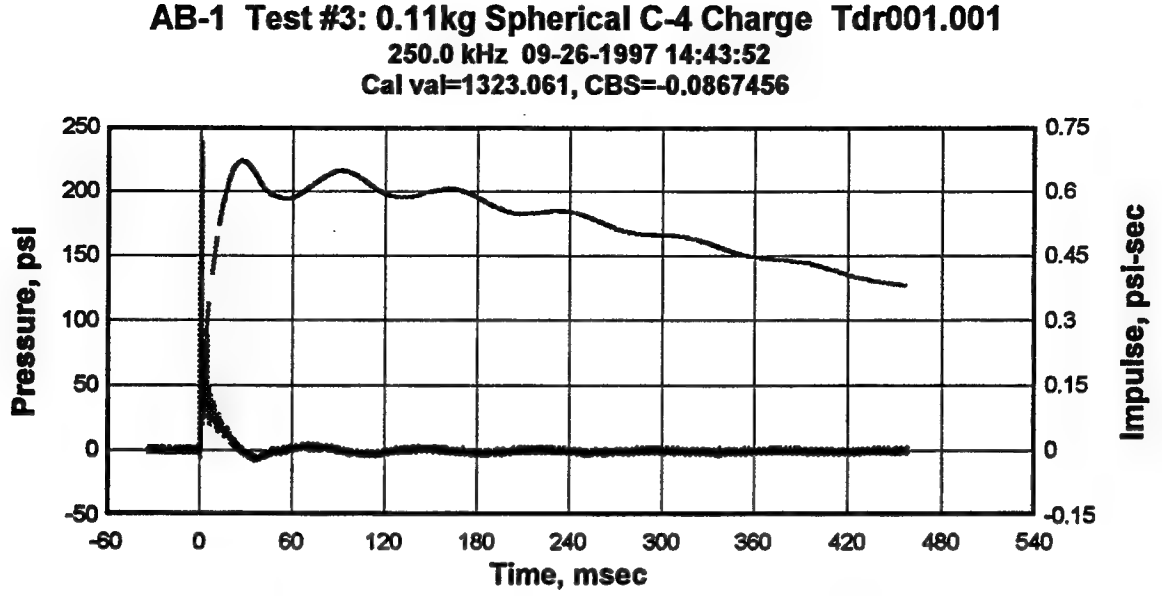

Figure C1. Pressure and impulse-time histories, Gage AB-1 on the rear wall of the detonation chamber at a horizontal distance of 0.90 m from the center of the explosive charge, Experiment 3.

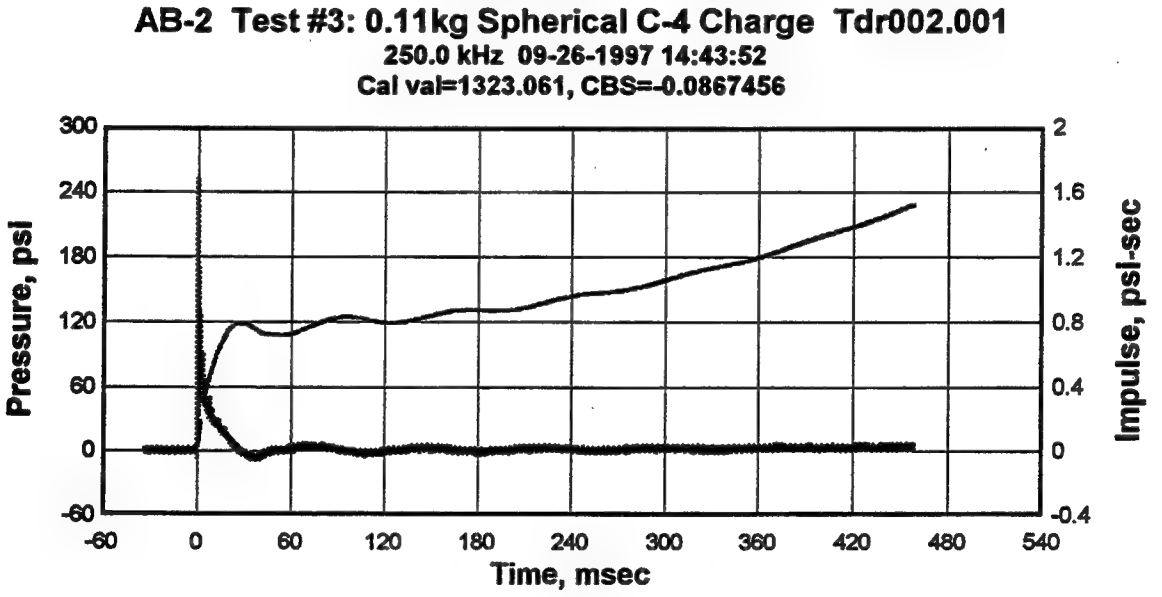

Figure C2. Pressure and impulse-time histories, Gage AB-2 on side wall of the detonation chamber at a horizontal distance of 0.45 m from the rear wall of the detonation chamber, Experiment 3.

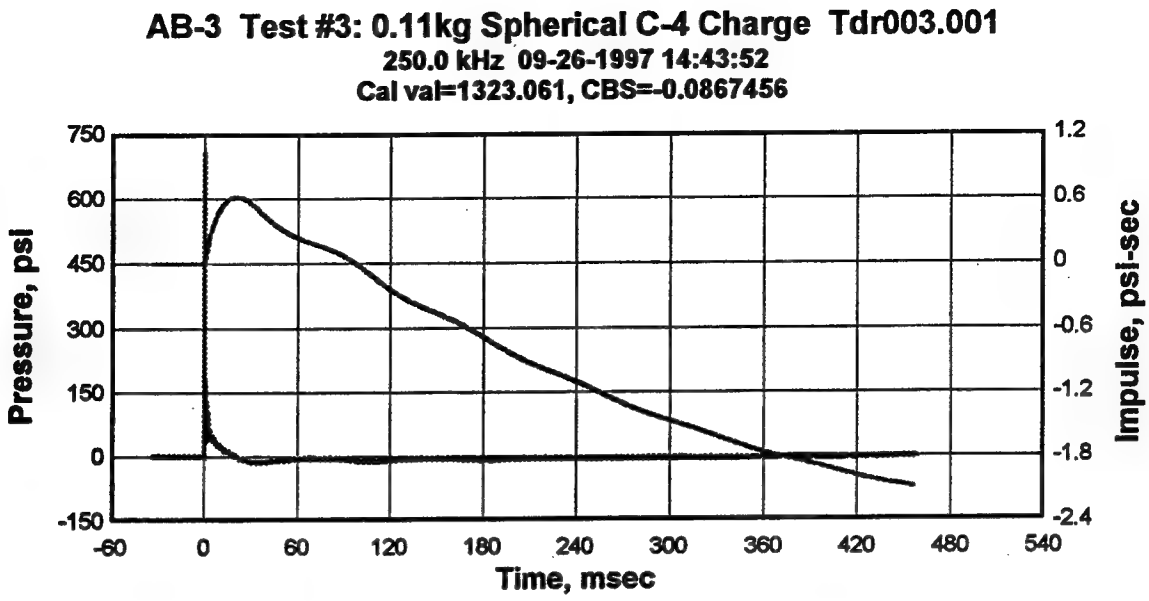

Figure C3. Pressure and impulse-time histories, Gage AB-3 on the side wall of the detonation chamber at a horizontal distance of 1.35 m from the rear wall of the detonation chamber, Experiment 3.

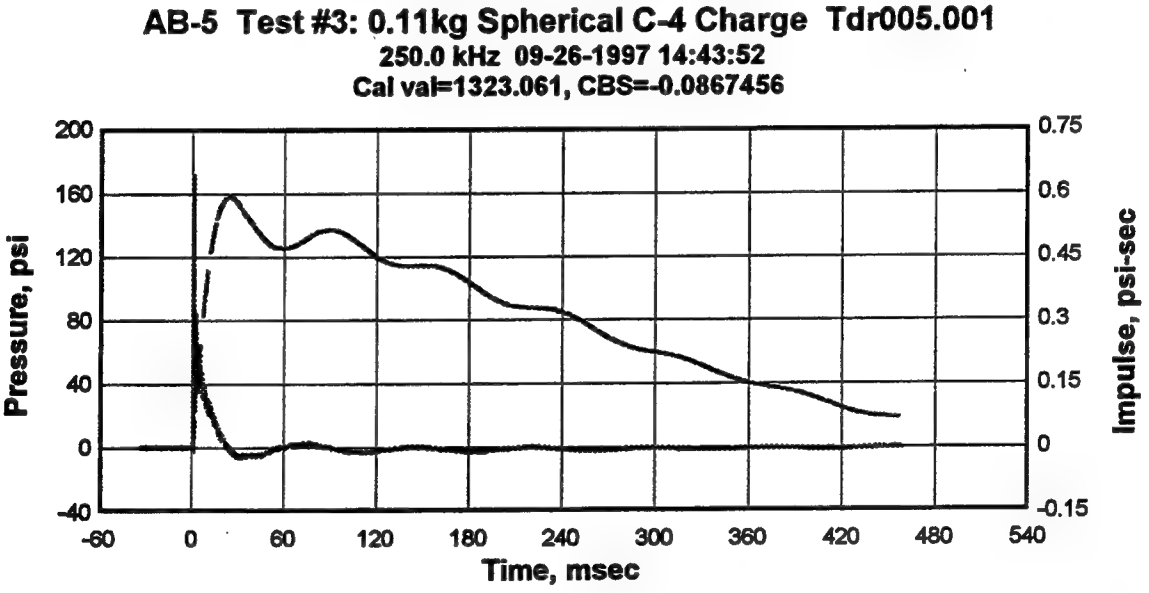

Figure C4. Pressure and impulse-time histories, Gage AB-5 on the wall of the access tunnel at a horizontal distance of 2.61 m from the rear wall of the detonation chamber, Experiment 3.

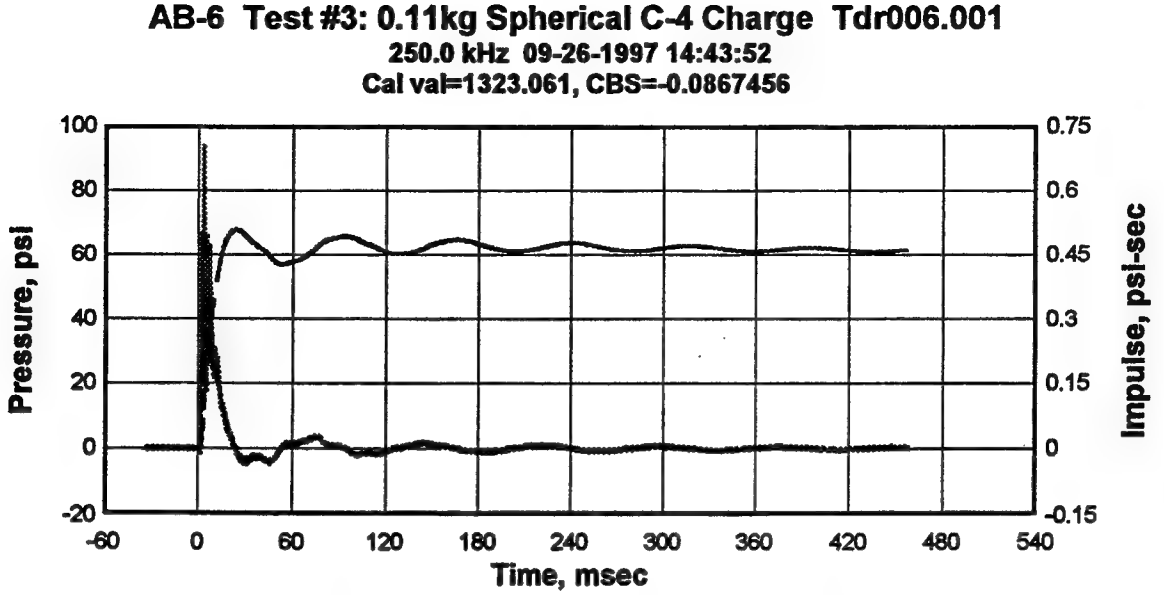

Figure C5. Pressure and impulse-time histories, Gage AB-6 in a baffled chamber on the side of probe mount at a horizontal distance of 3.37 m from the rear wall of the detonation chamber, Experiment 3.

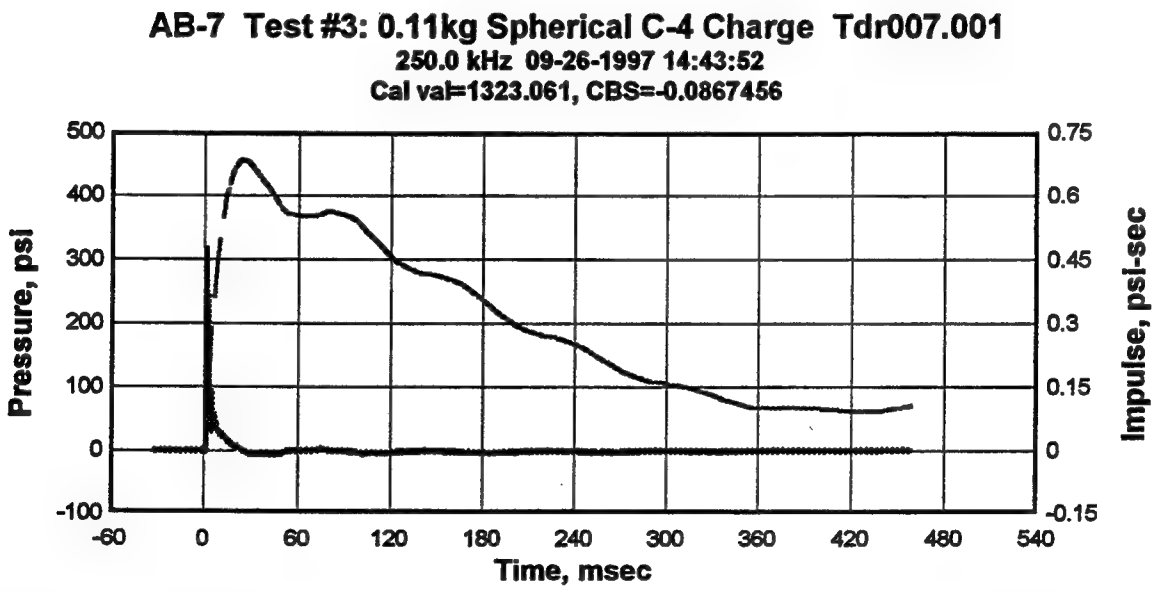

Figure C6. Total pressure and impulse-time histories, Gage AB-7 on probe mount at a horizontal distance of 3.30 m from the rear wall of the detonation chamber, Experiment 3.

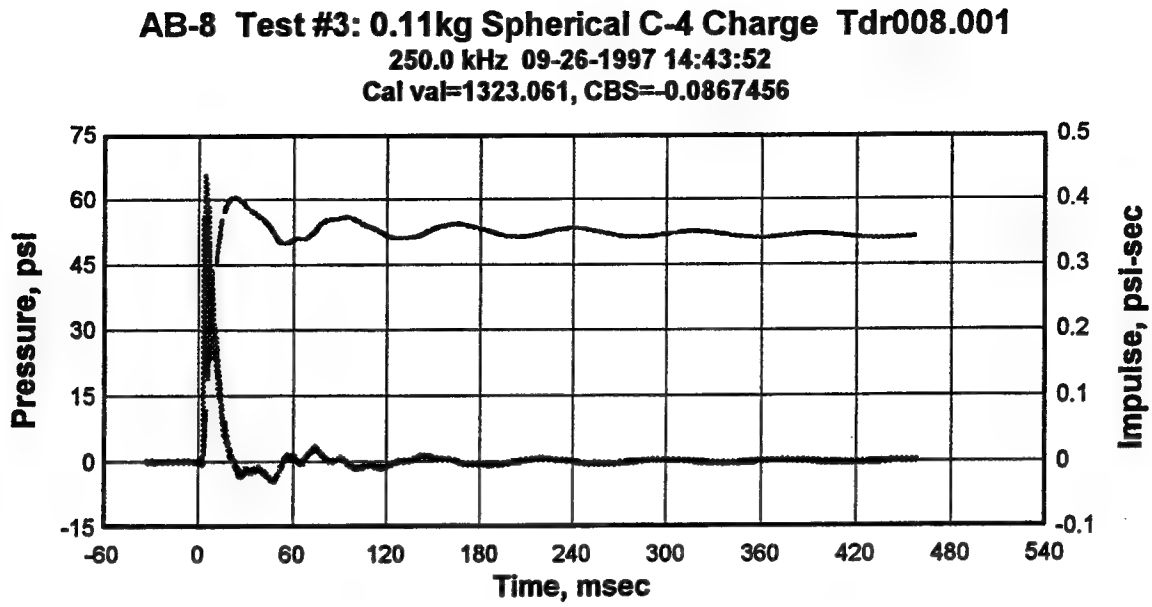

Figure C7. Pressure and impulse-time histories, Gage AB-8 in baffled chamber on the side of probe mount at a horizontal distance of 4.37 m from the rear wall of the detonation chamber, Experiment 3.

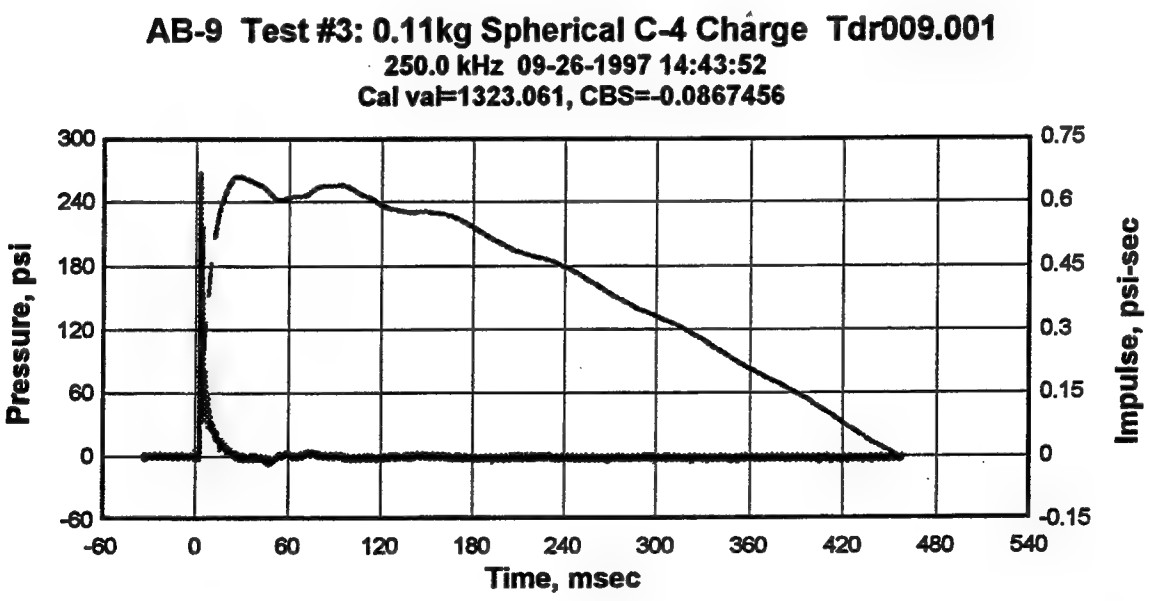

Figure C8. Total pressure and impulse-time histories, Gage AB-9 on probe mount at horizontal distance of 4.30 m from the rear wall of the detonation chamber, Experiment 3.

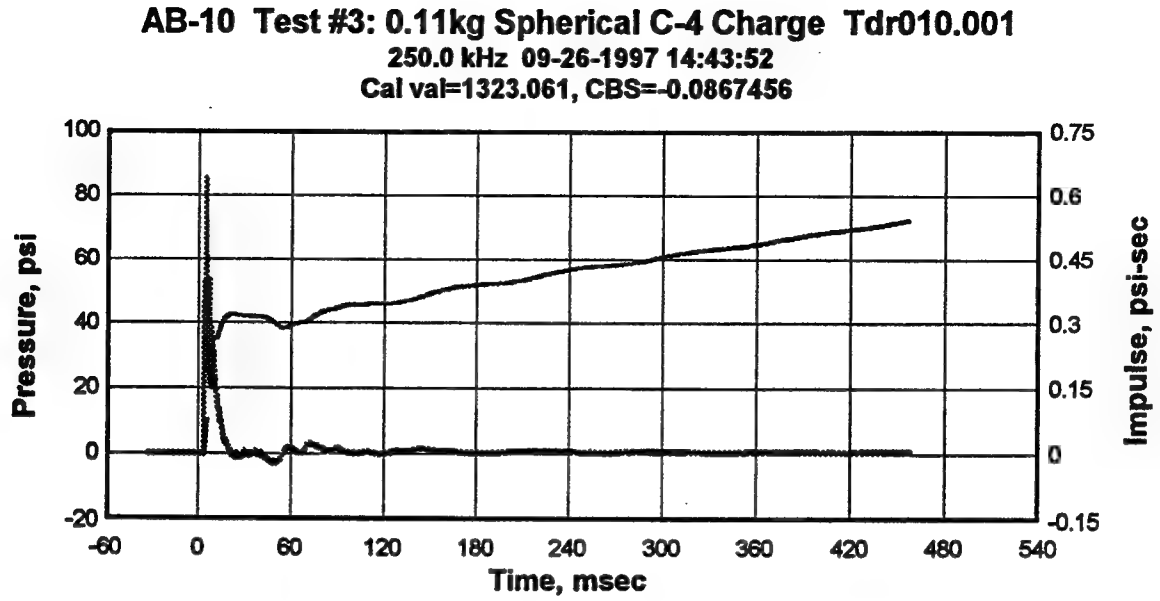

Figure C9. Pressure and impulse-time histories, Gage AB-10 on wall of access tunnel at a horizontal distance of 5.30 m from ther ear wall of the detonation chamber, Experiment 3.

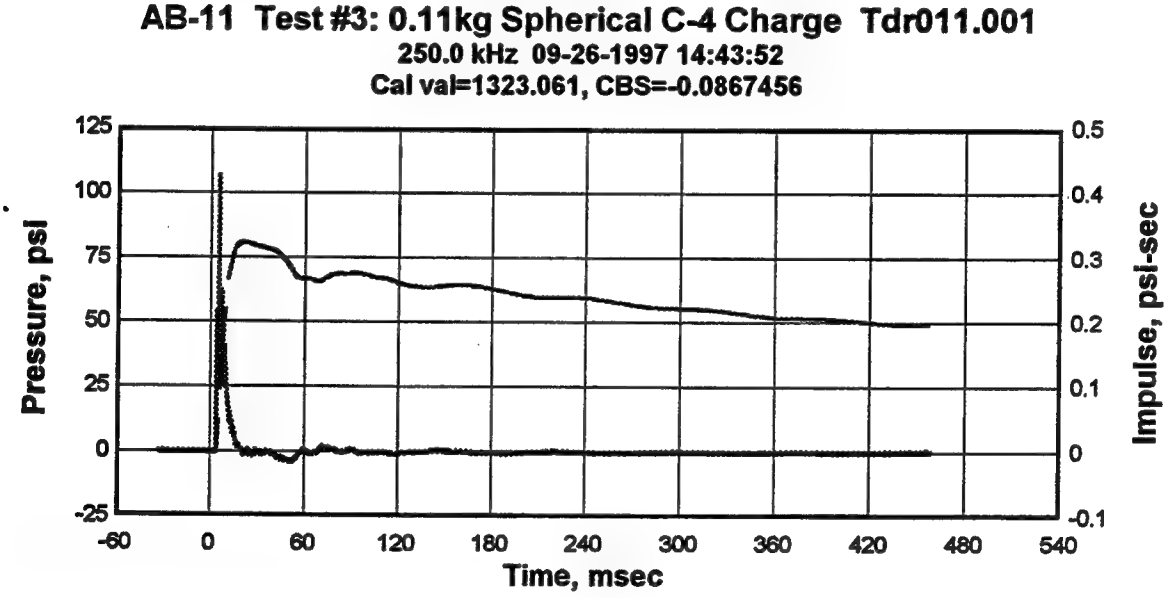

Figure C10. Pressure and impulse-time histories, Gage AB-11 on wall of the access tunnel at a horizontal distance of 5.61 m from the rear wall of the detonation chamber, Experiment 3.

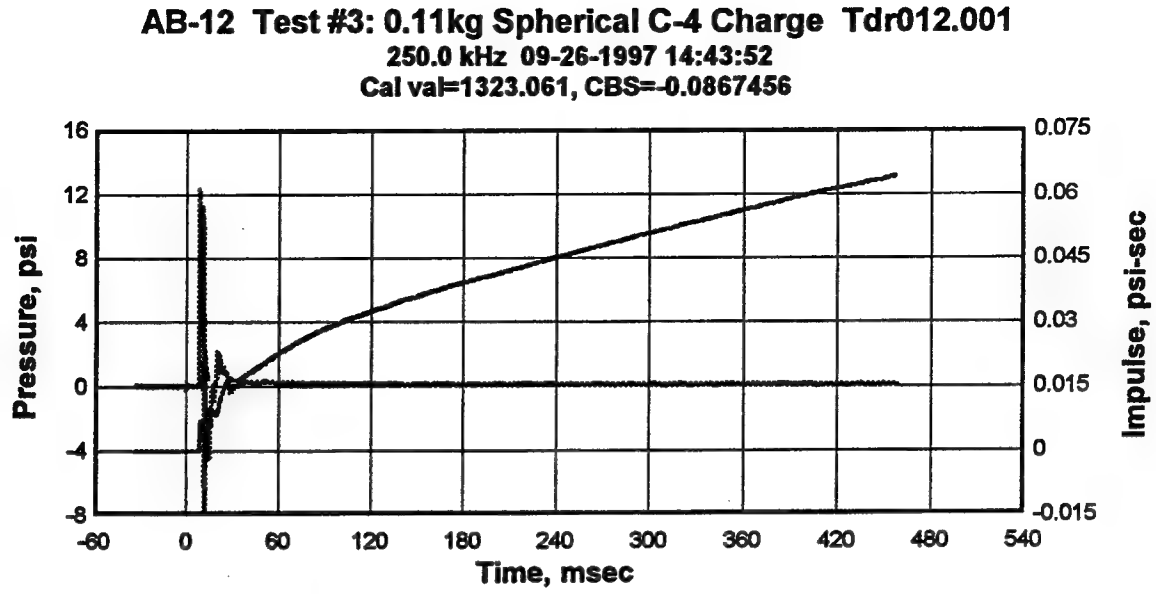

Figure C11. Pressure and impulse-time histories, free-field Gage AB-12 on the surface of the ground at a horizontal distance of 1.80 m from the portal, Experiment 3.

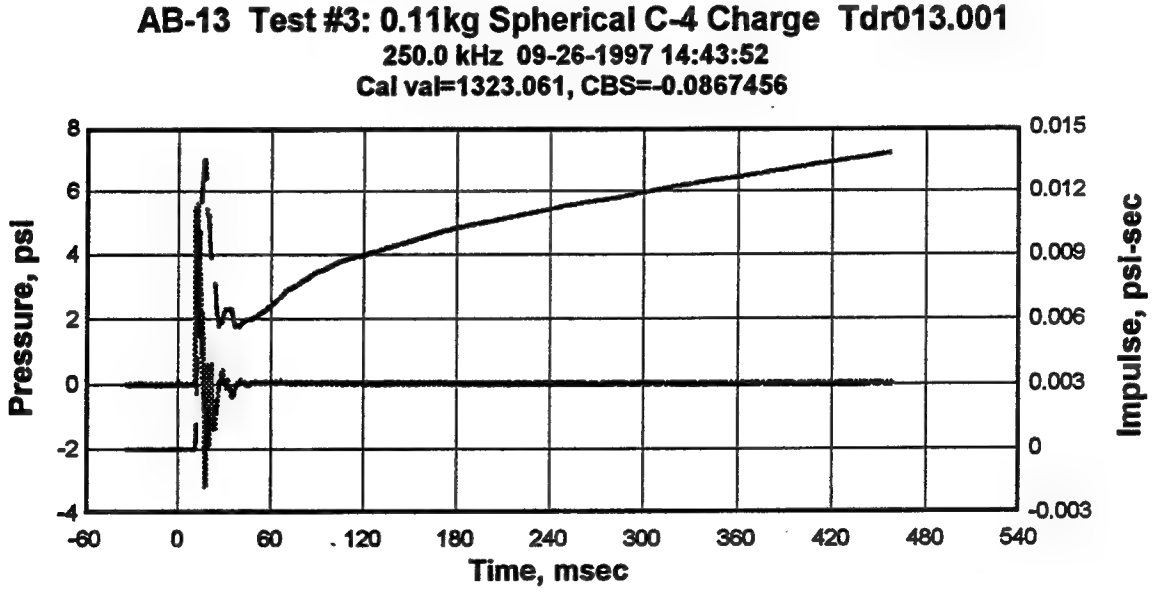

Figure C12. Pressure and impulse-time histories, free-field Gage AB-13 on surface of the ground at a horizontal distance of 3.00 m from the portal, Experiment 3.

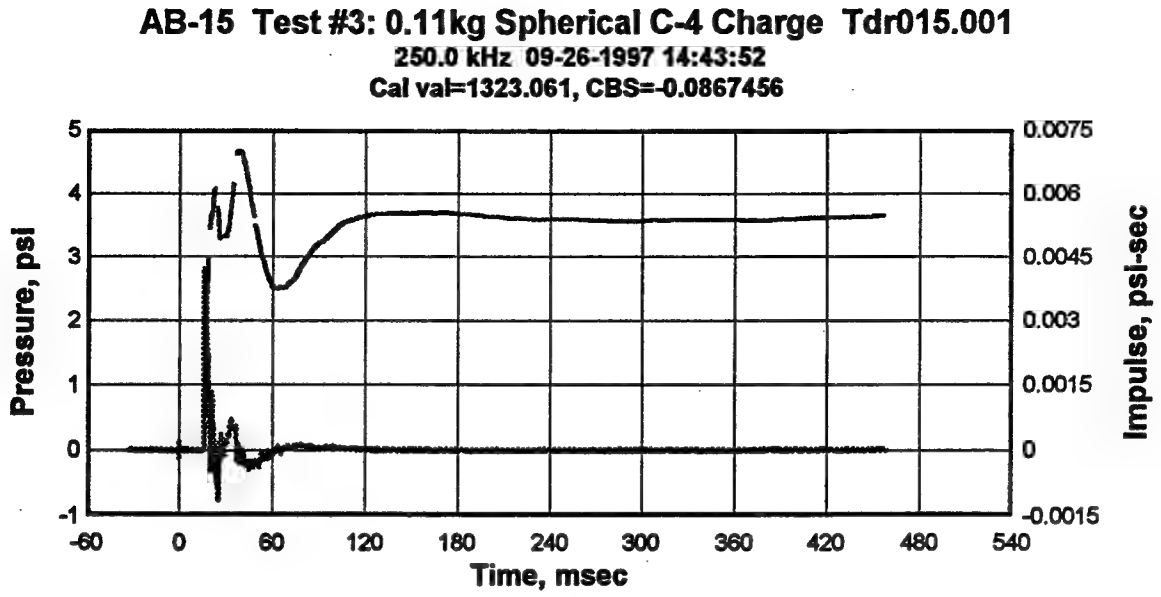

Figure C13. Pressure and impulse-time histories, free-field Gage AB-15 on the surface of the ground at a horizontal distance of 4.80 m from the portal, Experiment 3

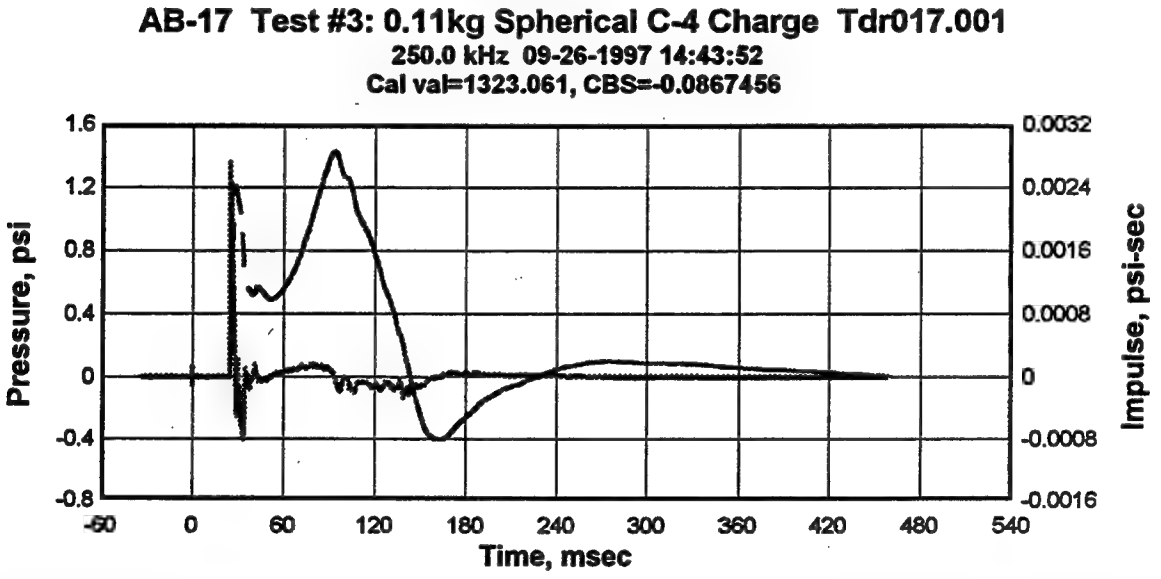

Figure C14. Pressure and impulse-time histories, free-field Gage AB-17 on the surface of the ground at a horizontal distance of 8.00 m from the portal, Experiment 3.

Appendix D
Airblast Effects Research Small-Scale Magazine Experiment 4

Pressure-Time Histories from the Detonation of 0.28 kg Spherical C-4 Charge

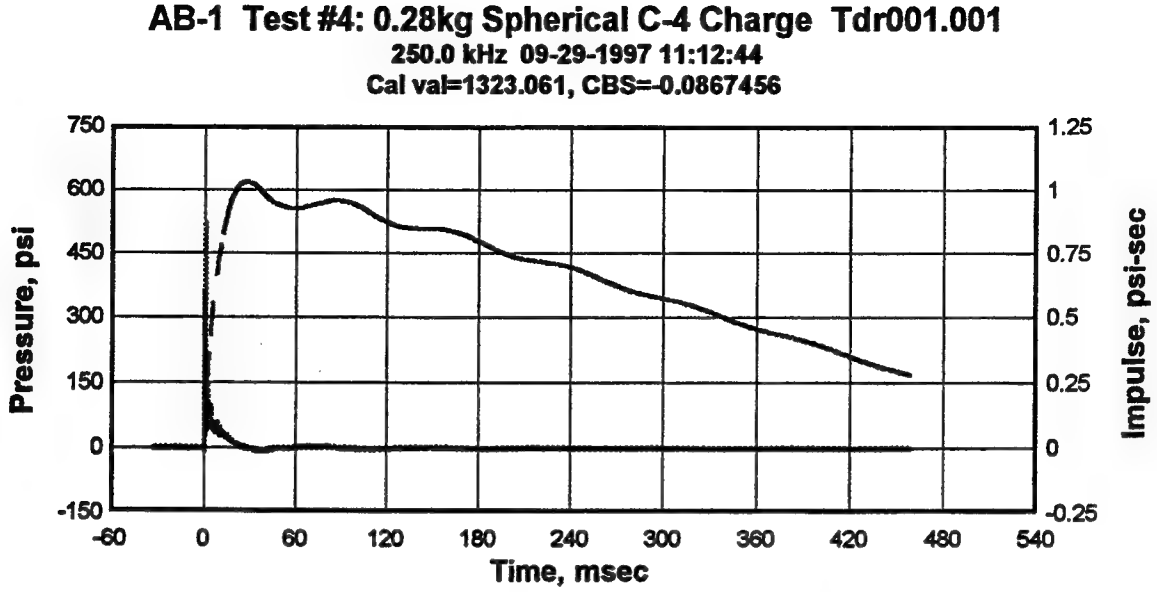

Figure D1. Pressure and impulse-time histories, Gage AB-1 on rear wall of the detonation chamber at a horizontal distance of 0.90 m from the center of the explosive charge, Experiment 4.

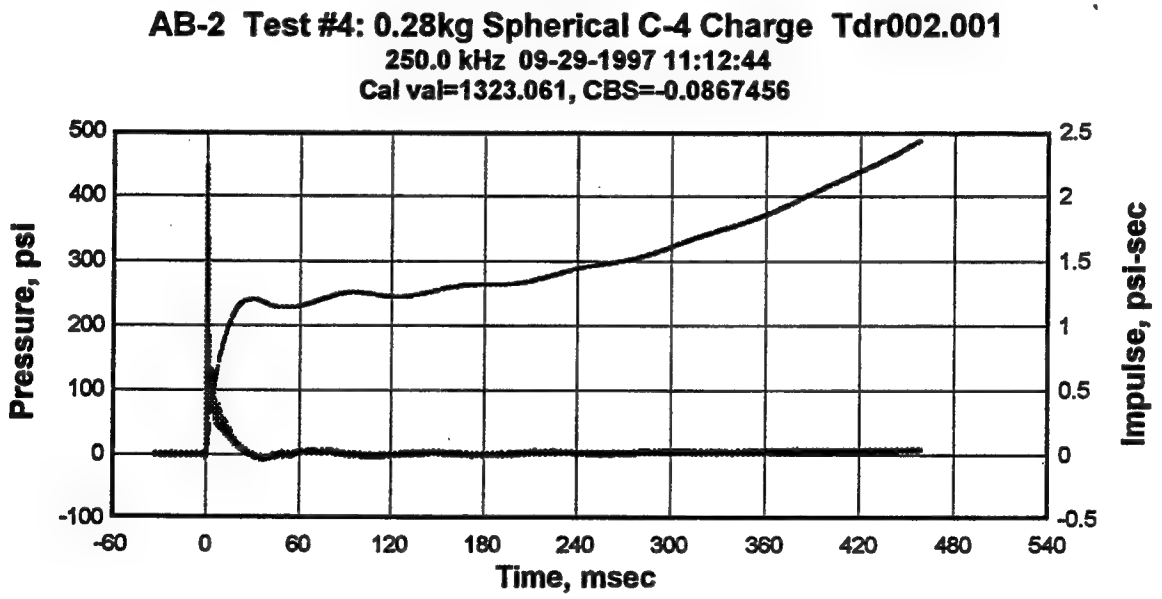

Figure D2. Pressure and impulse-time histories, Gage AB-2 on side wall fo the detonation chamber at a horizontal distance of 0.45 m from the rear wall of the detonation chamber, Experiment 4

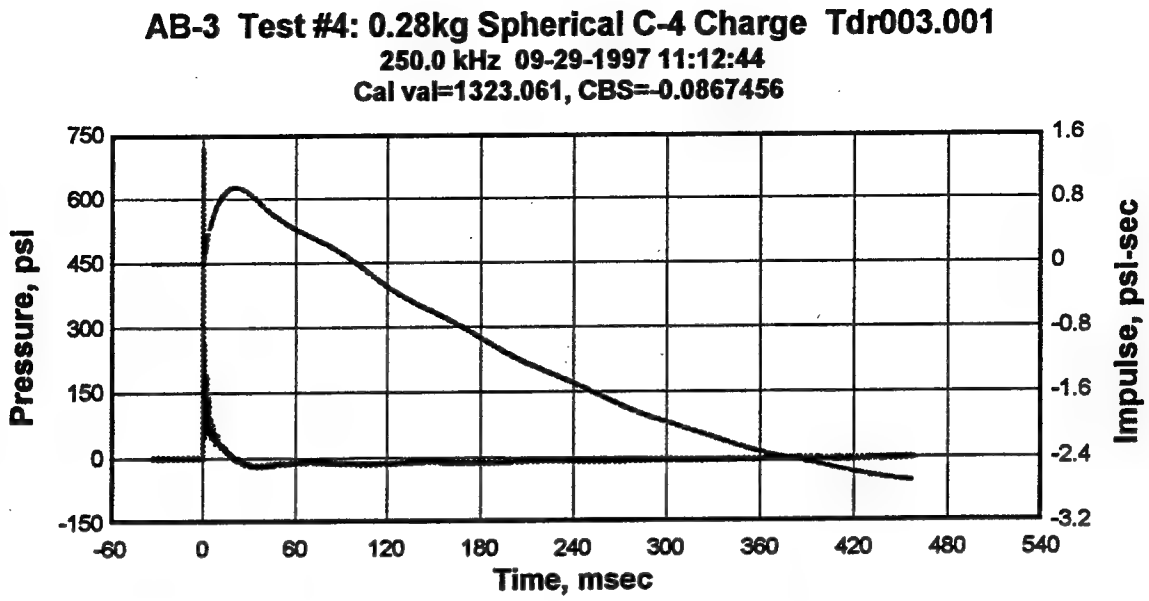

Figure D3. Pressure and impulse-time histories, Gage AB-3 on side wall of the detonation chamber at a horizontal distance of 1.35 m from the rear wall of the detonation chamber, Experiment 4.

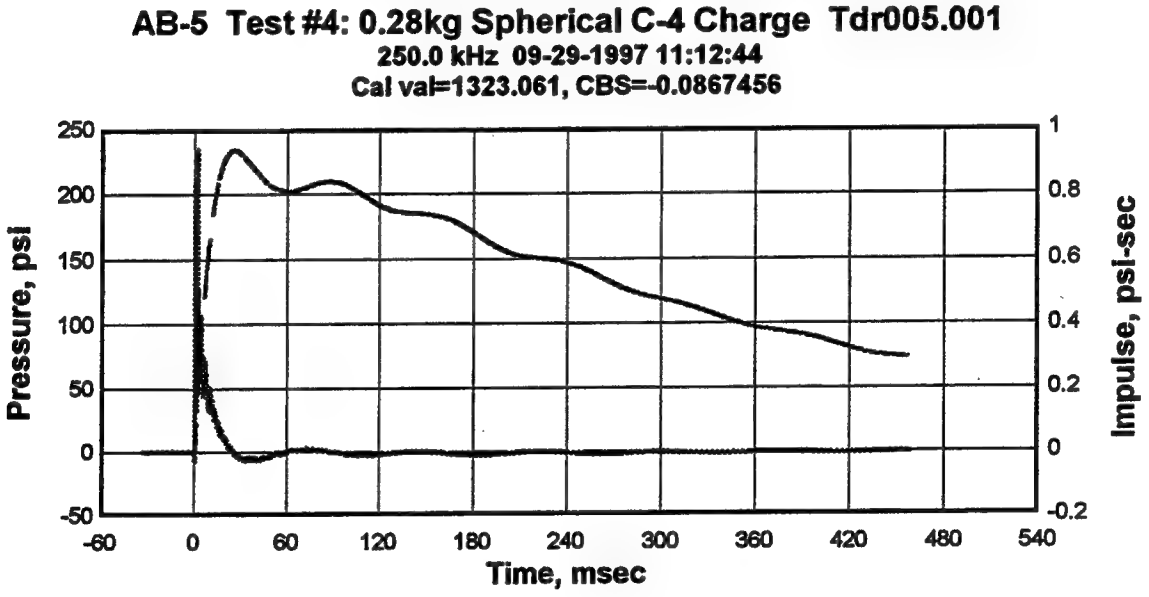

Figure D4. Pressure and impulse-time histories, Gage AB-5 on wall of the access tunnel at a horizontal distance of 2.61 m from the rear wall of the detonation chamber, Experiment 4.

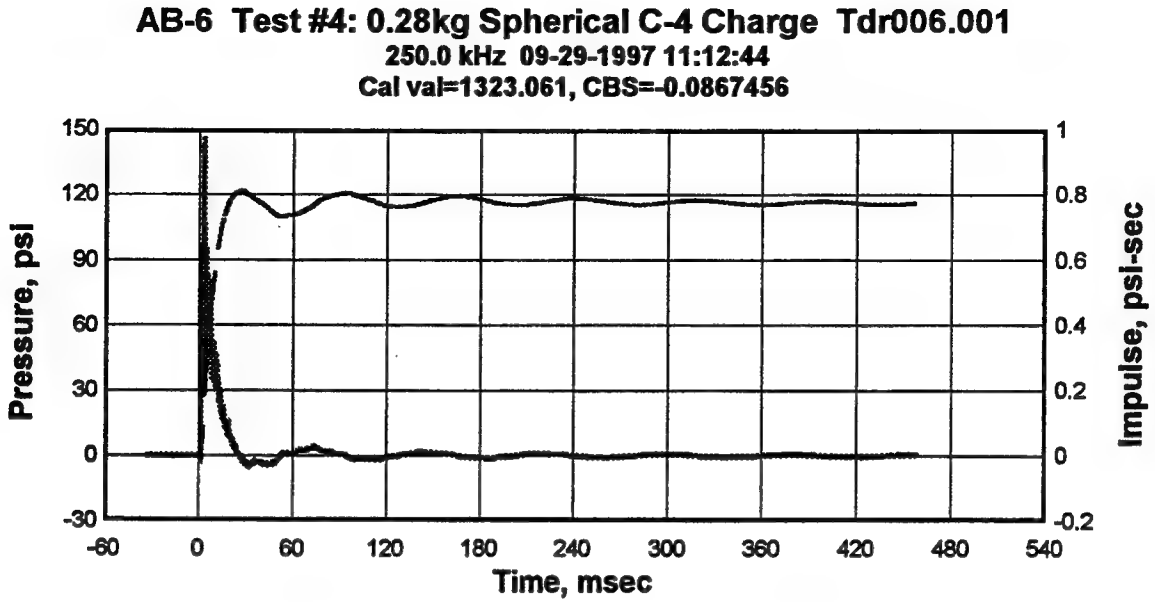

Figure D5. Pressure and impulse-time histories, Gage AB-6 in baffled chamber on the side of probe mount at a horizontal distance of 3.37 m from the rear wall of the detonation chamber, Experiment 4.

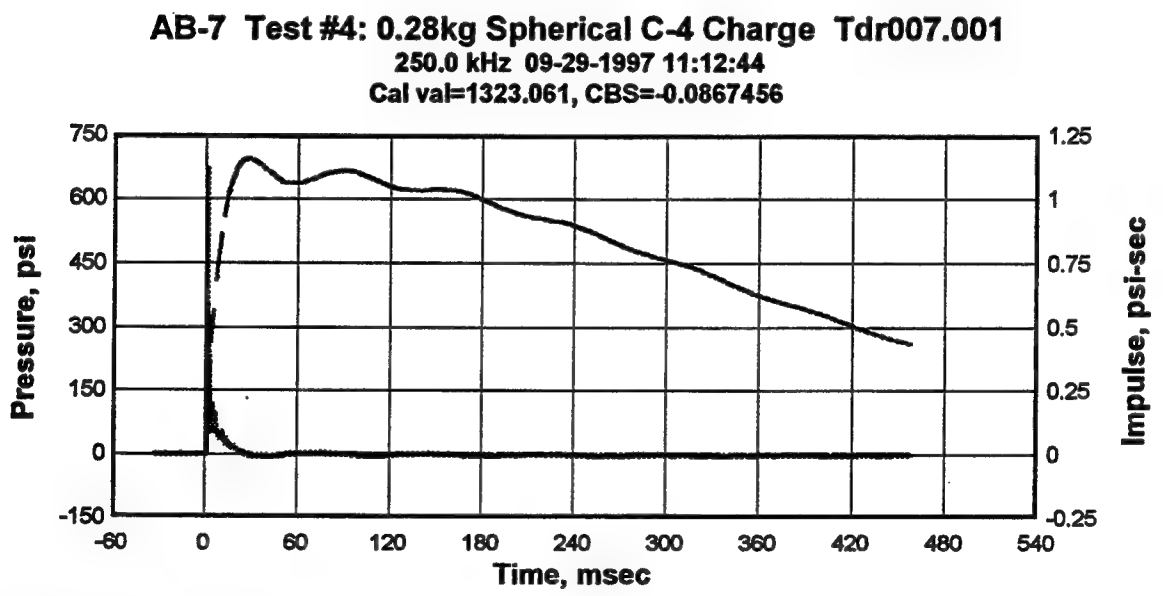

Figure D6. Total pressure and impulse-time histories, Gage AB-7 on probe mount at a horizontal distance of 3.30 m from the rear wall of the detonation chamber, Experiment 4.

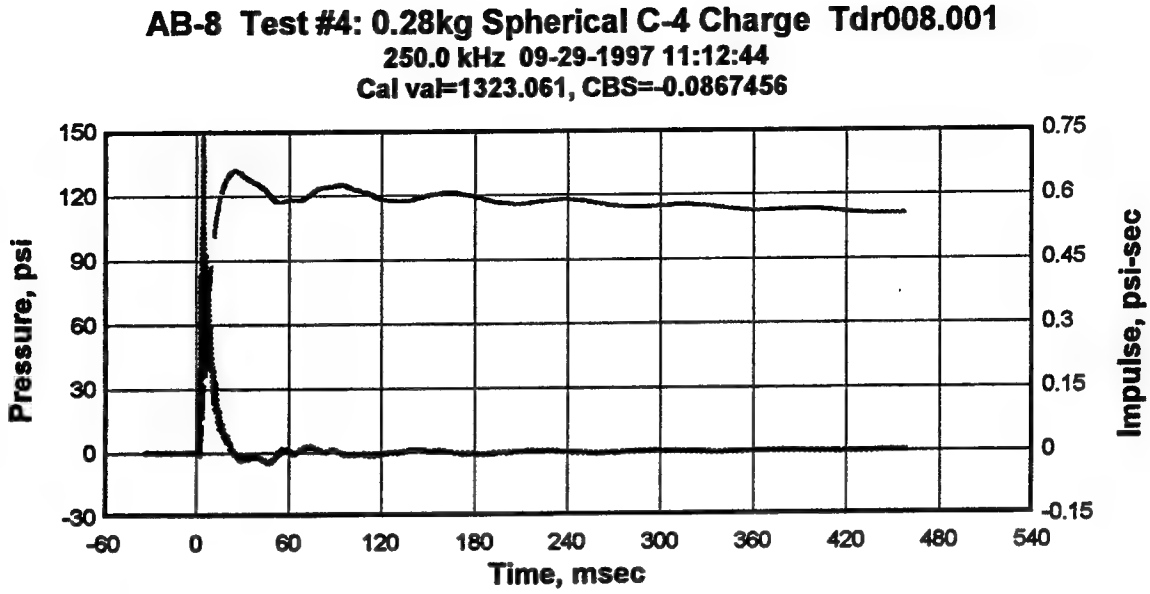

Figure D7. Pressure and impulse-time histories, AB-8 in baffled chamber on the side of the probe mount at a horizontal distance of 4.37 m from the rear wall of the detonation chamber, Experiment 4.

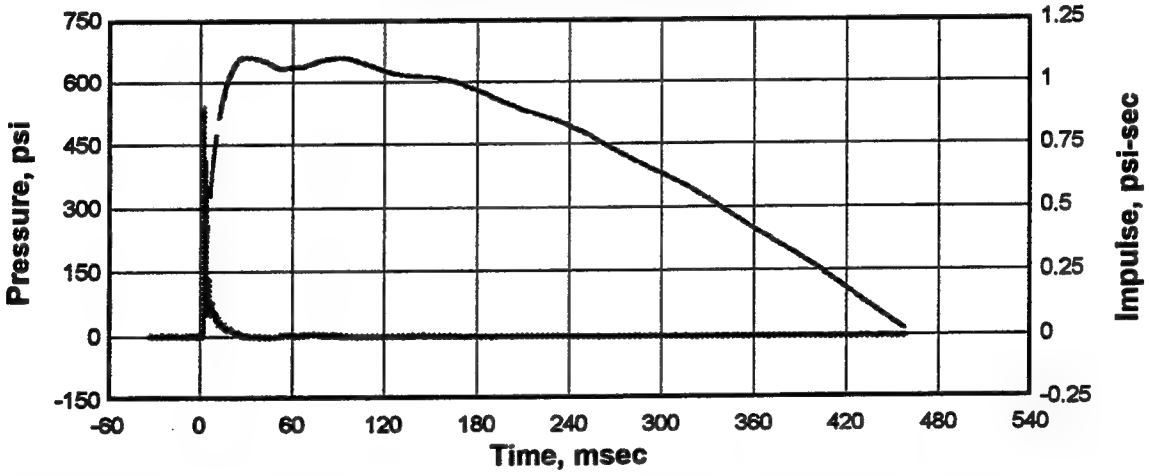

Figure D8. Total pressure and impulse-time histories, Gage AB-9 on probe mount at a horizontal distance of 4.30 m from the rear wall of the detonation chamber, Experiment 4.

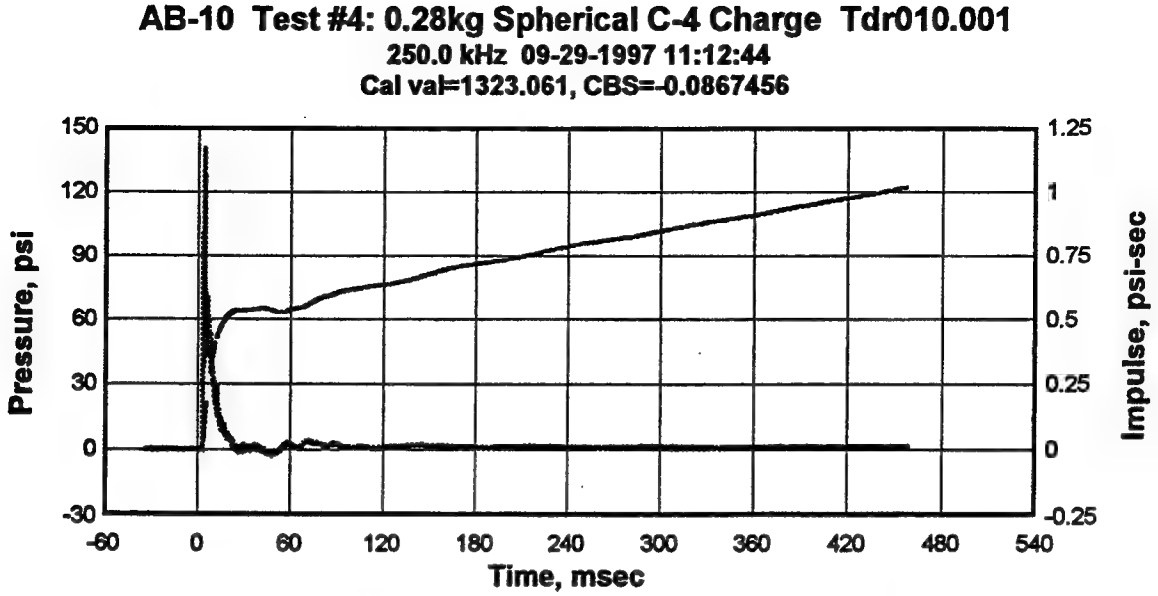

Figure D9. Pressure and impulse-time histories, Gage AB-10 on wall of access tunnel at a horizontal distance of 5.30 m from the rear wall of the detonation chamber, Experiment 4.

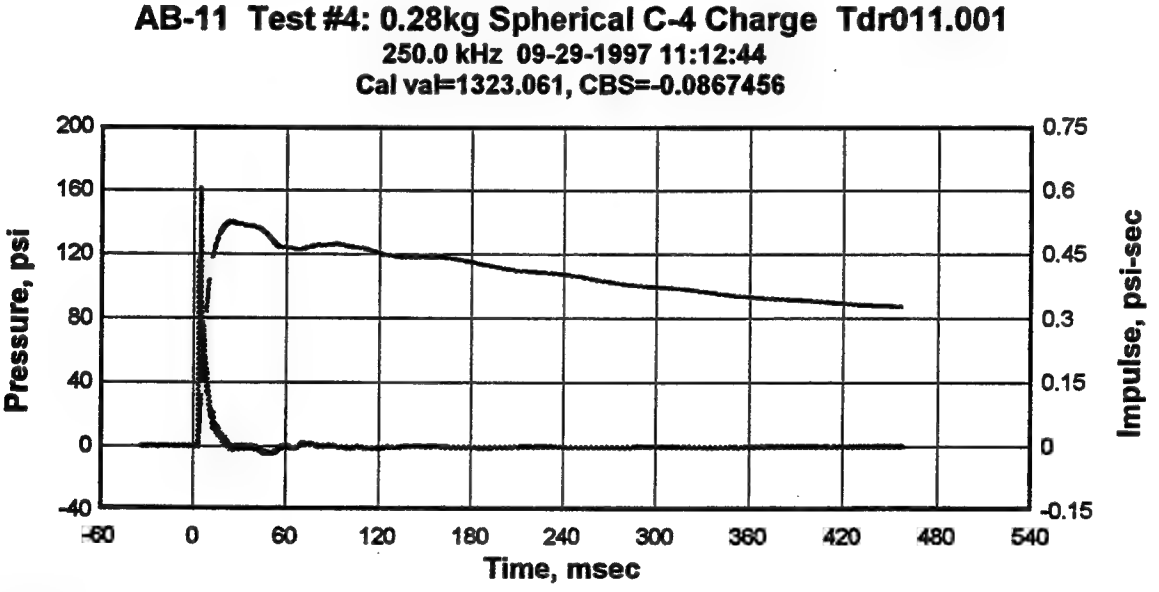

Figure D10. Pressure and impulse-time histories, Gage AB-11 on wall of the access tunnel at a horizontal distance of 5.61 m from the rear wall of the detonation chamber, Experiment 4.

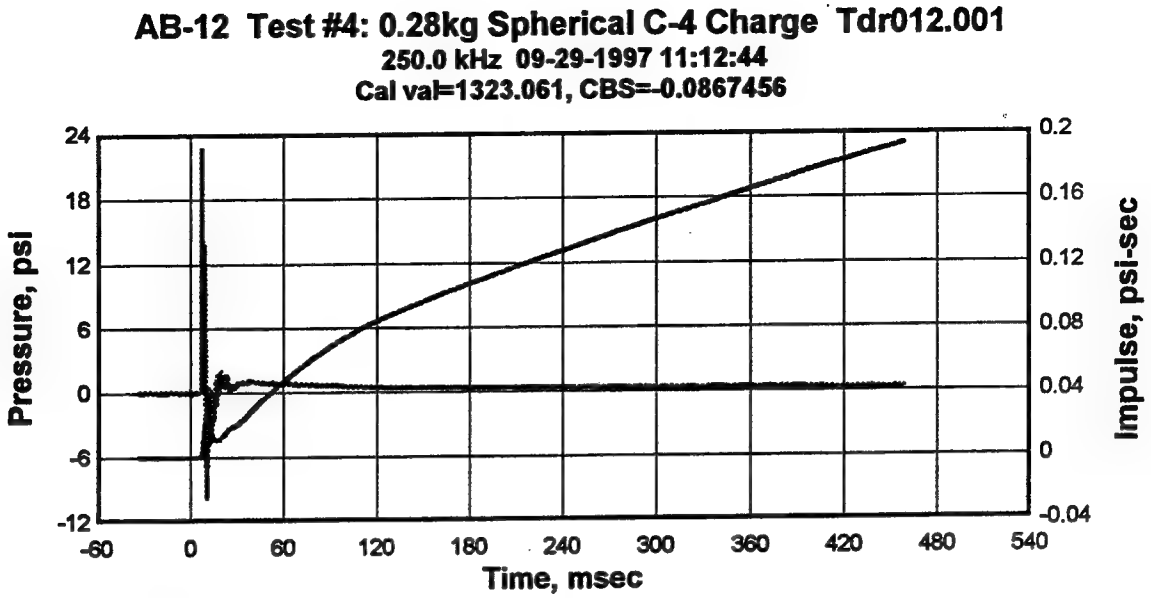

Figure D11. Pressure and impulse-time histories, free-field Gage AB-12 on the surface of the ground at a horizontal distance of 1.80 m from the portal, Experiment 4.

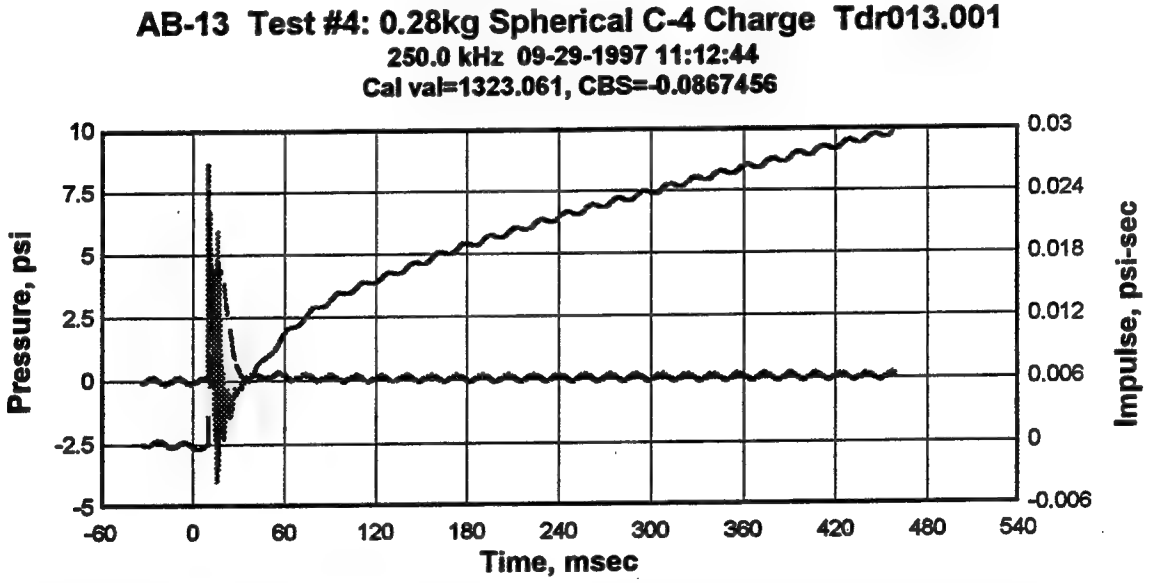

Figure D12. Pressure and impulse-time histories, free-field Gage AB-13 on the surface of the ground at a horizontal distance of 3.00 m from the portal, Experiment 4

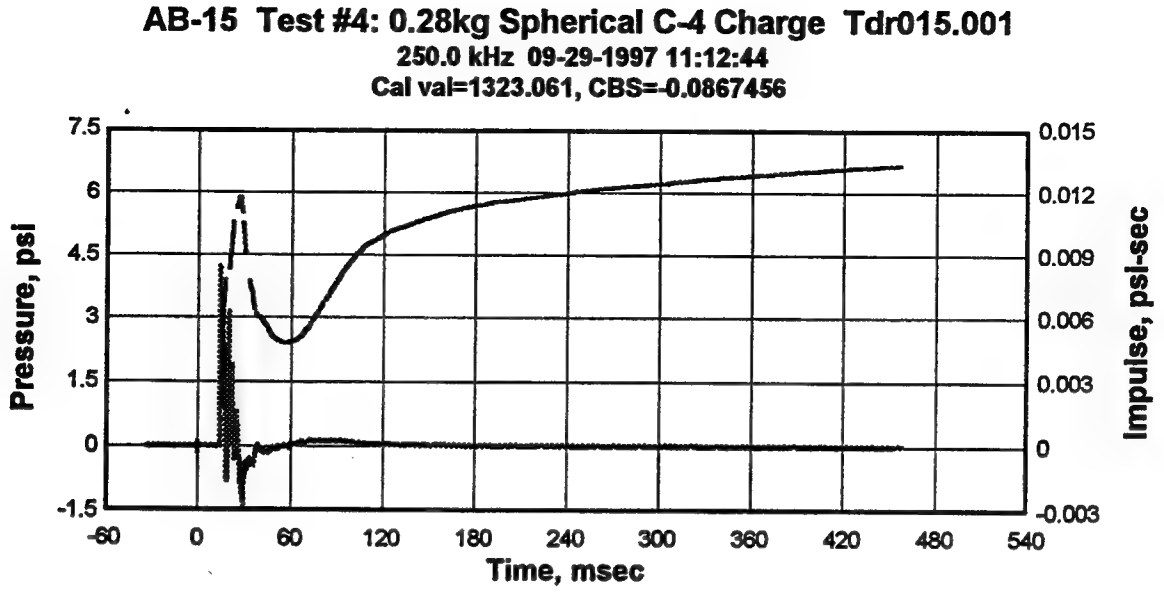

Figure D13. Pressure and impulse-time histories, free-field Gage AB-15 on surface of the ground at a horizontal distance of 4.80 m from the portal, Experiment 4

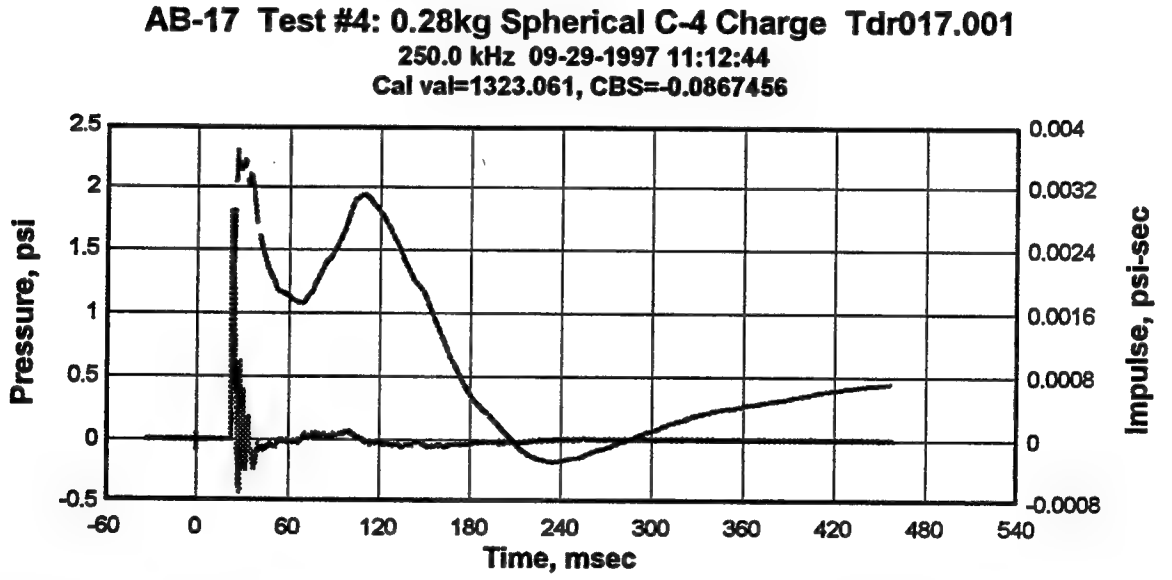

Figure D14. Pressure and impulse-time histories, free-field Gage AB-17 on the surface of the ground at a horizontal distance of 8.00 m from the portal, Experiment 4.

Appendix E
Airblast Effects Research Small-Scale Magazine Experiment 5

Pressure-Time Histories from the Detonation of 1.36 kg Spherical C-4 Charge

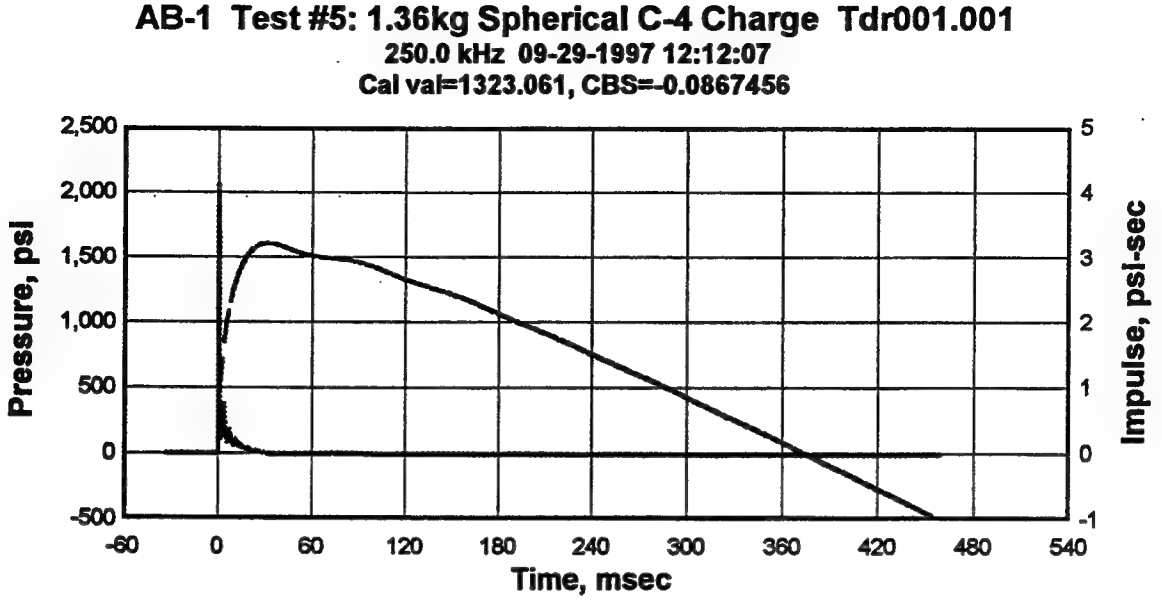

Figure E1. Pressure and impulse-time histories, Gage AB-1 on rear wall of the detonation chamber at a horizontal distance of 0.90 m from the center of the explosive charge, Experiment 5.

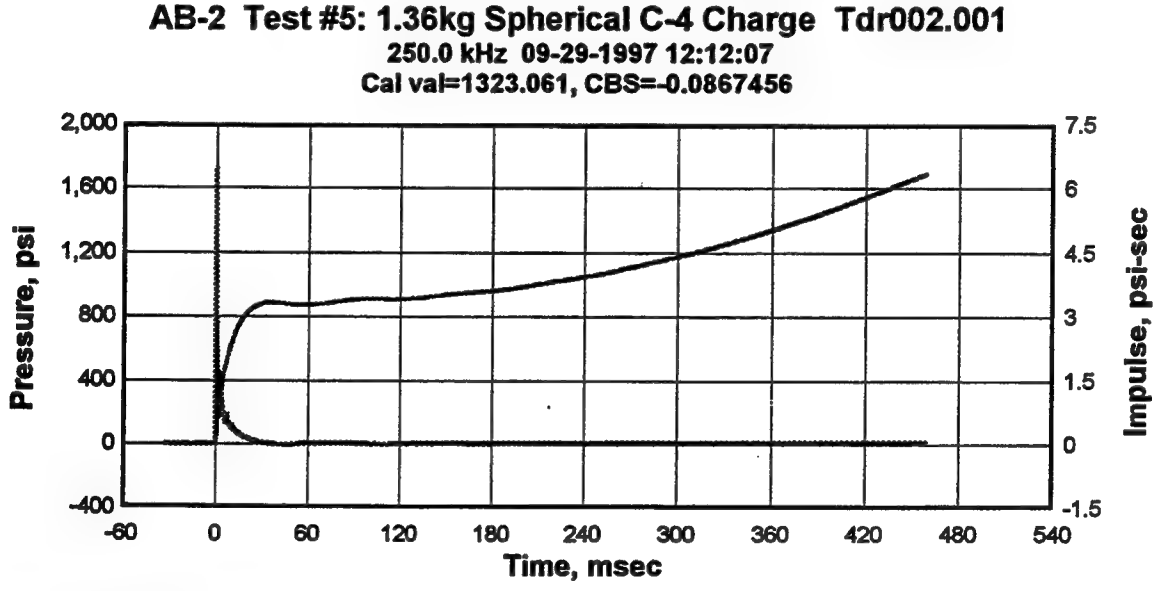

Figure E2. Pressure and impulse-time histories, Gage AB-2 on side wall of the detonation chamber at a horizontal distance of 0.45 m from the rear wall of the detonation chamber, Experiment 5.

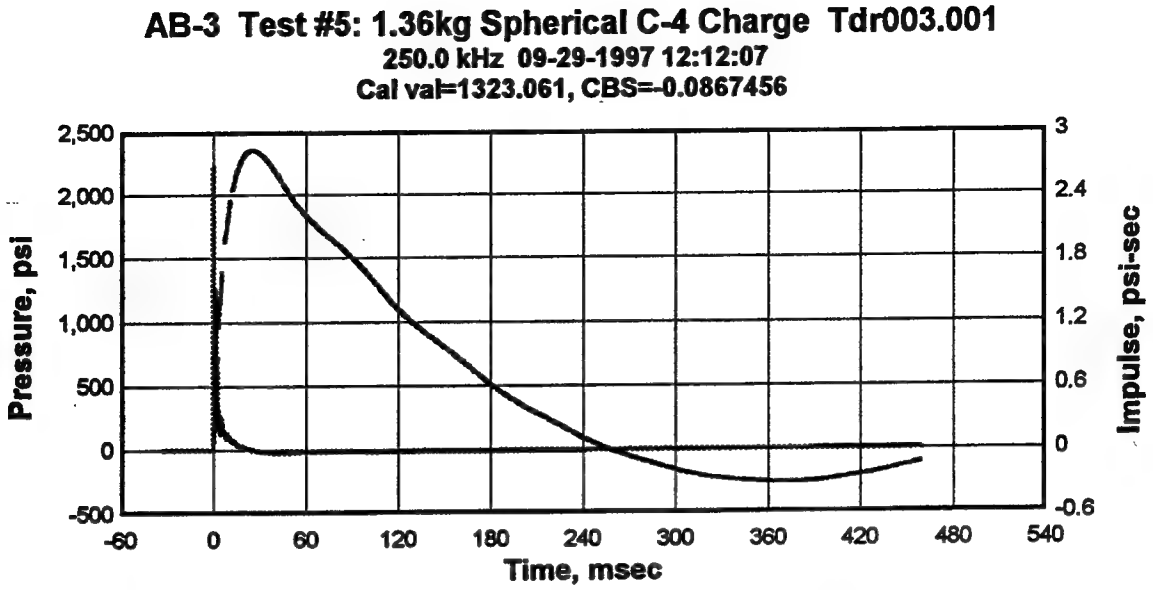

Figure E3. Pressure and impulse-time histories, Gage AB-3 on side wall of the detonation chamber at a horizontal distance of 1.35 m from the rear wall of the detonation chamber, Experiment 5.

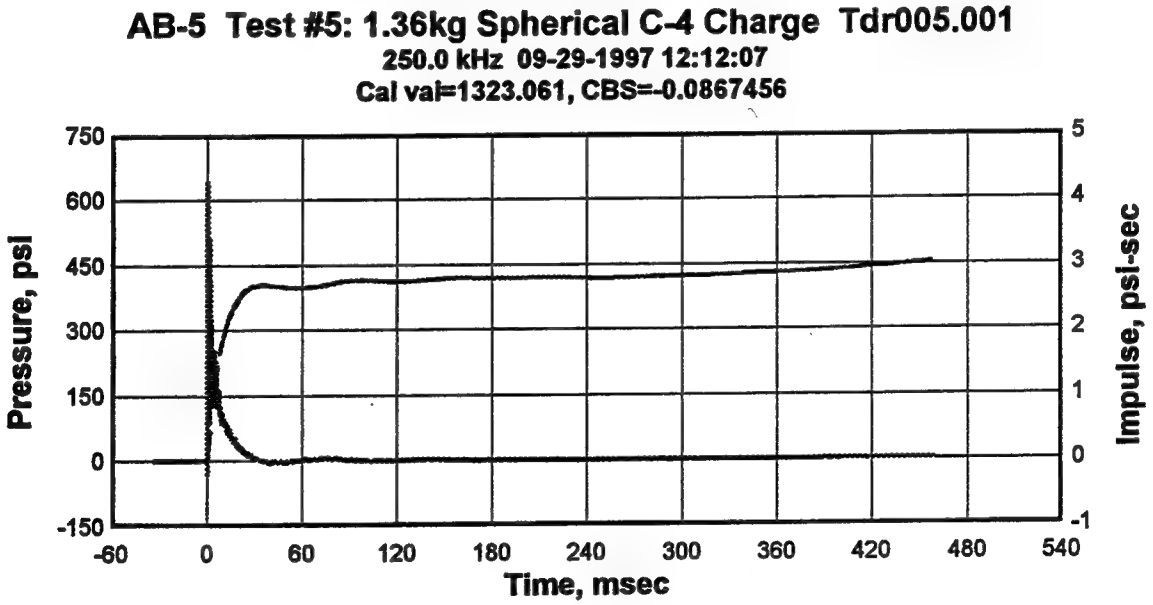

Figure E4. Pressure and impulse-time histories, Gage AB-5 on the wall of the access tunnel at a horizontal distance of 2.61 m from the rear wall of the detonation chamber, Experiment 5.

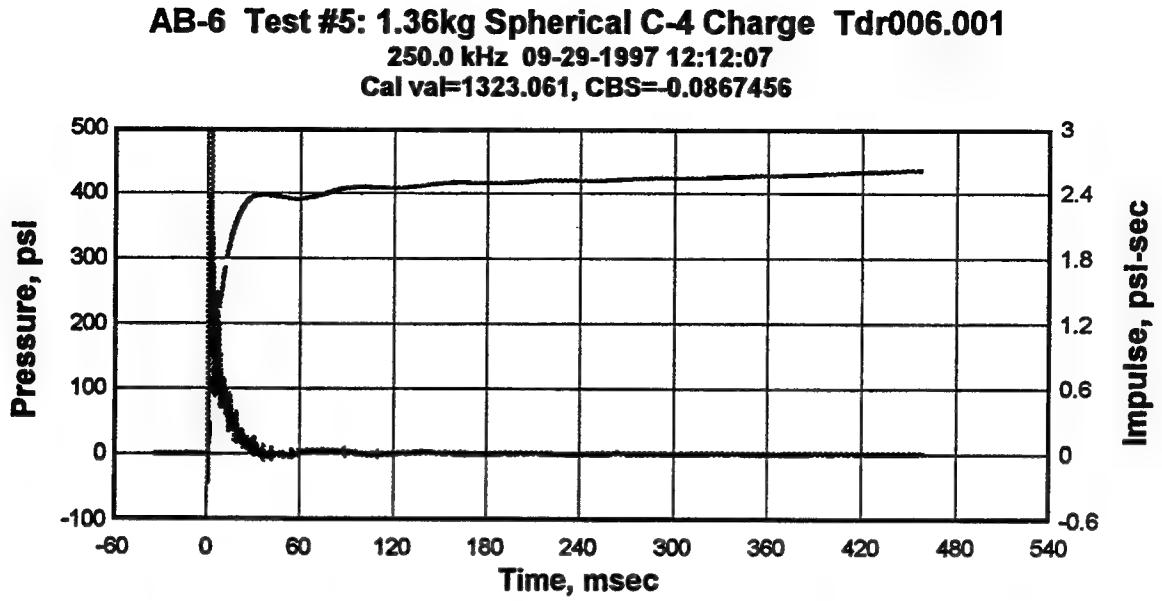

Figure E5. Pressure and impulse-time histories, Gage AB-6 in baffled chamber on side of the probe mount at a horizontal distance of 3.37 m from the rear of the detonation chamber, Experiment 5.

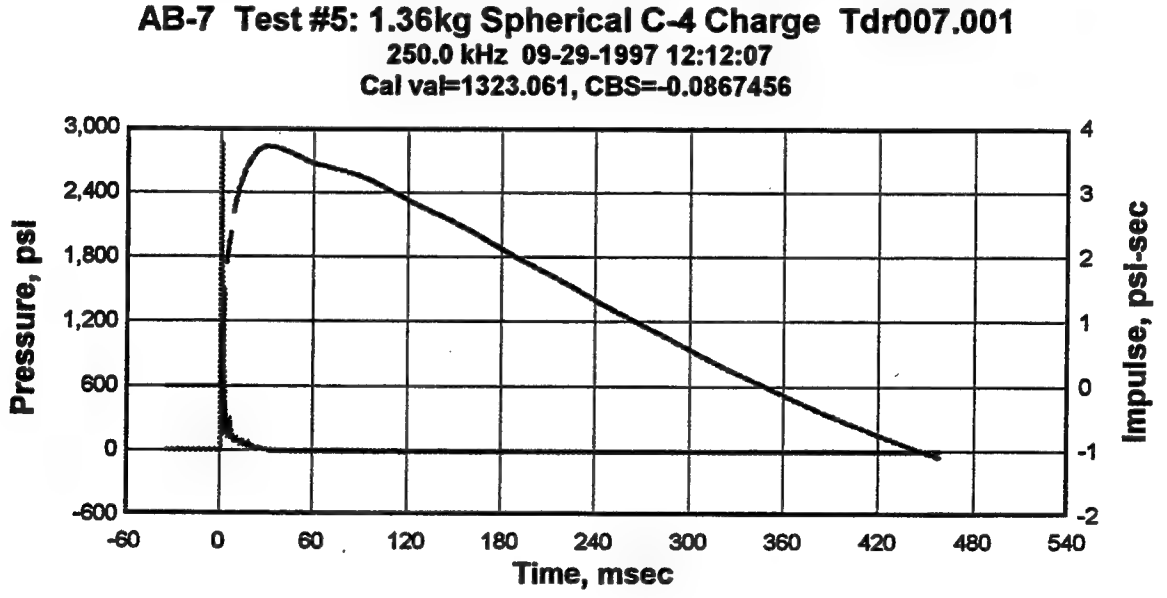

Figure E6. Total pressure and impulse-time histories, Gage AB-7 on probe mount at a horizontal distance of 3.30 m from the rear wall of the detonation chamber, Experiment 5.

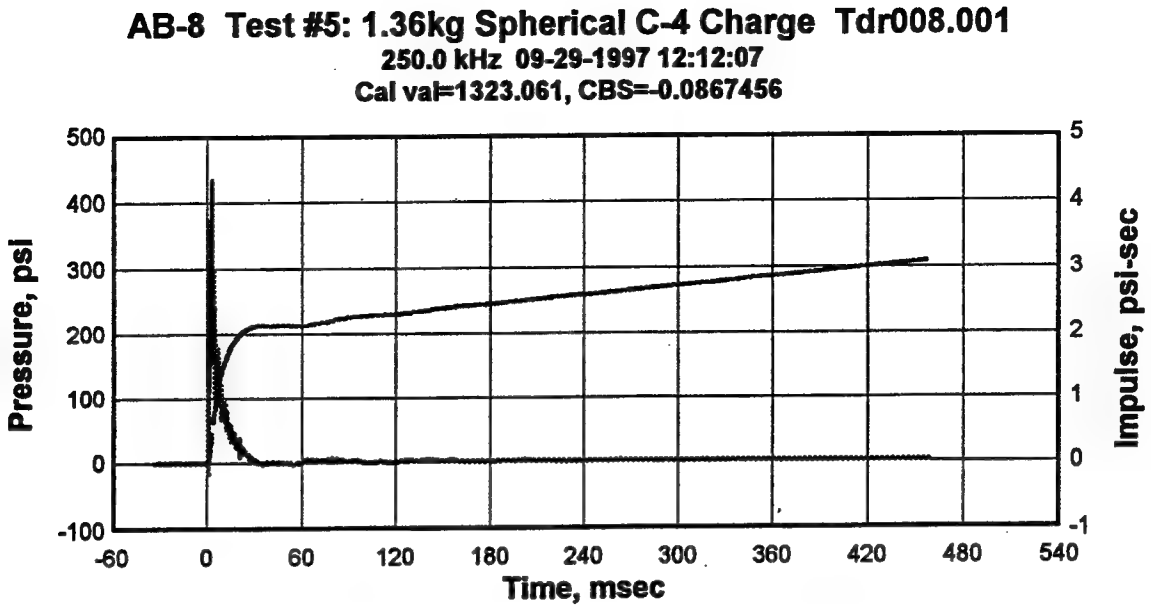

Figure E7. Pressure and impulse-time histories, Gage AB-8 in baffled chamber on the side of probe mount at a horizontal distance of 4.37 m from the rear wall of the detonation chamber, Experiment 5.

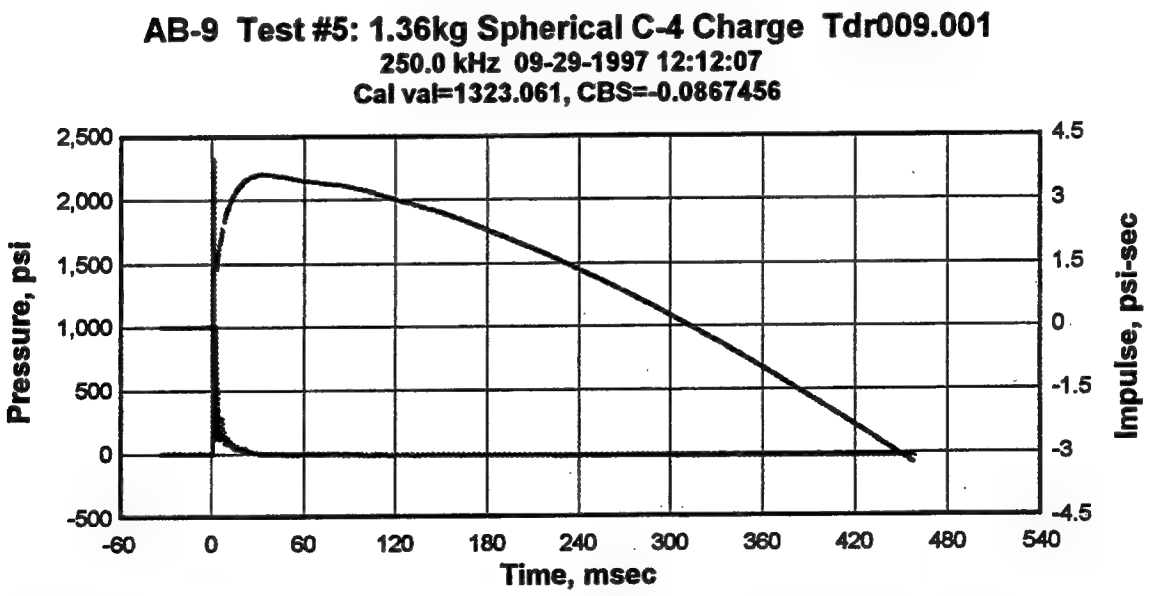

Figure E8. Total pressure and impulse-time histories, Gage AB-9 on probe mount at a horizontal distance of 4.30 m from the rear of the detonation chamber, Experiment 5

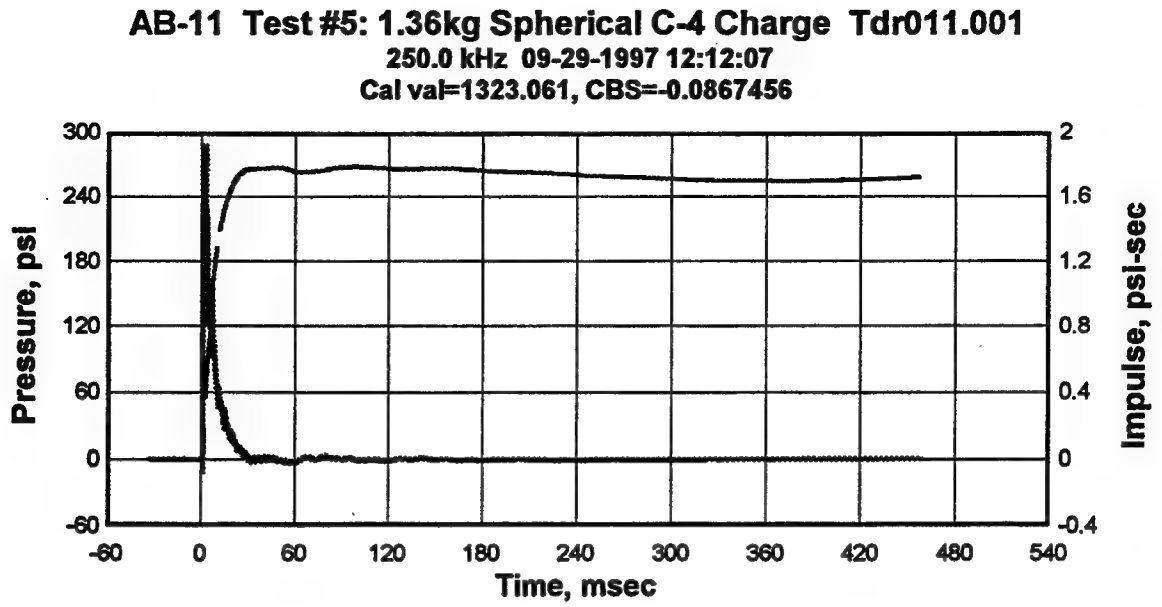

Figure E9. Pressure and impulse-time histories, Gage AB-11 on wall of the access tunnel at a horizontal distance of 5.61 m from the rear wall of the detonation chamber, Experiment 5.

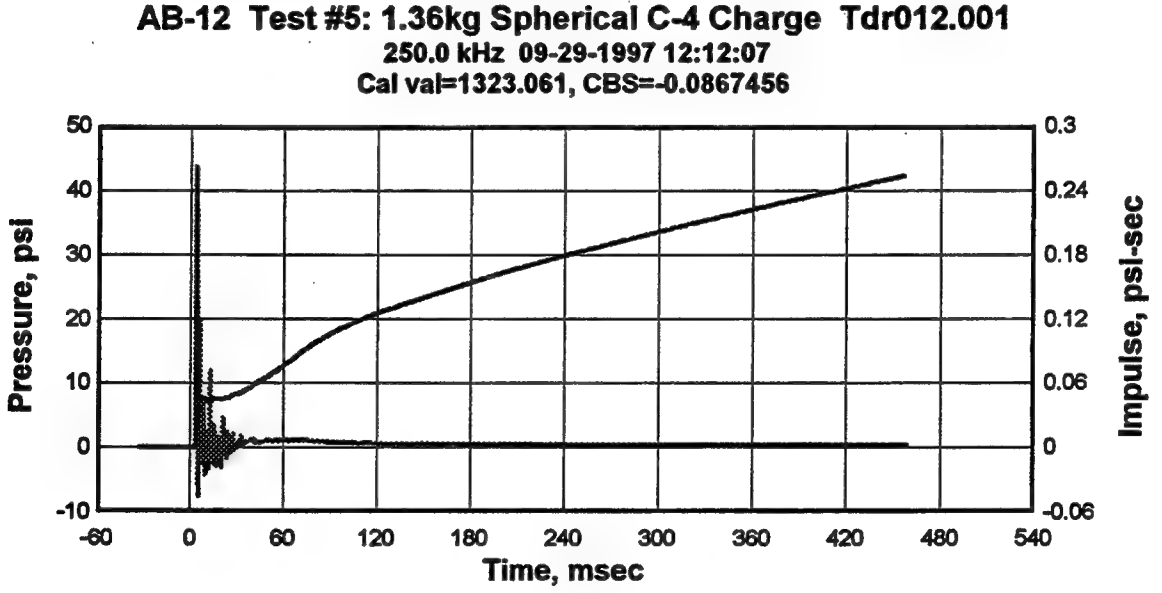

Figure E10. Pressure and impulse-time histories, free-field Gage AB-12 on the surface of the ground at a horizontal distance of 1.80m from the portal, Experiment 5.

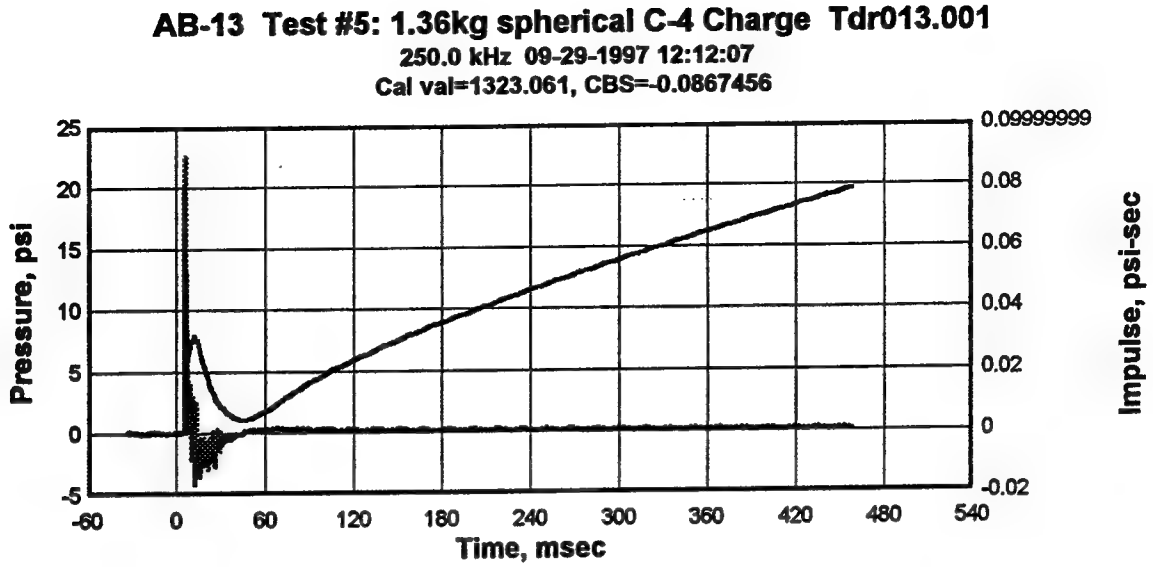

Figure E11. Pressure and impulse-time histories, free-field Gage AB-13 on the surface of the ground at a horizontal distance of 3.00 m from the portal, Experiment 5.

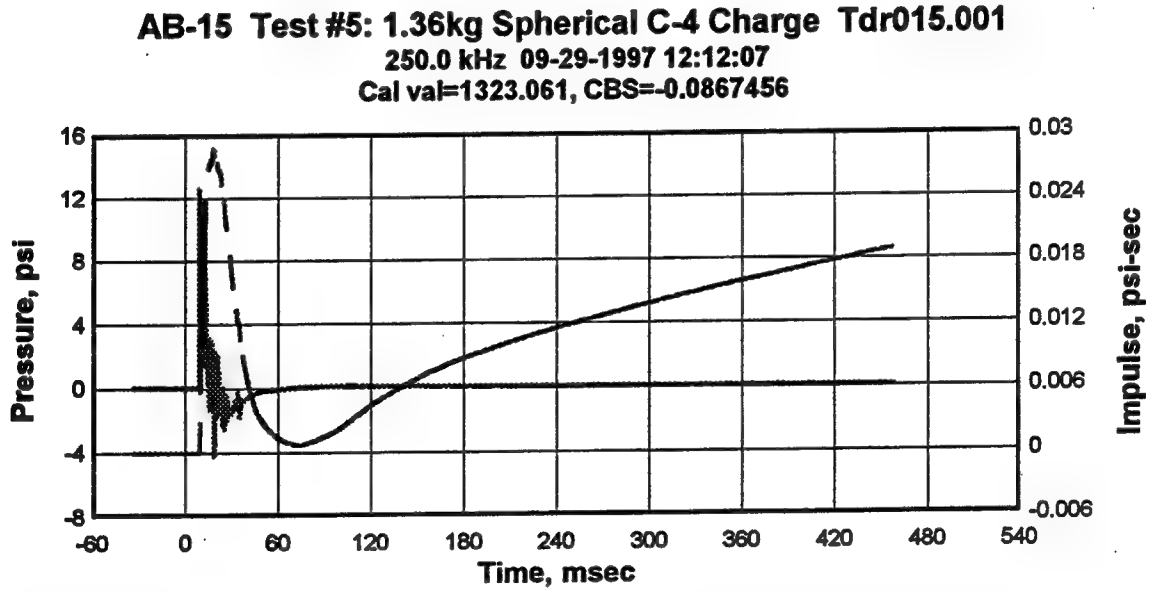

Figure E12. Pressure and impulse-time histories, free-field Gage AB-15 on the surface of the ground at a horizontal distance of 4.80 m from the portal, Experiment 5.

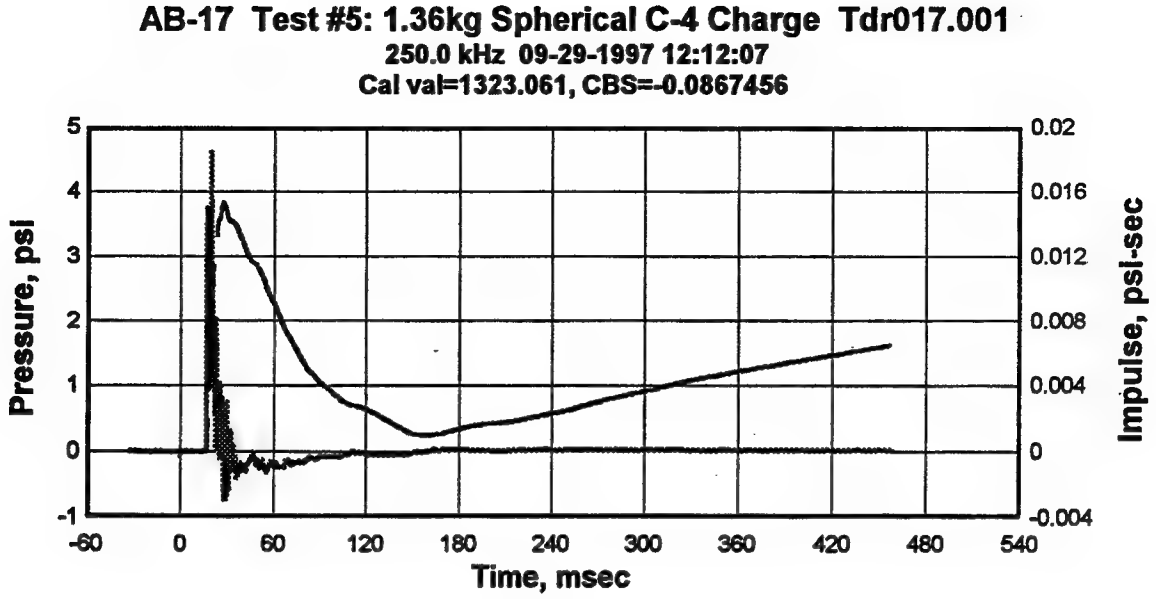

Figure E13. Pressure and impulse-time histories, free-field Gage AB-17 on the surface of the ground at a horizontal distance of 8.00 m from the portal, Experiment 5.

Appendix F
Airblast Effects Research Small-Scale Magazine Experiment 6

Pressure-Time Histories from the Detonation of 0.045 kg Spherical C-4 Charge

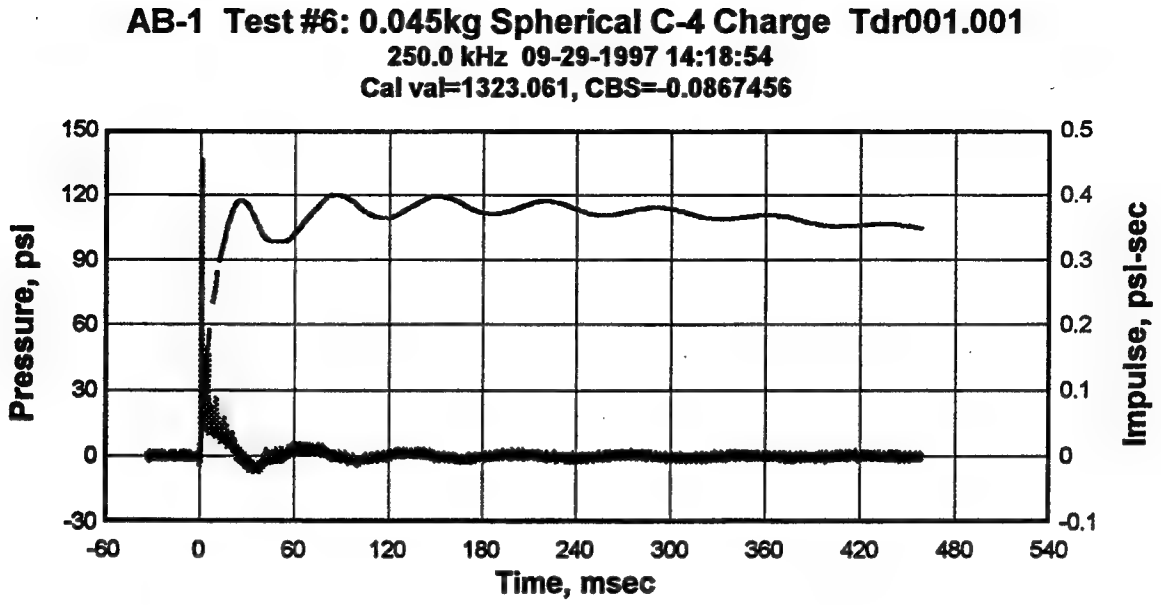

Figure F1. Pressure and impulse-time histories, Gage AB-1 on the rear wall of the detonation chamber at a horizontal distance of 0.90 m from the center of the explosive charge, Experiment 6.

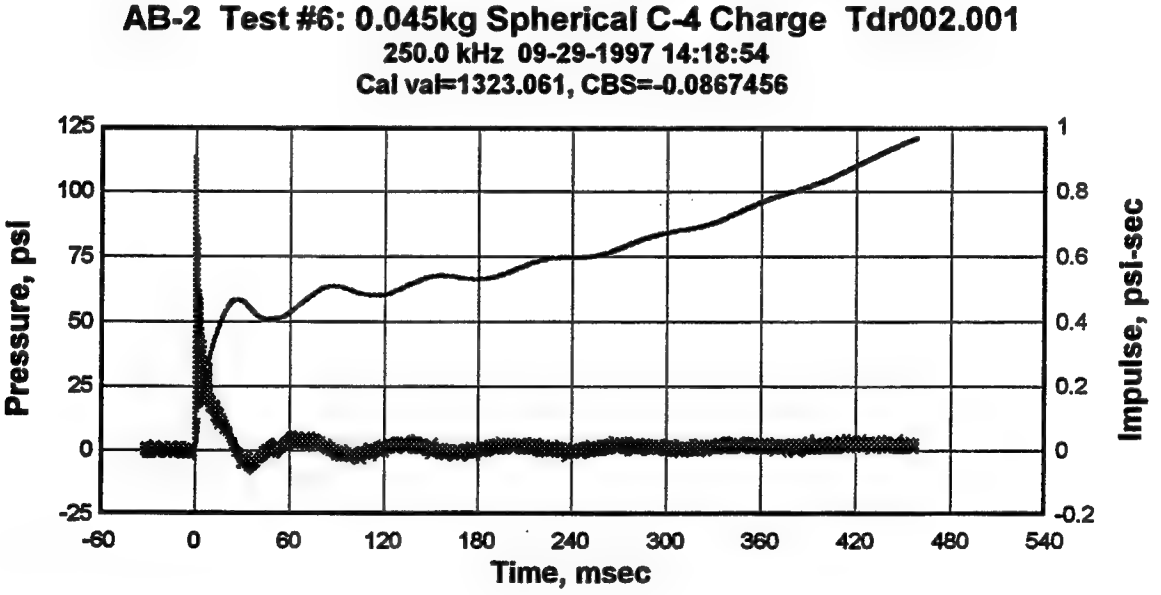

Figure F2. Pressure and impulse-time histories, Gage AB-2 on side wall of the detonation chamber at a horizontal distance of 0.45 m from the rear wall of the detonation chamber, Experiment 6.

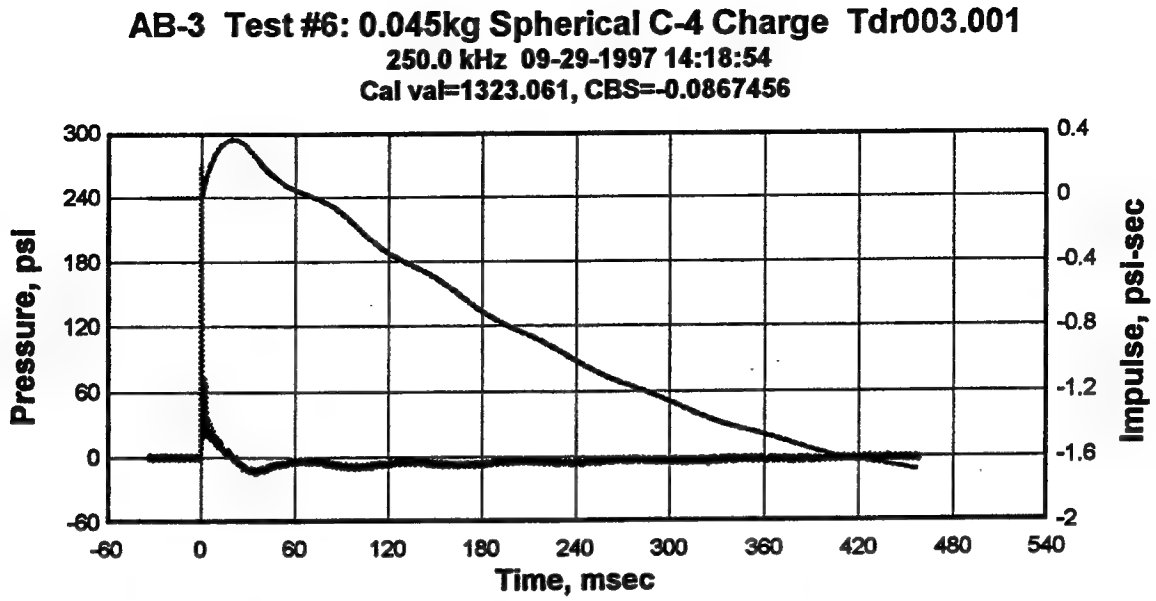

Figure F3. Pressure and impulse-time histories, Gage AB-3 on side wall of the detonation chamber at a horizontal distance of 1.35 m from the rear wall of the detonation chamber, Experiment 6

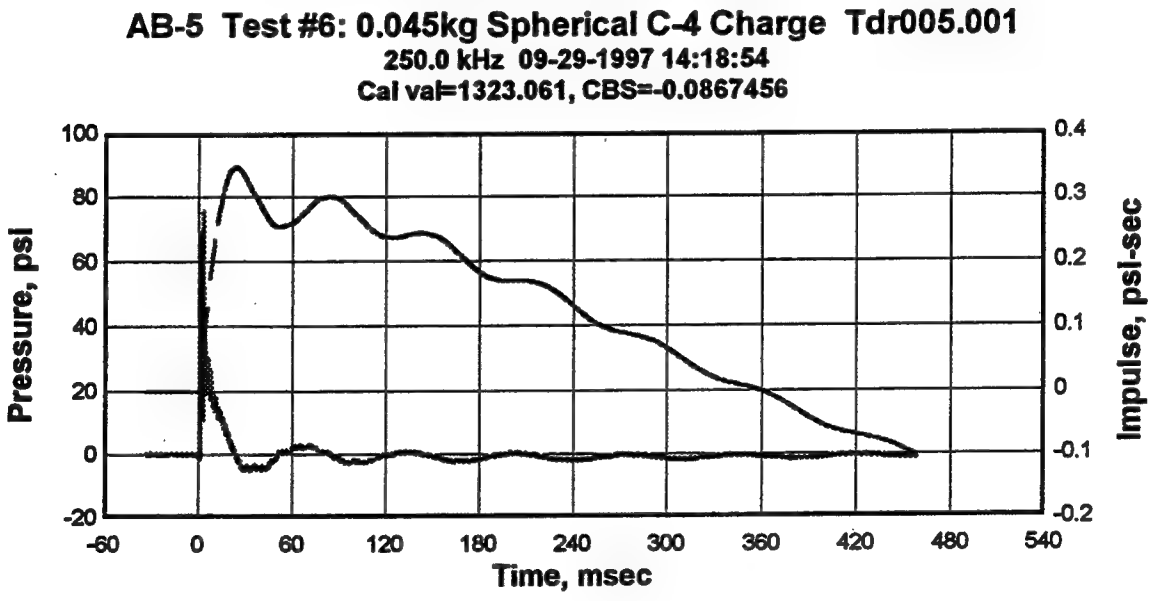

Figure F4. Pressure and Impulse-time histories, Gage AB-5 on wall of the access tunnel at a horizontal distance of 2.61 m from the rear wall of the detonation chamber, Experiment 6.

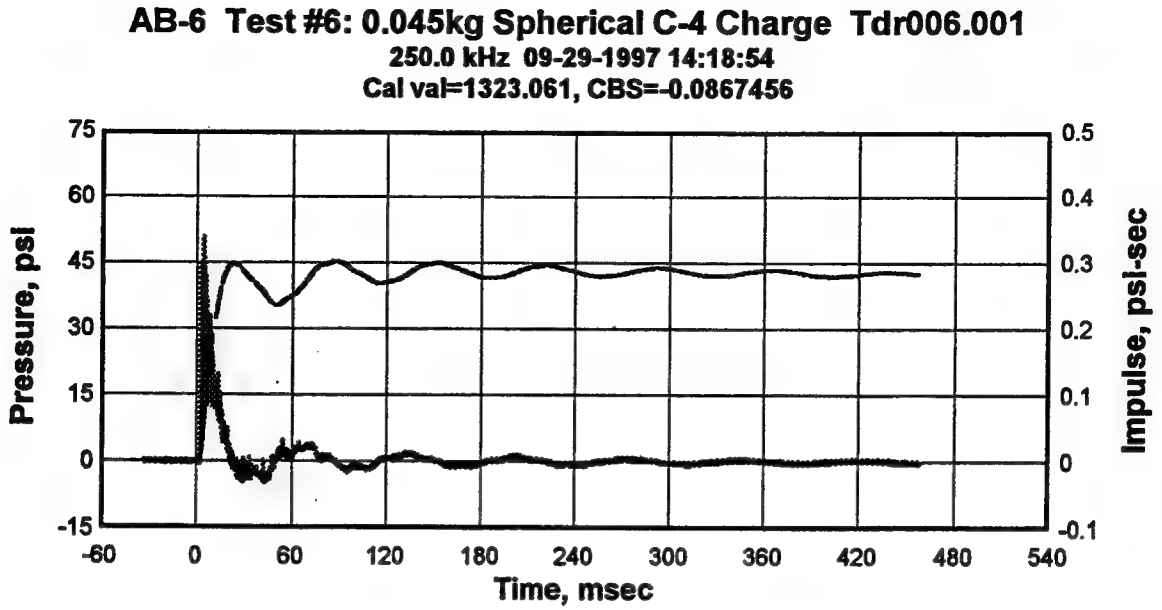

Figure F5. Pressure and impulse-time histories, Gage AB-6 in baffled chamber on the side of probe mount at a horizontal distance of 3.37 m from the rear wall of the detonation chamber, Experiment 6.

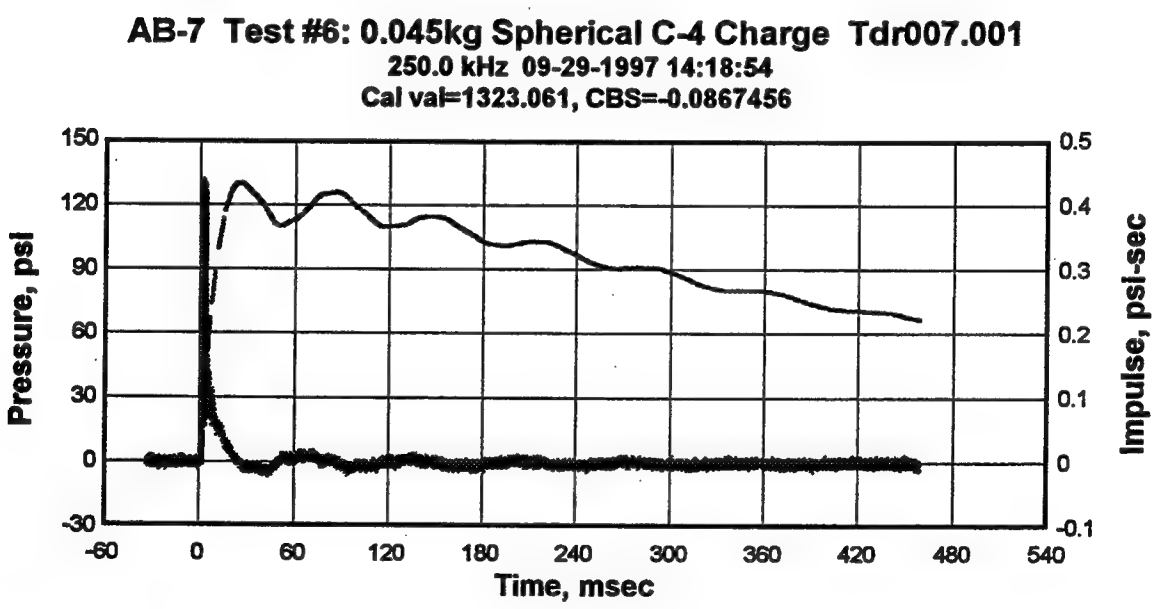

Figure F6. Total pressure and impulse-time histories, Gage AB-7 on probe mount at horizontal distance of 3.30 m from rear wall of detonation chamber, Experiment 6.

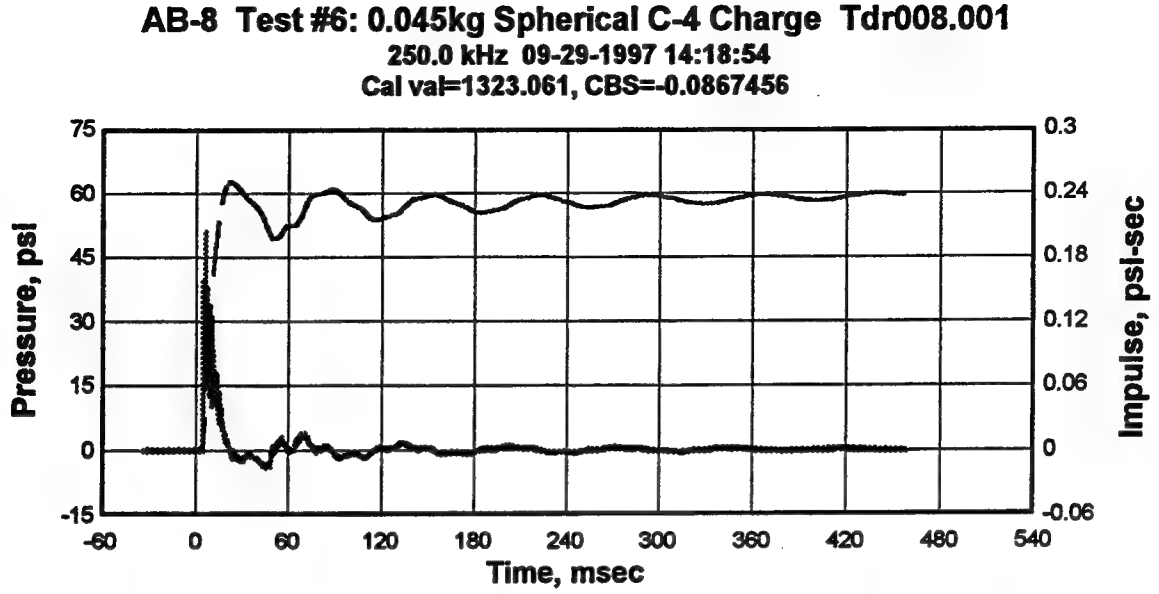

Figure F7. Pressure and impulse-time histories, Gage AB-8 in baffled chamber on the side of probe mount at a horizontal distance of 4.37 m from the rear of the detonation chamber, Experiment 6.

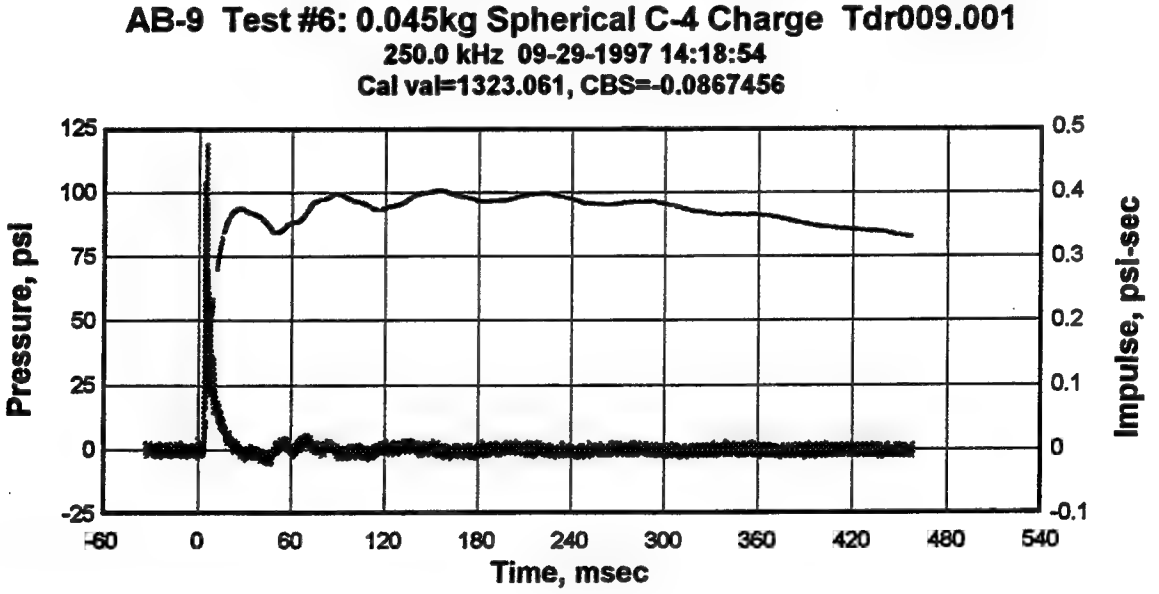

Figure F8. Total pressure and impulse-time histories, Gage AB-9 on probe mount at a horizontal distance of 4.30 m from the rear wall of the detonation chamber, Experiment 6.

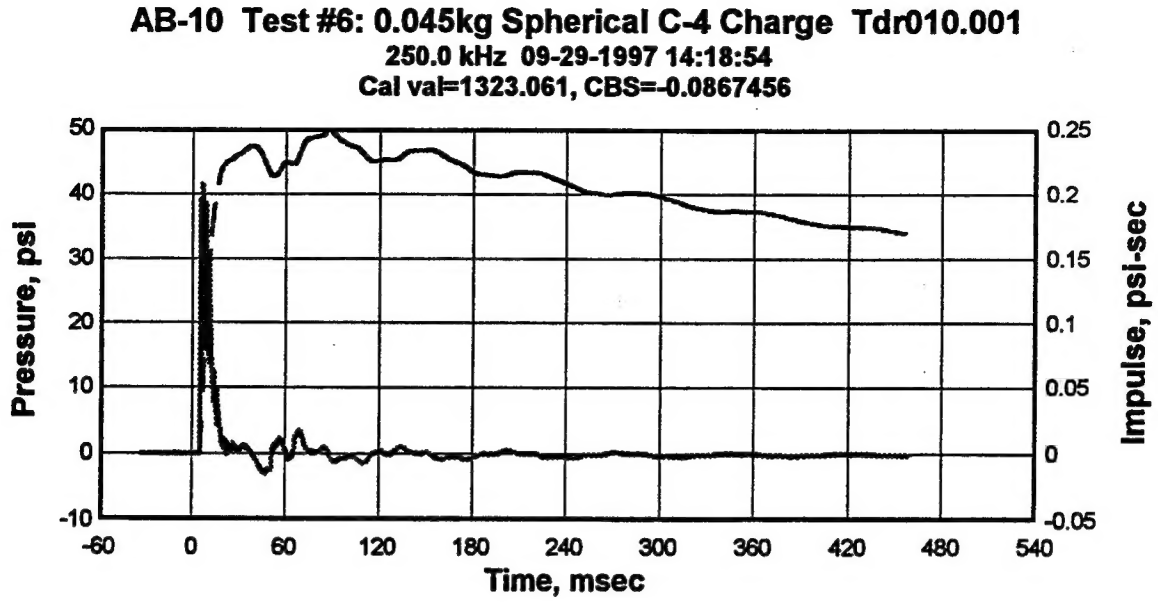

Figure F9. Pressure and impulse-time histories, Gage AB-10 on wall of access tunnel at a horizontal distance of 5.3 m from rear of the detonation chamber, Experiment 6.

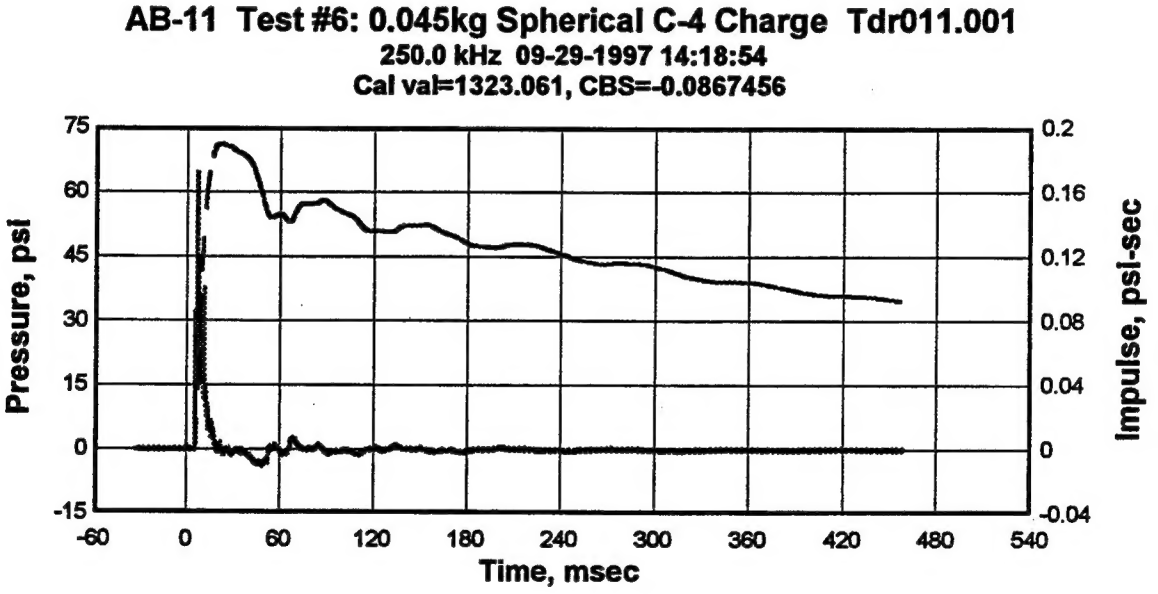

Figure F10. Pressure and impulse-time histories, Gage AB-11 on wall of the access tunnel at a horizontal distance of 5.61 m from the rear wall of the detonation chamber, Experiment 6.

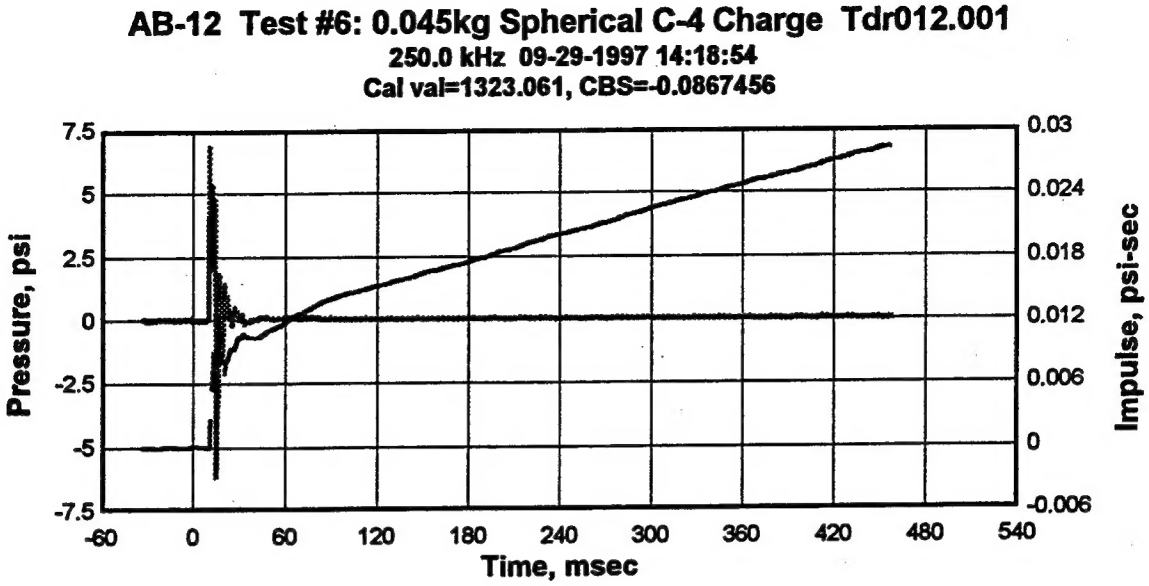

Figure F11. Pressure and impulse-time histories, free-field Gage AB-12 on the surface of the ground at a horizontal distance of 1.80 m from the portal, Experiment 6.

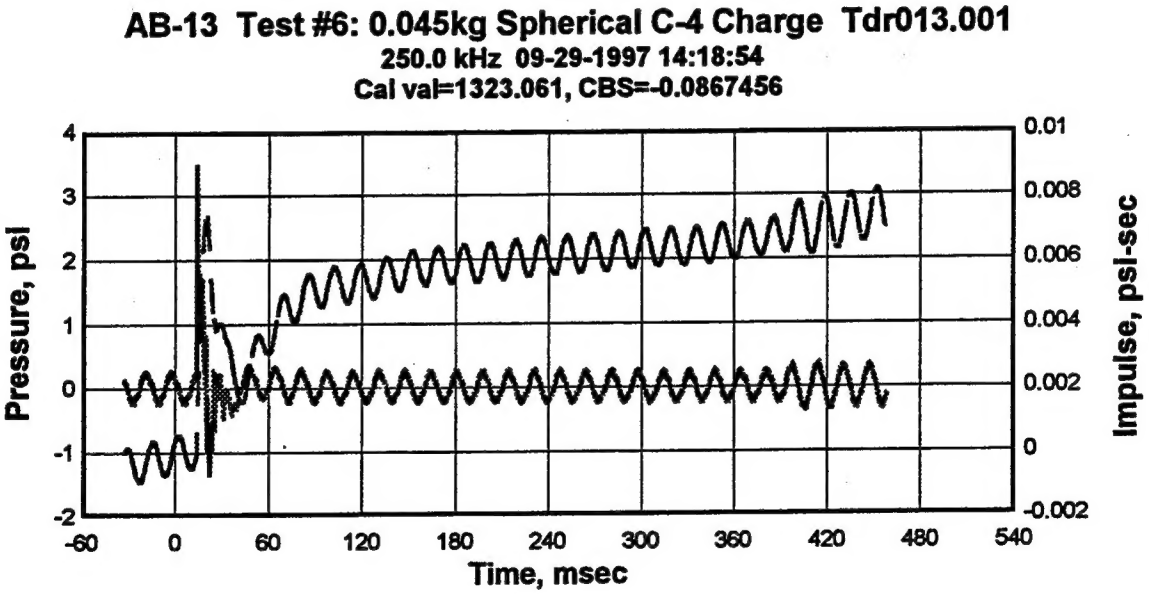

Figure F12. Pressure and impulse-time histories, free-field Gages AB-13 on surface of the ground at a horizontal distance of 3.00 m from the portal, Experiment 6.

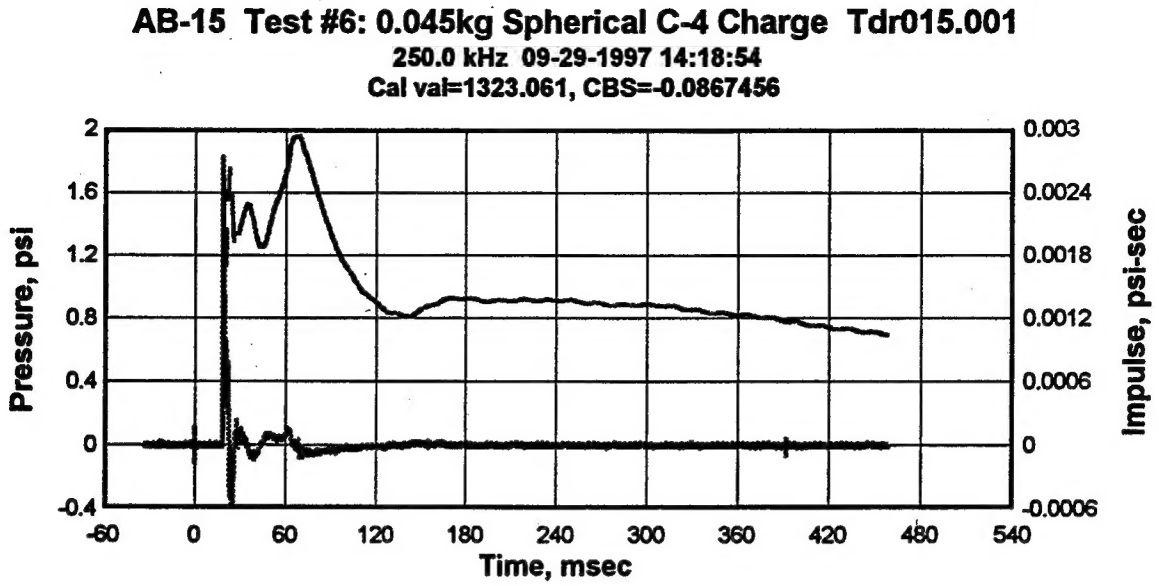

Figure F13. Pressure and impulse-time histories, free-field Gage AB-15 on the surface of the ground at a horizontal distance of 4.80 m from the portal, Experiment 6.

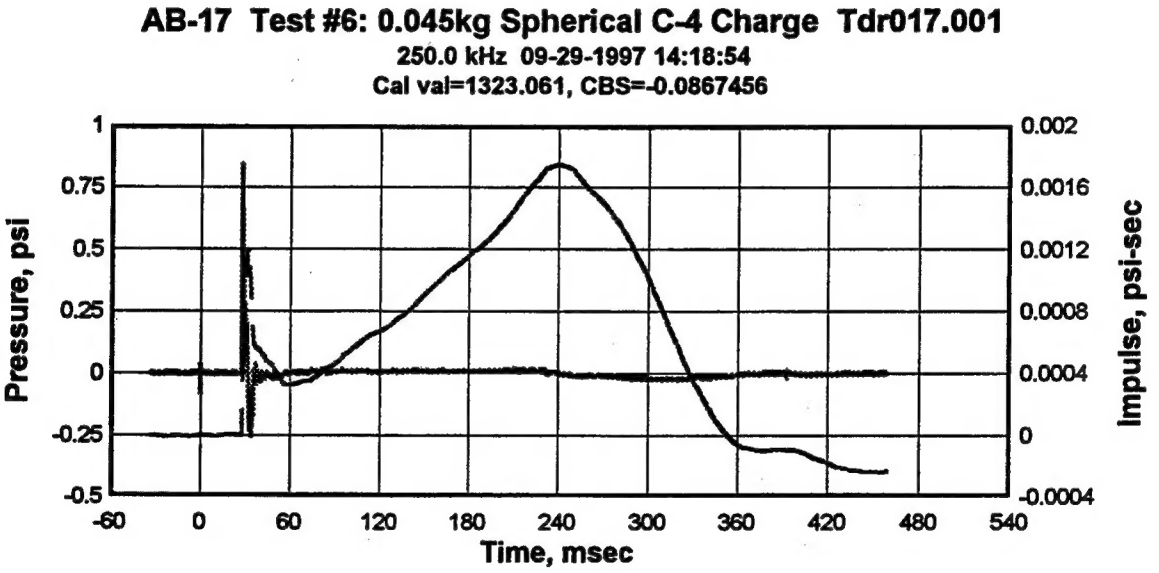

Figure F14. Pressure and impulse-time histories, free-field Gage AB-17 on the surface of the ground at a horizontal distance of 8.00 m from the portal, Experiment 6.

REPORT DOCUMENTATION PAGE

Form Approved
OMB No. 0704-0188

1. AGENCY USE ONLY *(Leave blank)*	2. REPORT DATE	3. REPORT TYPE AND DATES COVERED
	August 1999	Final report

4. TITLE AND SUBTITLE
Airblast Effects Research:
Small-Scale Experiments and Calculations

5. FUNDING NUMBERS

6. AUTHOR(S)
Charles E. Joachim, Gordon W. McMahon, Christo V. Lunderman,
Sharon B. Garner

7. PERFORMING ORGANIZATION NAME(S) AND ADDRESS(ES)
U.S. Army Engineer Waterways Experiment Station
3909 Halls Ferry Road
Vicksburg, MS 39180-6199

8. PERFORMING ORGANIZATION REPORT NUMBER
Technical Report SL-99-5

9. SPONSORING/MONITORING AGENCY NAME(S) AND ADDRESS(ES)
Army Materiel Command
Special Projects Support Activity
Fort Belvoir, Virginia 22060

10. SPONSORING/MONITORING AGENCY REPORT NUMBER

11. SUPPLEMENTARY NOTES
Available from National Technical Information Service, 5285 Port Royal Road, Springfield, VA 22161.

12a. DISTRIBUTION/AVAILABILITY STATEMENT
Approved for public release; distribution is unlimited.

12b. DISTRIBUTION CODE

13. ABSTRACT ***(Maximum 200 words)***

A series of 1:15-scale model experiments were conducted to investigate the effects of loading density on the dynamic airblast flow parameters produced by spherical charge detonations in an underground ammunition storage magazine (shotgun design). Chamber loading densities ranged from 0.4 to 5.0 kg/cubic meter (TNT Equivalent). Total pressure measurements were made on the center line of the model access tunnel using a miniaturized, probe-type, pressure mount. Side-on and total pressure measurements provide the data required to quantify the pressure regime at these locations within the model. The data also provide an estimate of the dynamic flow regime. Calculations for a full-scale magazine were performed using the CTH hydrocode.

Comparisons of the CTH calculated full-scale pressure waveforms with the scaled-up recorded waveforms are excellent. Detonations in an underground magazine are confined so that the blast wave follows a restricted flow path to the portal. Comparisons of the measured and calculated pressures show that this confinement drastically increases the pressures of the blast wave by an order of magnitude or more above that produced in the free field by the same explosion source.

14. SUBJECT TERMS
Airblast impulse
Airblast total pressure
CTH hydrocode calculations
Overpressure
Underground magazine

15. NUMBER OF PAGES
99

16. PRICE CODE

17. SECURITY CLASSIFICATION OF REPORT	18. SECURITY CLASSIFICATION OF THIS PAGE	19. SECURITY CLASSIFICATION OF ABSTRACT	20. LIMITATION OF ABSTRACT
UNCLASSIFIED	UNCLASSIFIED		